AD-A189 544

OPTIMAL THRUST VECTOR CONTROL OF

COPLANAR ORBITAL EVASIVE MANEUVERS

THESIS

Sharon A. Eide
Second Lieutenant, USAF

AFIT/GA/AA/87D-2

DTIC
ELECTE
MAR 0 3 1988

H

DEPARTMENT OF THE AIR FORCE
AIR UNIVERSITY
AIR FORCE INSTITUTE OF TECHNOLOGY

Wright-Patterson Air Force Base, Ohio

88 3 01 134

OPTIMAL THRUST VECTOR CONTROL OF

COPLANAR ORBITAL EVASIVE MANEUVERS

THESIS

Sharon A. Eide
Second Lieutenant, USAF

AFIT/GA/AA/87D-2

DTIC
ELECTE
S
MAR 0 3 1988
D

H

AFIT/GA/AA/87D-2

OPTIMAL THRUST VECTOR CONTROL OF COPLANAR

ORBITAL EVASIVE MANEUVERS

THESIS

Presented to the Faculty of the School of Engineering

of the Air Force Institute of Technology

Air University

In Partial Fulfillment of the

Requirement for the Degree of

Master of Science in Astronautical Engineering

Sharon A. Eide, B.S.

Second Lieutenant, USAF

December 1987

Preface

The purpose of this study was to develop a method of determining a sequence of optimal orbital evasive and rendezvous maneuvers using continuous, low thrust electric propulsion. I began my research with the intent of developing an algorithm which could be implemented on the tactical level to analyze the optimal avoidance trajectory for a spacecraft under attack. I made substantial progress towards this goal, and I believe this work forms the basis of a practical solution method.

Throughout this project, the unpredictable behavior of the Lagrange costates posed a major difficulty in that costate trajectories greatly affect the convergence of a numerical solution. For this reason, results include these trajectories and their quadratic curvefits with time in the hope that future researchers may find them useful in obtaining a converged solution.

Upon completion, I would like to add that this research was not the product of my efforts alone. I owe a debt of gratitude to my thesis advisor, Lt Col Joseph W. Widhalm, for the endless ideas he contributed and the direction he provided me over the course of my efforts. Finally, I give my greatest thanks to Keith for his continuous support and understanding throughout this endeavor.

Sharon A. Eide

ii

Table of Contents

List of Figures

List of Tables

Notation

$\underset{\sim}{x}$ System state vector

β Thrust vector control angle referred to +x axis

J Performance index

ϕ Function optimized at final time

$\underset{\sim}{\psi}$ System constraint vector

$\underset{\sim}{\nu}$ Vector of constant Lagrange multipliers

$\underset{\sim}{\lambda}$ Vector of costate Lagrange multipliers

$\mathcal{H}$ System Hamiltonian

x Spacecraft position in an inertial x direction

y Spacecraft position in an inertial y direction

u Spacecraft velocity in an inertial x direction

v Spacecraft velocity in an inertial y direction

r Radial distance of spacecraft from earth's center

r_o Radius of initial geosynchronous orbit

v_o Circular speed in initial geosynchronous orbit

x_{NOM} Nominal circular orbit position in inertial x direction

y_{NOM} Nominal circular orbit position in inertial y direction

u_{NOM} Nominal circular orbit velocity in inertial x direction

v_{NOM} Nominal circular orbit velocity in inertial y direction

μ Universal gravitation constant times mass of the earth

T Magnitude of thrust vector

m_o Initial spacecraft mass

$\dot{m}$ Time rate of change of spacecraft mass

t_o Initial time of evasive maneuver

t_1 Final time of evasive maneuver/nominal intercept time

t_f Time of rendezvous

τ Time parameterization variable

c Time parameter state

TOF   Time of flight

AFIT/GA/AA/87D-2

Abstract

Optimal in-plane orbital maneuvers enabling a target
spacecraft in geosynchronous orbit to avoid interception by
a threat in direct coasting ascent are examined. Given
constant magnitude, low thrust electric propulsion, the
thrust vector control history is determined to propel the
spacecraft to either a maximum or minimum orbit radius in a
specified time of flight. The evasive maneuver is studied
from two aspects. First, an orthogonality constraint is
applied at the final time of the maneuver, such that the
target spacecraft's position vector is orthogonal to its
velocity vector. This requirement is then removed to allow
the spacecraft to travel without influence of a terminal
constraint. Results demonstrate the adverse shaping effect
the orthogonality constraint applies over the entire evasive
maneuver.

Upon completion of the evasive maneuver, the spacecraft
returns in minimum time to its nominal orbit, in a position
as if no evasive thrusting had occurred. Results show the
time required to rendezvous with the nominal orbit may be
significantly greater than the time of flight of the evasive
maneuver.

Optimal control is applied to formulate the evasive and
rendezvous maneuvers using Euler-Lagrange theory and the

calculus of variations. The behavior of the Lagrange costates is examined in terms of their effect upon solution convergence. The resulting two point boundary value problem is solved by numerical methods to yield the optimal spaceflight trajectory.

OPTIMAL THRUST VECTOR CONTROL OF COPLANAR ORBITAL EVASIVE MANEUVERS

I. Introduction

In past years, numerous studies have dealt with the subject of optimal maneuvering in space, mainly pertaining to orbital transfer, rendezvous and satellite station keeping. Until recently, however, few authors have addressed the problem of avoiding an interception in space through evasive maneuvering. At this time, anti-satellite vehicles are capable of intercepting low altitude targets with no warning or up to three and one half hours warning. High altitude targets in geosynchronous orbit, however, may receive up to six hours warning of an interceptor's approach in direct coasting ascent. In view of these current and emerging interceptor capabilities, the intercept avoidance problem is becoming increasingly important to spacecraft mission planning in relation to anti-satellite, space reconnaissance and collision avoidance objectives.

Much of the current literature is concerned with optimal maneuvering using impulsive or continuous thrust. Burk (5) discusses the evasive problem in terms of minimum impulse orbital maneuvers. Kelley, Cliff and Lutze (8:14-17) present a method for optimization of attack and evasion sequences based on Clohessy-Wiltshire models.

1

Both Lawden (9) and Marec (10) develop theory directly applicable to optimal spaceflight trajectories, either in terms of intercept or evasive maneuvers. Differential game theory considers these two approaches simultaneously in a two spacecraft pursuit-evasion scheme (7).

This work follows on that of Preissinger (13), who developed a model determining orbital evasive maneuvers using various thrust magnitudes. The scenario presented herein is one side of the pursuit-evasion game, with the additional consideration of return of a spacecraft to its nominal orbit. A target spacecraft in geosynchronous orbit is considered to be under intercept by a non-maneuvering threat in direct coasting ascent. The point of intercept is specified on the nominal orbit either two, four or six hours ahead of the target spacecraft upon initiation of the evasive maneuver at a time t_o. Thus, with no maneuvering by the target spacecraft, the two crafts would collide at the nominal intercept time t_i. To avoid any further effects of the interceptor's self-detonation, the target spacecraft must achieve a maximum in-plane change in orbit radius such that it will be outside an explosion's lethal radius at the intercept time. To accomplish this change of radius, which may result in either a higher or a lower altitude trajectory than the nominal, the target spacecraft's orbit radius is maximized or minimized by applying two strategies of optimal control. First, the target spacecraft maneuvers subject to

2

a constraint specifying its terminal velocity vector as orthogonal to its terminal radius vector. The other strategy allows the spacecraft to travel with no terminal constraint. These two strategies may be compared in terms of the effect a terminal constraint applies over an evasive trajectory, as well as its effect on the spacecraft's ability to return to its nominal orbit.

The target spacecraft executes the evasive maneuver with a specified amount of fuel, such that the maneuver terminates when the threat reaches the nominal intercept point. Considering the spacecraft rocket propellant to be consumed at a small, constant rate by a continuous low thrust propulsion system, the solution of the problem is to control optimally the thrust direction with time. The position and velocity of the target spacecraft are measured in a non-rotating x-y coordinate system, oriented such that the positive x-axis passes through the point where the evasive maneuver initiates. The thrust vector control angle is measured relative to the +x-axis, as shown in Figure 1.

Immediately upon completion of the evasive maneuver at t_1, the spacecraft returns to its nominal orbit. The return maneuver is performed with a minimum amount of fuel, such that the problem solution is time optimal. The evasive and rendezvous maneuvers occur in sequence over the time interval t_o to t_f and remain in the plane of the nominal orbit, as depicted in Figure 2.

3
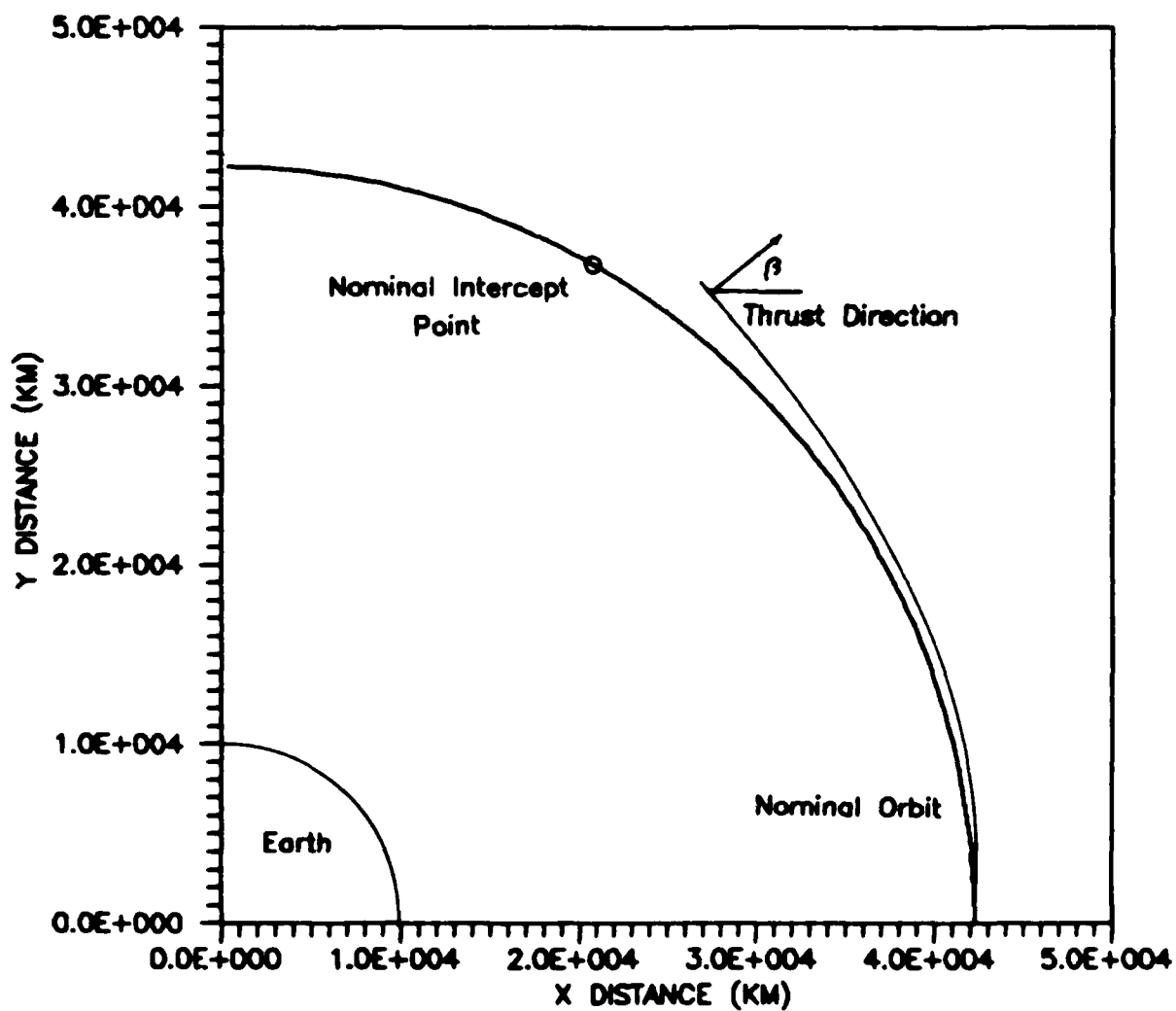
Figure 1.   Reference Coordinate System
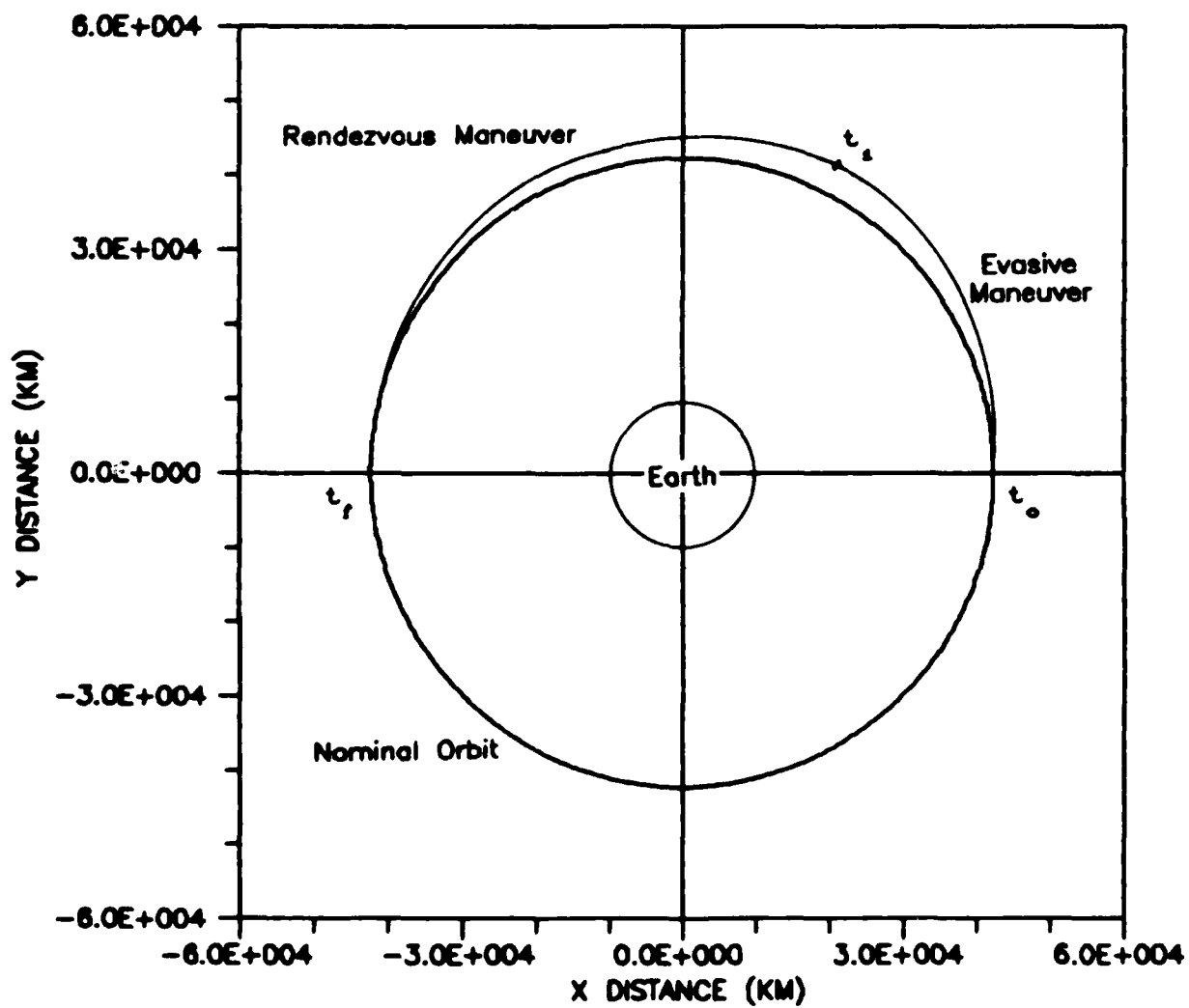
Figure 2. Evasion and Rendezvous Maneuver

For each maneuver examined, the application of
Euler-Lagrange theory (4:47-89) and the calculus of
variations results in a two point boundary value problem
describing necessary conditions an optimal solution must
satisfy. The differential equations associated with each
optimal control problem are nonlinear, and thus must be
solved by numerical methods.

From another perspective, the evasive maneuver may be
viewed in the context of intercepting a specified radius in
minimum time. Two strategies are again implemented, such
that the terminal orthogonality constraint is first applied
and then removed. This viewpoint is considered to ensure
the numerical solutions aquired for the evasive maneuvers
are valid.

II. Euler-Lagrange Theory

Optimal control problems such as those discussed in in this study are developed using the calculus of variations. Bryson and Ho (4:47-89) discuss the following method of applied optimal control as the Euler-Lagrange equations. This theory completely defines a two point boundary value problem to be solved by analytical or numerical means, with either a fixed or free terminal time t_f.

The system under consideration is described by a set of nonlinear differential equations

$$\dot{\underset{\sim}{x}} = \underset{\sim}{f}[x(t),\beta(t),t] \qquad (1)$$

where the states are specified at an initial time t_o.

A performance index, composed of functions to be maximized or minimized, is written in the scalar form

$$\iota = \phi[x(t_f),t_f] + \int_{t_o}^{t_f} \mathcal{L}[x(t),\beta(t),t]dt \qquad (2)$$

A set of functions of the terminal state constrains the system at the final time:

$$\underset{\sim}{\psi}[x(t_f),t_f] = 0 \qquad (3)$$

7

Adjoining these constraints and the system state equations (1) to the performance index (2) by a set of constant multipliers $\underset{\sim}{\nu}$ and costate multipliers $\underset{\sim}{\lambda}$ yields

$$J = \phi[x(t_f),t_f] + \underset{\sim}{\nu}^T \underset{\sim}{\psi}[x(t_f),t_f] + \int_{t_o}^{t_f} \{\mathcal{L}[x(t),\beta(t),t]$$

$$+ \underset{\sim}{\lambda}^T(\underset{\sim}{f} - \underset{\sim}{\dot{x}})\}dt \qquad (4)$$

A dimensionless scalar function $\mathcal{H}$, the Hamiltonian, is defined as

$$\mathcal{H}[x(t),\beta(t),\lambda(t),t] = \mathcal{L}[x(t),\beta(t),t]$$

$$+ \underset{\sim}{\lambda}^T(t)\underset{\sim}{f}[x(t),\beta(t),t] \qquad (5)$$

Substituting for $\mathcal{H}$ in Eq (4) and taking the differential to allow for infinitesimal changes in the terminal time t_f, considering t_o fixed, yields

$$dJ = \left\{ \left[\frac{\partial\phi}{\partial t} + \underset{\sim}{\nu}^T\frac{\partial\psi}{\partial t} + \mathcal{L} \right]dt + \left[\frac{\partial\phi}{\partial\underset{\sim}{x}} + \underset{\sim}{\nu}^T\frac{\partial\psi}{\partial\underset{\sim}{x}} \right]d\underset{\sim}{x} \right\}_{t_f}$$

$$+ \int_{t_o}^{t_f} \left\{ \frac{\partial\mathcal{H}}{\partial\underset{\sim}{x}} \delta\underset{\sim}{x} + \frac{\partial\mathcal{H}}{\partial u} \delta u - \underset{\sim}{\lambda}^T\delta\underset{\sim}{\dot{x}} \right\}dt \qquad (6)$$

Integrating the last term on the right hand side of Eq (6) by parts and substituting for the variation of x in terms of the differential dx

8

$$\delta x = dx - \dot{x}dt \qquad (7)$$

to combine terms in dx gives

$$dJ = \left\{ \left[\frac{\partial \phi}{\partial t} + \underset{\sim}{\nu}^T \frac{\partial \psi}{\partial t} + \mathcal{L} + \underset{\sim}{\lambda}^T \dot{\underset{\sim}{x}} \right] dt_f + \left[\frac{\partial \phi}{\partial \underset{\sim}{x}} + \underset{\sim}{\nu}^T \frac{\partial \psi}{\partial \underset{\sim}{x}} - \underset{\sim}{\lambda}^T \right] d\underset{\sim}{x} \right\}_{t_f}$$

$$+ \left. (\underset{\sim}{\lambda}^T \delta \underset{\sim}{x}) \right|_{t_o} + \int_{t_o}^{t_f} \left\{ \left[\frac{\partial \mathcal{H}}{\partial \underset{\sim}{x}} + \dot{\underset{\sim}{\lambda}}^T \right] \delta \underset{\sim}{x} + \frac{\partial \mathcal{H}}{\partial u} \delta u \right\} dt \qquad (8)$$

Choosing the multiplier functions $\underset{\sim}{\lambda}(t)$ to cause the coefficients of $\delta x(t)$, $dx(t_f)$ and dt_f, if the final time is undetermined, to vanish gives a set of conditions necessary for the existence of a stationary value of J. These necessary conditions include an optimality condition determining the control $\beta(t)$

$$\frac{\partial \mathcal{H}}{\partial \beta} = 0 \qquad (9)$$

as well as a set of Lagrange costate equations

$$\dot{\underset{\sim}{\lambda}}^T = - \frac{\partial \mathcal{H}}{\partial \underset{\sim}{x}} \qquad (10)$$

with boundary conditions given by

$$\underset{\sim}{\lambda}^T(t_f) = \left. \left[\frac{\partial \phi}{\partial \underset{\sim}{x}} + \underset{\sim}{\nu}^T \frac{\partial \psi}{\partial \underset{\sim}{x}} \right] \right|_{t_f} \qquad (11)$$

9

An additional transversality condition applies if the terminal time t_f is unspecified:

$$\left[\frac{\partial \phi}{\partial t} + \underset{\sim}{\nu}^T \frac{\partial \psi}{\partial t} + \mathcal{H} \right]\bigg|_{t_f} = 0 \qquad (12)$$

On the optimal trajectory, Eq (9) shows that the optimal control $\beta(t)$ maximizes or minimizes the Hamiltonian. It then follows that to maximize $\mathcal{H}$, and thus maximize J, the following statement known as the Legendre-Clebsch condition in the calculus of variations must be enforced:

$$\frac{\partial^2 \mathcal{H}}{\partial \beta^2} \leq 0 \qquad (13)$$

To minimize $\mathcal{H}$, and thus J, however, the Legendre-Clebsch condition must take the form

$$\frac{\partial^2 \mathcal{H}}{\partial \beta^2} \geq 0 \qquad (14)$$

Thus, the two point boundary value problem is completely described by the state equations (1) with the initial states specified, and the costate equations (10) with boundary conditions given as in Eq (11). The control is determined by the optimality condition (9), subject to the Legendre-Clebsch condition of Eq (13) or (14). The remaining boundary conditions are recovered from the

10

constraint functions of Eq (3). If the terminal time is
unspecified, an additional final boundary condition is given
by the transversality condition of Eq (12).

III. Orbital Evasive Manuevers

A target spacecraft is considered to be threatened by a coasting craft in a direct-ascent collision course with its nominal geosynchronous orbit. To avoid intercept by the threat craft and any possible effects of its self-detonation, the target craft must maneuver in an optimal manner to achieve a maximum change in its orbit radius. This change in the spacecraft's trajectory may be directed to the exterior of its nominal course, or to the interior providing it does not pass within a lethal radius centered on the ascending interceptor. In the context of optimal control, these two types of trajectory changes are effected by maximizing and minimizing the entire radius of the target spacecraft's orbit.

The evasive maneuver initiates at time t_o, prior to the nominal intercept time t_1 by a specified time of flight. Continuous, low thrust electric propulsion is employed over the entire maneuver, wherein control is provided by a thrust vector free to gimbal in any desired direction. Both the maximum and the minimum radius maneuvers are accomplished in two ways. First, the target spacecraft's orbit radius is maximized under the influence of a terminal orthogonality constraint, such that the spacecraft's velocity vector is orthogonal to its position vector at the final time of the maneuver, t_1. The constraint is then removed to allow the spacecraft to travel unhindered by any shaping effect the

12

terminal condition might have on the maneuver. These two classes of evasion maneuvers may be compared in terms of total fuel required to achieve a maximal radius change at t_1 followed by a rendezvous with the nominal orbit at time t_f.

Equations of Motion

The spacecraft travels in a plane surrounding the earth, such that its position is described in non-rotating, earth-centered coordinates x and y. The spacecraft velocity components are given by u and v along the x and y axes, respectively. The two body equation of motion for a spacecraft operating in an inverse square gravitational field without influence of external forces is developed by Bate (3:14) and Baker (1:58). Neglecting perturbative effects and taking the rocket thrust force into consideration, the equations of motion may then be written in first order form as given by Preissenger (13:7):

$$\dot{x} = u \tag{15}$$

$$\dot{y} = v \tag{16}$$

$$\dot{u} = \frac{-\mu x}{r^3} + \frac{T}{m_o - \dot{m}t} \cos\beta \tag{17}$$

$$\dot{v} = \frac{-\mu y}{r^3} + \frac{T}{m_o - \dot{m}t} \sin\beta \tag{18}$$

where β is the thrust vector control angle measured with respect to the +x-axis. Assuming the orientation of the

13

x-axis is described as passing through the point where the evasive maneuver initiates, the target spacecraft position and velocity states are specified at the initial time t_o as

$$x(t_o) = 42241.1225 \text{ km}$$

$$y(t_o) = 0.0 \text{ km}$$

$$u(t_o) = 0.0 \text{ km/sec}$$

$$v(t_o) = 3.0719 \text{ km/sec}$$

Maneuver with Terminal Orthogonality Constraint

In order to observe the effect of a terminal constraint on an evasive maneuver, as well as the spacecraft's ability to return to its nominal orbit, a constraint is applied at the final time forcing the spacecraft's velocity vector to be orthogonal to its position vector. This orthogonality constraint is expressed as a function of the states at the final time t_1, as given in Eq (3):

$$\psi(t_1) = xu + yv \Big|_{t_1} = 0 \qquad (19)$$

Maximum Radius Maneuver. To achieve a maximum change in orbit radius to a higher altitude, the requirement that the evasive manuever reach a maximum possible radius in a specified time of flight is defined through the function

14

$$\phi[x(t_\text{i}), t_\text{i}] = r(t_\text{i}) = (x^2 + y^2)^{1/2}\Big|_{t_\text{i}} \tag{20}$$

Adjoining the constraint of Eq (19) to Eq (20) yields a performance index posed as in Eq (4):

$$J = r(t_\text{i}) + \nu(xu + yv)\Big|_{t_\text{i}} \tag{21}$$

where the multiplier ν is to be determined by the boundary conditions on the Lagrange costates. The problem is now to determine the thrust vector control angle β to maximize this performance index.

Following the Lagrange method described by Bryson and Ho (4), the system Hamiltonian is constructed as given by Eq (5):

$$\mathcal{H} = \lambda_x u + \lambda_y v + \lambda_u \left[\frac{-\mu x}{r^3} + \frac{T}{m_o - \dot{m}t} \cos\beta \right]$$

$$+ \lambda_v \left[\frac{-\mu y}{r^3} + \frac{T}{m_o - \dot{m}t} \sin\beta \right] \tag{22}$$

The thrust control angle producing a stationary value of the performance index Eq (21) is given by the optimality condition of Eq (9), resulting in a bilinear tangent control law:

$$\beta = \tan^{-1}\left[\frac{\lambda_v}{\lambda_u}\right] \qquad (23)$$

To ensure the control β maximizes the Hamiltonian, the Legendre-Clebsch condition of Eq (13) must be satisfied as

$$\mathcal{H}_{\beta\beta} = -\left[\lambda_u \frac{T}{m_o - \dot{m}t} \cos\beta + \lambda_v \frac{T}{m_o - \dot{m}t} \sin\beta\right] \leq 0 \qquad (24)$$

where the subscript denotes partial differentiation with respect to the associated variable. This condition, combined with the control law of Eq (23) yields the appropriate definitions of the thrust control angle to apply to the state equations (15) through (18):

$$\cos\beta = \frac{\lambda_u}{(\lambda_u^2 + \lambda_v^2)^{1/2}} \qquad (25)$$

$$\sin\beta = \frac{\lambda_v}{(\lambda_u^2 + \lambda_v^2)^{1/2}} \qquad (26)$$

thus enforcing the Legendre-Clebsch condition as

$$\mathcal{H}_{\beta\beta} = -\frac{T}{m_o - \dot{m}t} (\lambda_u^2 + \lambda_v^2)^{1/2} \qquad (27)$$

To determine the Lagrange multipliers $\underset{\sim}{\lambda}$, the costate equations are developed from Eq (10) as

$$\dot{\lambda}_x = \lambda_u \left[\frac{\mu}{r^3} - \frac{3\mu x^2}{r^5} \right] - \lambda_v \left[\frac{3\mu xy}{r^5} \right] \tag{28}$$

$$\dot{\lambda}_y = \lambda_v \left[\frac{\mu}{r^3} - \frac{3\mu y^2}{r^5} \right] - \lambda_u \left[\frac{3\mu xy}{r^5} \right] \tag{29}$$

$$\dot{\lambda}_u = -\lambda_x \tag{30}$$

$$\dot{\lambda}_v = -\lambda_y \tag{31}$$

Necessary boundary conditions on the costates at the final time of the evasive maneuver are determined from Eq (11):

$$\lambda_x(t_1) = \frac{x}{r} + \nu u \bigg|_{t_1} \tag{32}$$

$$\lambda_y(t_1) = \frac{y}{r} + \nu v \bigg|_{t_1} \tag{33}$$

$$\lambda_u(t_1) = \nu x \bigg|_{t_1} \tag{34}$$

$$\lambda_v(t_1) = \nu y \bigg|_{t_1} \tag{35}$$

Combining these boundary conditions with the orthogonality constraint function of Eq (19) as well as the specified initial state values to eliminate the multiplier ν yields a set of boundary conditions implemented to solve the

17

resulting two point boundary value problem:

$$\underset{\sim}{x}(t_o) \text{ Specified}$$

$$xu + yv = 0 \Big|_{t_1} \tag{36}$$

$$\lambda_v x - \lambda_u y = 0 \Big|_{t_1} \tag{37}$$

$$\lambda_x x - \frac{x^2}{r} - \lambda_u u = 0 \Big|_{t_1} \tag{38}$$

$$\lambda_y y - \frac{y^2}{r} - \lambda_v v = 0 \Big|_{t_1} \tag{39}$$

These boundary conditions (36) through (39) are not unique in form, but they must be independent at time t_1.

The two point boundary value problem is now described by the four state equations (15) through (18) with the appropriate definitions of the control angle applied, Eqs (25) and (26), the four costate equations (28) through (31), four specified initial states, and the above four final boundary conditions on the costates.

<u>Minimum Radius Maneuver.</u> Depending upon the approach path of the attacker, an avoidance maneuver to the interior of the nominal spacecraft orbit may be practical. Such a trajectory is best modeled as a minimum radius maneuver or, alternatively, a maximum negative radius maneuver. The development of the two point boundary value problem defining the maneuver follows that of the maximum orbit radius

18

maneuver, with merely a sign change in the boundary
conditions.

To maximize the negative of the spacecraft orbit
radius, subject to the orthogonality constraint on the
spacecraft velocity and position vectors at the final time,
the performance index is written as

$$J = -r(t_{\textit{f}}) + \nu(xu + yv) \Big|_{t_{\textit{f}}} \tag{40}$$

Since the performance index is again to be maximized,
the Hamiltonian Eq (22), control law Eq (23),
Legendre-Clebsch condition Eq (24), control angle
definitions Eqs (25) and (26), and costate equations (28)
through (31) determined previously apply. However, the
necessary boundary conditions on the costate equations
are now

$$\lambda_x(t_{\textit{f}}) = -\frac{x}{r} + \nu u \Big|_{t_{\textit{f}}} \tag{41}$$

$$\lambda_y(t_{\textit{f}}) = -\frac{y}{r} + \nu v \Big|_{t_{\textit{f}}} \tag{42}$$

$$\lambda_u(t_{\textit{f}}) = \nu x \Big|_{t_{\textit{f}}} \tag{43}$$

$$\lambda_v(t_{\textit{f}}) = \nu y \Big|_{t_{\textit{f}}} \tag{44}$$

Eliminating the multiplier ν and considering the

19

orthogonality constraint Eq (19) yields the following set of boundary conditions to apply to the two point boundary value problem:

$$\underline{x}(t_o) \text{ Specified}$$

$$xu + yv = 0 \Big|_{t_1} \tag{45}$$

$$\lambda_v x - \lambda_u y = 0 \Big|_{t_1} \tag{46}$$

$$\lambda_x x + \frac{x^2}{r} - \lambda_u u = 0 \Big|_{t_1} \tag{47}$$

$$\lambda_y y + \frac{y^2}{r} - \lambda_v v = 0 \Big|_{t_1} \tag{48}$$

Again, these boundary conditions are independent at time t_1.

Maneuver with no Terminal Constraint

In some situations, the spacecraft may receive little warning of an attacker's approach. It may then be necessary for the spacecraft to travel as far away from the threat as possible in a specified time without regard for the final orientation of its velocity vector. In effect, this allows the target spacecraft to achieve the same radial distance change as achieved with a terminal constraint in a much shorter time period.

Maximum Radius Maneuver. The requirement of achieving maximum radius is still expressed by the function of Eq (20). In this case, however, the performance index to be

20

maximized is simply

$$J = r(t_4) \tag{49}$$

The system Hamiltonian is again given by Eq (22), so the bilinear tangent control law of Eq (23) applies. The Legendre-Clebsch condition demands the same definition of control angle, Eqs (25) and (26).

The costate equations are again given by Eqs (28) through (31), but the necessary boundary conditions on the costates are now

$$\lambda_x(t_4) = \frac{x}{r}\Big|_{t_4} \tag{50}$$

$$\lambda_y(t_4) = \frac{y}{r}\Big|_{t_4} \tag{51}$$

$$\lambda_u(t_4) = 0 \tag{52}$$

$$\lambda_v(t_4) = 0 \tag{53}$$

The boundary conditions on the λ_u and λ_v costates yield a singularity in the control angle β at the final time t_4, as seen from Eqs (23) through (26). This singularity is eliminated by applying L'Hôspital's rule to the bilinear tangent control law at the final time of the manuever. Combining the result with the costate equations (30) and (31), at the final time the control law becomes

21

$$\beta(t_1) = \tan^{-1}\left[\frac{\lambda_v}{\lambda_u}\right]_{t_1} = \tan^{-1}\left[\frac{\lambda_x}{\lambda_y}\right]_{t_1} \qquad (54)$$

The definitions of the control angle β must then be converted at the final time from Eqs (25) and (26) to

$$\cos\beta(t_1) = \frac{\lambda_x}{(\lambda_x^{\;2} + \lambda_y^{\;2})^{1/2}} \Big|_{t_1} \qquad (55)$$

$$\sin\beta(t_1) = \frac{\lambda_y}{(\lambda_x^{\;2} + \lambda_y^{\;2})^{1/2}} \Big|_{t_1} \qquad (56)$$

The Legendre-Clebsch condition is then satisfied at the final time as

$$\mathscr{H}_{\beta\beta}(t_1) = -\frac{T}{m_o - \dot{m}t} (\lambda_x^{\;2} + \lambda_y^{\;2})^{1/2} \Big|_{t_1} \qquad (57)$$

The two point boundary value problem is now given completely by the state equations (15) through (18) with the appropriate control definitions applied over the maneuver and at the final time, the costate equations (28) through (31), the boundary conditions on the costates at the final time, Eqs (50) through (53), and the specified states at the initial time.

22

Minimum Radius Maneuver. Again, the unconstrained
minimum radius maneuver is expressed as a maximum negative
radius maneuver, with the performance index written as

$$J = -r(t_1) \tag{58}$$

Noting that all necessary conditions derived for the
unconstrained maximum radius maneuver again apply, the
boundary conditions on the costates become

$$\lambda_x(t_1) = -\left.\frac{x}{r}\right|_{t_1} \tag{59}$$

$$\lambda_y(t_1) = -\left.\frac{y}{r}\right|_{t_1} \tag{60}$$

$$\lambda_u(t_1) = 0 \tag{61}$$

$$\lambda_v(t_1) = 0 \tag{62}$$

Once L'Hôspital's rule is applied to the control law as
in Eqs (54) through (56), the two point boundary value
problem is completely defined through the state equations
(15) through (18) using the appropriate control angle
substitution over the maneuver and at the final time, the
costate equations (28) through (31), the four boundary
conditions on the states at the initial time and the four
costate boundary conditions given above.

23

IV. Minimum Time Rendezvous Maneuvers

Once the target spacecraft has completed an evasive manevuer at time t_1, the concern is to return the spacecraft to its nominal orbit in a time optimal manner. Ideally, the point of rendezvous is the nominal geosynchronous position of the target spacecraft had it never performed the evasive maneuver.

Equations of Motion

The state equations (15) through (18) again govern the spacecraft motion with time. However, in order to numerically determine the final optimal time of the rendezvous maneuver over a fixed time interval, a change of variables is performed such that

$$t = c\tau \qquad (63)$$

where τ is defined over the interval $\tau = 0$ to $\tau = 1$. c is then a time parameter state with a constant value equal to t_f, the final time of the return maneuver. Applying the transformation

$$\frac{d(\ )}{d\tau} = c \frac{d(\ )}{dt} \qquad (64)$$

to the state equations yields the parameterized state equations:

24

$$x' = cu \tag{65}$$

$$y' = cv \tag{66}$$

$$u' = c\left[\frac{-\mu y}{r^3} + \frac{T}{m_o - \dot{m}t} \cos\beta \right] \tag{67}$$

$$v' = c\left[\frac{-\mu y}{r^3} + \frac{T}{m_o - \dot{m}t} \sin\beta \right] \tag{68}$$

where the prime symbol indicates differentiation with respect to τ. The time parameter adds an additional state equation:

$$c' = 0 \tag{69}$$

Assuming the rendezvous maneuver initiates immediately following completion of an evasion, the initial conditions given to the state variables $\underset{\sim}{x}(t_1)$ are the terminal state values determined at the final time of the avoidance maneuver.

Minimum Time Maneuver

The rendezvous is performed in minimum time, such that the performance index is written from Eq (2) as

$$J = \int_{t_1}^{t_f} 1 \, dt \tag{70}$$

Applying Eq (64) to the above yields the transformed

25

performance index

$$J = \int_0^1 c d\tau \qquad (71)$$

At the final time of the return maneuver, constraints are placed on each of the state variables such that the spacecraft motion matches exactly that of the nominal orbit:

$$\psi_x(t_f) = x(t_f) - x_{NOM}(t_f) \qquad (72)$$

$$\psi_y(t_f) = y(t_f) - y_{NOM}(t_f) \qquad (73)$$

$$\psi_u(t_f) = u(t_f) - u_{NOM}(t_f) \qquad (74)$$

$$\psi_v(t_f) = v(t_f) - v_{NOM}(t_f) \qquad (75)$$

where the nominal orbit states are given parametrically as

$$x_{NOM} = r_o \cos\left\{ \frac{v_o}{r_o} \left[t + (t_1 - t_o) \right] \right\} \qquad (76)$$

$$y_{NOM} = r_o \sin\left\{ \frac{v_o}{r_o} \left[t + (t_1 - t_o) \right] \right\} \qquad (77)$$

$$u_{NOM} = -v_o \sin\left\{ \frac{v_o}{r_o} \left[t + (t_1 - t_o) \right] \right\} \qquad (78)$$

26

$$v_{NOM} = v_o \cos\left\{ \frac{v_o}{r_o} \left[t + (t_1 - t_o) \right] \right\} \qquad (79)$$

In these equations, r_o is the radius of the nominal geosynchronous orbit, v_o is the nominal circular speed, and $(t_1 - t_o)$ is the time of flight of the original evasive maneuver.

Again parameterizing time as done for the performance index, the nominal orbit equations become

$$x_{NOM} = r_o \cos\left\{ \frac{v_o}{r_o} \left[c\tau + (t_1 - t_o) \right] \right\} \qquad (80)$$

$$y_{NOM} = r_o \sin\left\{ \frac{v_o}{r_o} \left[c\tau + (t_1 - t_o) \right] \right\} \qquad (81)$$

$$u_{NOM} = -v_o \sin\left\{ \frac{v_o}{r_o} \left[c\tau + (t_1 - t_o) \right] \right\} \qquad (82)$$

$$v_{NOM} = v_o \cos\left\{ \frac{v_o}{r_o} \left[c\tau + (t_1 - t_o) \right] \right\} \qquad (83)$$

The constraints of Eqs (72) through (75) are then evaluated at the final time $\tau = 1$.

Adjoining the constraint equations to the performance index of Eq (71) leads to an expression to be minimized:

27

$$J = \left[\nu_x(x - x_{NOM}) + \nu_y(y - y_{NOM}) + \nu_u(u - u_{NOM}) \right.$$

$$\left. + \nu_v(v - v_{NOM}) \right]\Big|_{\tau=1} + \int_0^1 c\,d\tau \quad (84)$$

The system Hamililtonian is now assembled as in Eq (5):

$$\mathscr{H} = c\left\{ 1 + \lambda_x u + \lambda_y v + \lambda_u \left[\frac{-\mu x}{r^3} + \frac{T}{m_o - \dot{m}t} \cos\beta \right] \right.$$

$$\left. + \lambda_v \left[\frac{-\mu y}{r^3} + \frac{T}{m_o - \dot{m}t} \sin\beta \right] \right\} \quad (85)$$

The performance index J is again given a stationary value subject to the optimality condition of Eq (9). As pertained to the evasive maneuvers, the bilinear tangent control law applies, but the thrust control angle definition changes such that

$$\beta = \tan^{-1}\left[\frac{-\lambda_v}{-\lambda_u} \right] \quad (86)$$

This change is attributed to the Legendre-Clebsch condition, which, from Eq (14), for a minimization problem requires

$$\mathscr{H}_{\beta\beta} = -c\left[\lambda_u \frac{T}{m_o - \dot{m}t} \cos\beta + \lambda_v \frac{T}{m_o - \dot{m}t} \sin\beta \right] \geq 0 \quad (87)$$

28

To satisfy this condition, the thrust control angle must be appropriately defined in the state equations (65) through (68) as:

$$\cos\beta = -\frac{\lambda_u}{\sqrt{\lambda_u^2 + \lambda_v^2}} \tag{88}$$

$$\sin\beta = -\frac{\lambda_v}{\sqrt{\lambda_u^2 + \lambda_v^2}} \tag{89}$$

thus yielding the control law given in Eq (86) and satisfying the Legendre-Clebsch condition as

$$\mathcal{H}_{\beta\beta} = \frac{T}{m_o - \dot{m}t}\sqrt{\lambda_u^2 + \lambda_v^2} \tag{90}$$

The costate equations are transformed from those of Eqs (28) through (31) as

$$\lambda_x' = c\left\{\lambda_u\left[\frac{\mu}{r^3} - \frac{3\mu x^2}{r^5}\right] - \lambda_v\left[\frac{3\mu xy}{r^5}\right]\right\} \tag{91}$$

$$\lambda_y' = c\left\{\lambda_v\left[\frac{\mu}{r^3} - \frac{3\mu y^2}{r^5}\right] - \lambda_u\left[\frac{3\mu xy}{r^5}\right]\right\} \tag{92}$$

$$\lambda_u' = -c\lambda_x \tag{93}$$

$$\lambda_v{}' = -c\lambda_y \qquad (94)$$

The boundary conditions on the costates at the final time are given by Eq (11) as constant multipliers:

$$\underset{\sim}{\lambda}(\tau=1) = \underset{\sim}{\nu} \qquad (95)$$

Since these multipliers are unknown, boundary conditions on the states at the final time of the rendezvous are recovered from the constraint equations (72) through (75) as

$$x - x_{NOM} \bigg|_{\tau=1} = 0 \qquad (96)$$

$$y - y_{NOM} \bigg|_{\tau=1} = 0 \qquad (97)$$

$$u - u_{NOM} \bigg|_{\tau=1} = 0 \qquad (98)$$

$$v - v_{NOM} \bigg|_{\tau=1} = 0 \qquad (99)$$

An additional boundary condition is provided by the transversality condition Eq (12) to allow determination of the time parameter c:

30

$$\mathcal{K}(\tau=1) + \left[\lambda_x y_{NOM} - \lambda_y x_{NOM} + \lambda_u v_{NOM} \right.$$

$$\left. - \lambda_v u_{NOM} \right]\Big|_{\tau=1} \frac{v_o}{r_o} = 0 \quad (100)$$

where the Hamiltonian $\mathcal{K}$ is given by Eq (85) and the nominal orbit states are given by Eqs (76) through (79). It should again be noted that the final time t_f corresponds to a value of $\tau = 1$. Additionally, the constant Lagrange multipliers $\underset{\sim}{v}$ were eliminated from Eq (100) by applying boundary conditions on the costates given by Eq (95).

Thus, the two point boundary value problem is completely defined by the state equations (65) through (68), the costate equations (91) through (94), four boundary conditions specifying the initial state at t_i, four boundary conditions on the final state at t_f, and the transversality condition of Eq (99).

V. Verification of Fixed Time Solutions

Since the maximum radius evasive maneuvers yield
optimal trajectories over a specified time, the two point
boundary value problem describing a minimum time intercept
of a specified radius should ideally generate an identical
solution. The formulation of the time optimal intercept is
similar to that of the rendezvous problem, and it provides a
convenient means of verifying the evasive maneuver control
history.

Maneuver with Terminal Constraint

The requirement of intercepting a specified orbit
radius at the final time of the maneuver t_1 is expressed
through the constraint function

$$\psi_1[t_1, x(t_1)] = x(t_1)^2 + y(t_1)^2 - r(t_1)^2 \qquad (101)$$

where $r(t_1)$ is the maximized orbital radius achieved in the
evasive maneuver. Similarly, the orthogonality requirement
is defined through the constraint

$$\psi_2[t_1, x(t_1)] = xu + yv \Big|_{t_1} \qquad (102)$$

By adjoining the constraint equations (101) and (102) to the
minimum time performance index , Eq (71), with a pair of

multipliers $\underset{\sim}{\nu}$, the two point boundary value problem is developed to minimize the new performance index

$$J = \nu_1(x^2 + y^2 - r^2)\Big|_{\tau=1} + \nu_2(xu + yv)\Big|_{\tau=1} + \int_0^1 c\,d\tau \qquad (103)$$

where time has been parameterized through Eq (64).

Since the formulation of the intercept problem pertains to minimum time, the state equations (65) through (68), Hamiltonian Eq (85), control law Eq (86), Legendre-Clebsch condition Eq (87), control angle definitions Eqs (88) and (89), and costate equations (91) through (94) of the rendezvous problem apply. However, the necessary boundary conditions on the costates at the final time t_1, are changed to give, from Eq (11)

$$\lambda_x(\tau=1) = 2\nu_1 x + \nu_2 u \qquad (104)$$

$$\lambda_y(\tau=1) = 2\nu_1 y + \nu_2 v \qquad (105)$$

$$\lambda_u(\tau=1) = \nu_2 x \qquad (106)$$

$$\lambda_v(\tau=1) = \nu_2 y \qquad (107)$$

Since the final time of the maneuver is unspecified, an additional boundary condition is formulated through the

33

transversality condition of Eq (12) as

$$\mathcal{H}(\tau=1) = 0 \qquad\qquad (108)$$

where the Hamiltonian is again given by Eq (85).

Eliminating the multipliers ν in the costate boundary
conditions and recovering the remaining boundary conditions
from the constraint equations (101) and (102) results in a
set of boundary conditions implemented to solve the two
point boundary value problem. These conditions are

$$\underset{\sim}{x}(\tau=0) \text{ Specified}$$

$$xu + yv = 0 \Big|_{\tau=1} \qquad\qquad (109)$$

$$x^2 + y^2 - r^2 = 0 \Big|_{\tau=1} \qquad\qquad (110)$$

$$\lambda_u y - \lambda_v x = 0 \Big|_{\tau=1} \qquad\qquad (111)$$

$$x(x\lambda_y - v\lambda_u) + y(u\lambda_u - x\lambda_x) = 0 \Big|_{\tau=1} \qquad\qquad (112)$$

and the transversality condition Eq (108). Note that Eqs
(111) and (112) are not the only means of combining the
costate equations to eliminate the multipliers ν. In
general, the form of the boundary conditions is not unique,
but the conditions must be independent.

34

The two point boundary value problem is now completely defined by the state equations (65) through (68), with initial conditions specified at the starting point of the evasive maneuver, the costate equations (91) through (94), the transversality condition Eq (108), and the boundary conditions Eqs (109) through (112). The control angle definition of Eqs (88) and (89) apply to the state equations.

Maneuver with no Terminal Constraint

To verify the unconstrained maximum radius maneuvers, the orthogonality constraint is removed from Eq (103) to give the performance index

$$J = \nu_1(x^2 + y^2 - r^2)\Big|_{\tau=1} + \int_0^1 c\,d\tau \qquad (113)$$

Again, the Hamiltonian of Eq (85), control law Eq (86), Legendre-Clebsch condition (87), control angle definitions Eqs (88) and (89), and costate equations (91) through (94) of the rendezvous problem apply. In this case, the necessary boundary conditions on the costates at the final time t_1, or $\tau = 1$, are derived from Eq (11) as

$$\lambda_x(\tau=1) = 2\nu_1 x \qquad (114)$$

$$\lambda_y(\tau=1) = 2\nu_1 y \qquad (115)$$

35

$$\lambda_u(\tau=1) = 0 \tag{116}$$

$$\lambda_v(\tau=1) = 0 \tag{117}$$

As was found for the unconstrained maximum radius maneuvers, the boundary conditions on the λ_u and λ_v costates yield a singularity in the control law of Eq (86) at the final time. Applying L'Hôspital's rule and the costate equations (93) and (94), the control law at t_1 can be found as

$$\beta(\tau=1) = \tan^{-1}\left[\frac{-\lambda_v}{-\lambda_u} \right]_{\tau=1} = \tan^{-1}\left[\frac{-\lambda_x}{-\lambda_y} \right]_{\tau=1} \tag{118}$$

which, when combined with the Legendre-Clebsch condition, gives the following control angle definitions applicable to the state equations at the final time:

$$\cos\beta(\tau=1) = \frac{-\lambda_x}{(\lambda_u^2 + \lambda_v^2)^{1/2}} \bigg|_{\tau=1} \tag{119}$$

$$\sin\beta(\tau=1) = \frac{-\lambda_y}{(\lambda_u^2 + \lambda_v^2)^{1/2}} \bigg|_{\tau=1} \tag{120}$$

thus satisfying the Legendre-Clebsch condition at $\tau = 1$ as

36

$$\mathcal{H}_{\beta\beta}(\tau=1) = \frac{T}{m_o - \dot{m}t} \left. (\lambda_x{}^2 + \lambda_y{}^2)^{1/2} \right|_{\tau=1} \geq 0 \qquad (121)$$

The two point boundary value problem is now completely defined as for the constrained intercept maneuver, with the exception of directly applying the costate boundary conditions (114) through (117) and converting the control angle definitions to those of Eqs (119) and (120) at the final time.

VI. Method of Solution

The formulation of the two point boundary value problem using optimal control theory produces a set of nonlinear ordinary differential equations which must be solved by numerical methods. Each of the two point boundary value problems developed previously were solved directly using the IMSL routine DVCPR. The algorithm applied in DVCPR is a variable order, variable step size finite difference method with deferred corrections, based upon Lentini and Pereyra's PASVA3 program (12:67-88). DVCPR solves two point boundary value problems over a fixed time interval, thus the transformation over the interval $\tau = 0$ to $\tau = 1$ applied in the minimum time maneuvers.

As shown by Carnahan, Luther and Wilkes (6:405-506), no known numerical methods exist to guarantee a solution for a given boundary value problem. Bryson and Ho (4:214-215) additionally comment that small errors in guessing initial conditions often produce extremely volatile state space trajectories, wherein the values of the states and costates may well exceed the computer's numerical limits. The greatest difficulty in producing an accurate solution to a well-posed two point boundary value problem is then to provide the algorithm with a trial solution suitably close to satisfying the differential equations and boundary conditions.

VI. Method of Solution

The formulation of the two point boundary value problem using optimal control theory produces a set of nonlinear ordinary differential equations which must be solved by numerical methods. Each of the two point boundary value problems developed previously were solved directly using the IMSL routine DVCPR. The algorithm applied in DVCPR is a variable order, variable step size finite difference method with deferred corrections, based upon Lentini and Pereyra's PASVA3 program (12:67-88). DVCPR solves two point boundary value problems over a fixed time interval, thus the transformation over the interval $\tau = 0$ to $\tau = 1$ applied in the minimum time maneuvers.

As shown by Carnahan, Luther and Wilkes (6:405-506), no known numerical methods exist to guarantee a solution for a given boundary value problem. Bryson and Ho (4:214-215) additionally comment that small errors in guessing initial conditions often produce extremely volatile state space trajectories, wherein the values of the states and costates may well exceed the computer's numerical limits. The greatest difficulty in producing an accurate solution to a well-posed two point boundary value problem is then to provide the algorithm with a trial solution suitably close to satisfying the differential equations and boundary conditions.

The IMSL routine DVCPR demands input of an initial grid
to begin Newtonian iteration on estimates of unspecified
initial or terminal conditions in order to satisfy the
differential equations and specified boundary conditions.
This grid consists of trial state and costate trajectories
over the entire time interval of a maneuver. The input grid
for the maximum radius maneuver with the orthogonality
constraint applied at a final time of six hours was
constructed first, since output for a similar maneuver was
available from the work of Preissinger (13). Curvefits with
time over both the states and the costates of Preissinger's
solution provided a suitable grid allowing DVCPR to converge
upon a solution. The form in which the final boundary
conditions were specified was also a consideration since,
by trial and error, some forms were found to be more
conducive to convergence than others. For maximum radius
maneuvers over the two hour and four hour times of flight
with the orthogonality constraint applied at the final time,
the six hour grid was scaled over the appropriate time
interval before input to achieve a converged solution.
Sample subroutines called by DVCPR for these maneuvers are
listed in appendix A.

Maximum radius maneuvers with no constraint at the
final time were considered next, since these involved merely
eliminating portions of the final boundary conditions
specified in the previous maneuver. The input grid for

each time of flight was the output for the same time of
flight with the tangency constraint applied at the final
time. Appendix B contains subroutines called by DVCPR for
these maneuvers.

A similar procedure was followed for the minimum radius
maneuvers. Again, the grid input to the algorithm was the
output grid for the same time of flight from the maximum
radius maneuver with the corresponding constraints at the
final time, an orthogonality constraint or no constraint.

For the minimum time intercept maneuvers used to
confirm the maximum radius results, the grid was normalized
over time to achieve convergence. Additionally, due to the
change in control angle definition derived from the
Legendre-Clebsch condition, a change in sign of two of the
costates was required. Again, boundary conditions were a
consideration in that the form they were written in
influenced the ability of DVCPR to produce a converged
solution.

Rendezvous maneuvers, however, posed a difficulty since
the states were shifted greatly from those found in the
evasive maneuvers. In this case, the input grid consisted
of states approximated in the appropriate nominal orbit
position, and costates output from the solution of the
minimum time intercept maneuvers. The rendezvous position
was initially specified as a stationary point on the nominal
orbit. A continuation scheme was then applied such that the

final boundary conditions were moved from a stationary position to the moving nominal orbit. For these maneuvers, DVCPR called subroutines given in appendix C.

Overall, reasonable state trajectories were fairly easily determined from any input. The costate trajectories, however, did indeed require an input grid very close to the true solution for convergence to be achieved, as discussed in the results.

VII. Results

Results were calculated for a nominal 2400 kilogram
spacecraft propelled by ten 30 centimeter diameter primary
propulsion electric thrusters normally used for satellite
stationkeeping or interplanetary spaceflight. The
propulsion system delivers 1.3 Newton total thrust, with a
total mass flow rate of 6.9×10^{-5} kilogram per second
(11:14-19).

Numerical solutions for each optimal control problem
were generated using the IMSL routine DVCPR on the ASC
VAX-11/785 system. All optimal trajectories were determined
to an accuracy within a range of 10^{-11} to 10^{-12}, as
specified by the tolerance parameter internal to the IMSL
routine DVCPR. The grid sizes required by DVCPR for
convergence varied between 200 and 300 subintervals for the
evasive maneuvers. Rendezvous maneuvers, on the other hand,
required grid sizes on the order of 300 to 600 subintervals.
The small tolerance parameter and large grid sizes give an
indication of the quality of the solution.

Control Histories and State Trajectories

For all maneuvers with a specified terminal time, two,
four and six hour times of flight were considered. During
these fixed time maneuvers, the nominal orbit traveled
one-twelfth, one-sixth and one-quarter of a geosynchronous
orbit. Each maneuver consumed less than 0.1 percent of the

total fuel mass allotted to the spacecraft, such that the
target spacecraft could maneuver over the entire design
lifetime of the propulsion system, if necessary.

Evasive Maneuver with Terminal Constraint. Figures 3,
4 and 5 show the thrust vector control histories for two,
four and six hour time of flight maneuvers, respectively, to
a maximum orbit radius with the orthogonality constraint
applied at the final time. The two and four hour thrust
angle profiles show similar control characteristics; the
spacecraft initially thrusts into the first quadrant to
increase its radial position, as expected. Note, however,
that the terminal control angle is in the third quadrant, in
effect reversing the thrust direction to achieve
orthogonality at the final time of the maneuver. The
control angle behaves in a different manner over a six hour
time of flight. Initially, the spacecraft thrusts into the
second quadrant, anticipating its terminal position nearly a
quarter orbit away. The thrust angle gimbals in a direction
opposite to that of the two and four hour time of flight
maneuvers, and is directed nearly along the negative y-axis
at the final time in order to achieve orthogonality.

For all three constrained evasive maneuvers, the
control characteristic of reversing thrust direction to
satisfy the tangency constraint at the final time shapes the
maneuver over the entire time of flight. This shaping
adversely affects the increase in orbit radius achieved at

43

Figure 3. Thrust Control Angle vs Time for 2 Hour Time of
Flight to Maximum Radius with Orthogonality Constraint

44

Figure 4. Thrust Control Angle vs Time for 4 Hour Time of
Flight to Maximum Radius with Orthogonality Constraint

45
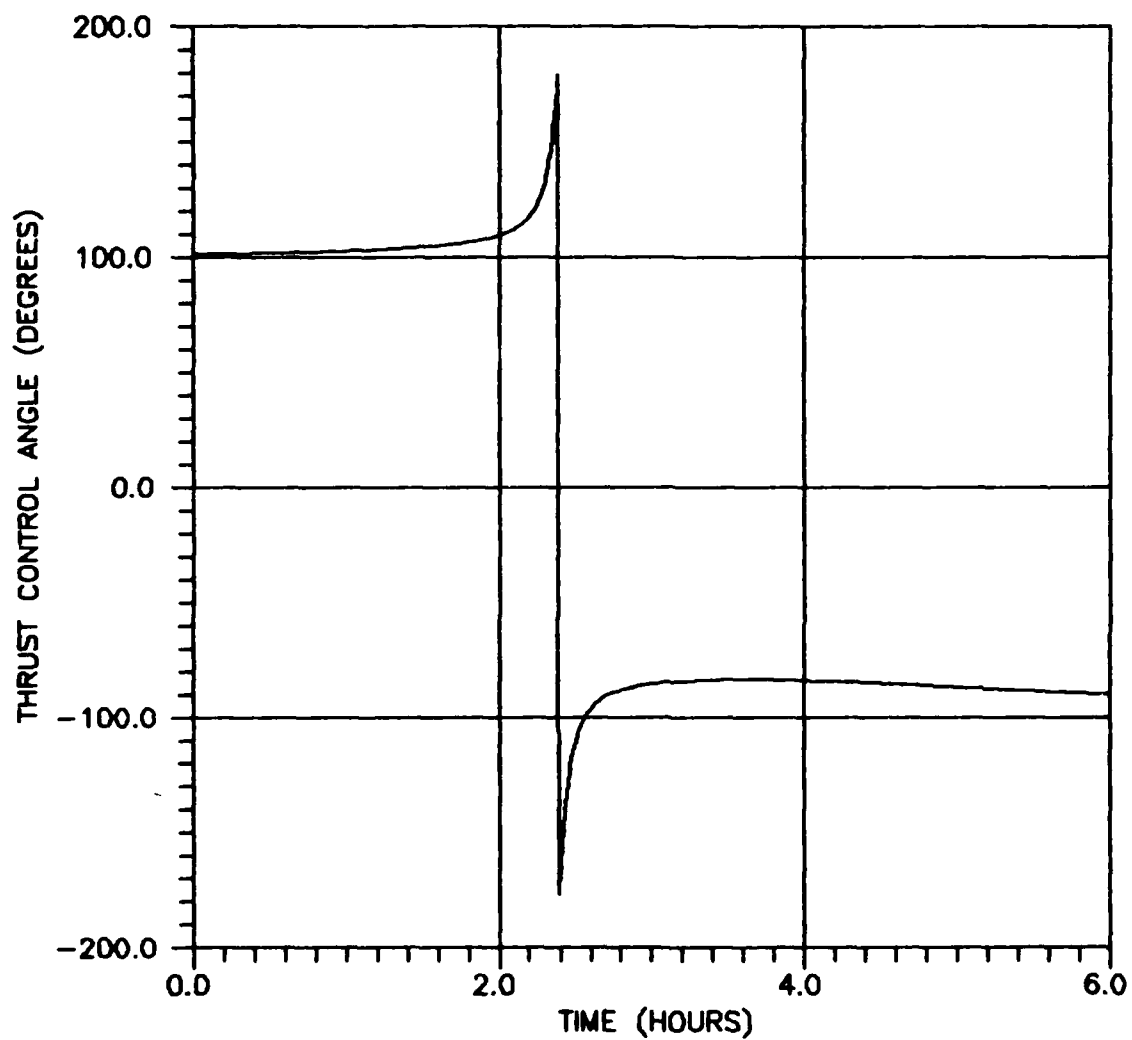
Figure 5.   Thrust Control Angle vs Time for 6 Hour Time of
Flight to Maximum Radius with Orthogonality Constraint

the final time, as will be seen in the discussion of the
unconstrained evasive maneuver. The six hour evasive
maneuver also shows a unique feature in that it terminates
on the +y-axis, on the same radius vector as the nominal
orbit and thus retaining the nominal orbit period. In
contrast, the two and four hour maneuvers achieve
a greater relative increase in orbit radius at the expense
of orbit drift, an expected phenomenon wherein the orbital
period of a spaceflight trajectory increases with increasing
orbit radius. As a result, at the terminal time of the two
and four hour evasive maneuvers, the target spacecraft's
motion lags behind the nominal orbit. The effect herein is
evidenced in the slight radial distance benefit gained by
increasing the time of flight from four to six hours, as
opposed to the great amount gained by increasing the time of
flight from two to four hours. Table I summarizes the
distance increases achieved in the radial direction for each
time of flight.

Table I. Radial Increase for Maximum Radius
Evasive Maneuver with Terminal Constraint

Time of Flight (hrs)	Radial Increase (km)
2	14.1825
4	64.4491
6	71.6190

For the purpose of verifying boundary conditions and the
orthogonality constraint, Tables II and III give the
terminal position and velocity states of the target
spacecraft upon completion of the evasive maneuver.

Table II. Terminal Position States for Maximum Radius
Evasive Maneuver with Terminal Constraint

Time of Flight (hrs)	x (km)	y (km)
2	36600.8575	21116.0609
4	21216.5804	36600.7937
6	0.0	42312.7415

Table III. Terminal Velocity States for Maximum Radius
Evasive Maneuver with Terminal Constraint

Time of Flight (hrs)	u (km/s)	v (km/s)
2	-1.5335	2.6580
4	-2.6501	1.5362
6	-3.0691	0.0

Figures 6, 7 and 8 illustrate the control histories of
minimum radius evasive maneuvers for two, four and six hour
times of flight, respectively. Each thrust angle profile
shows the same characteristics as the parallel maximum
radius control history, however the control angle is shifted
by 180 degrees. This shift results in nearly identical
changes in orbit radius at the terminal time, but in a
radially opposite direction. Table IV lists the results.

48
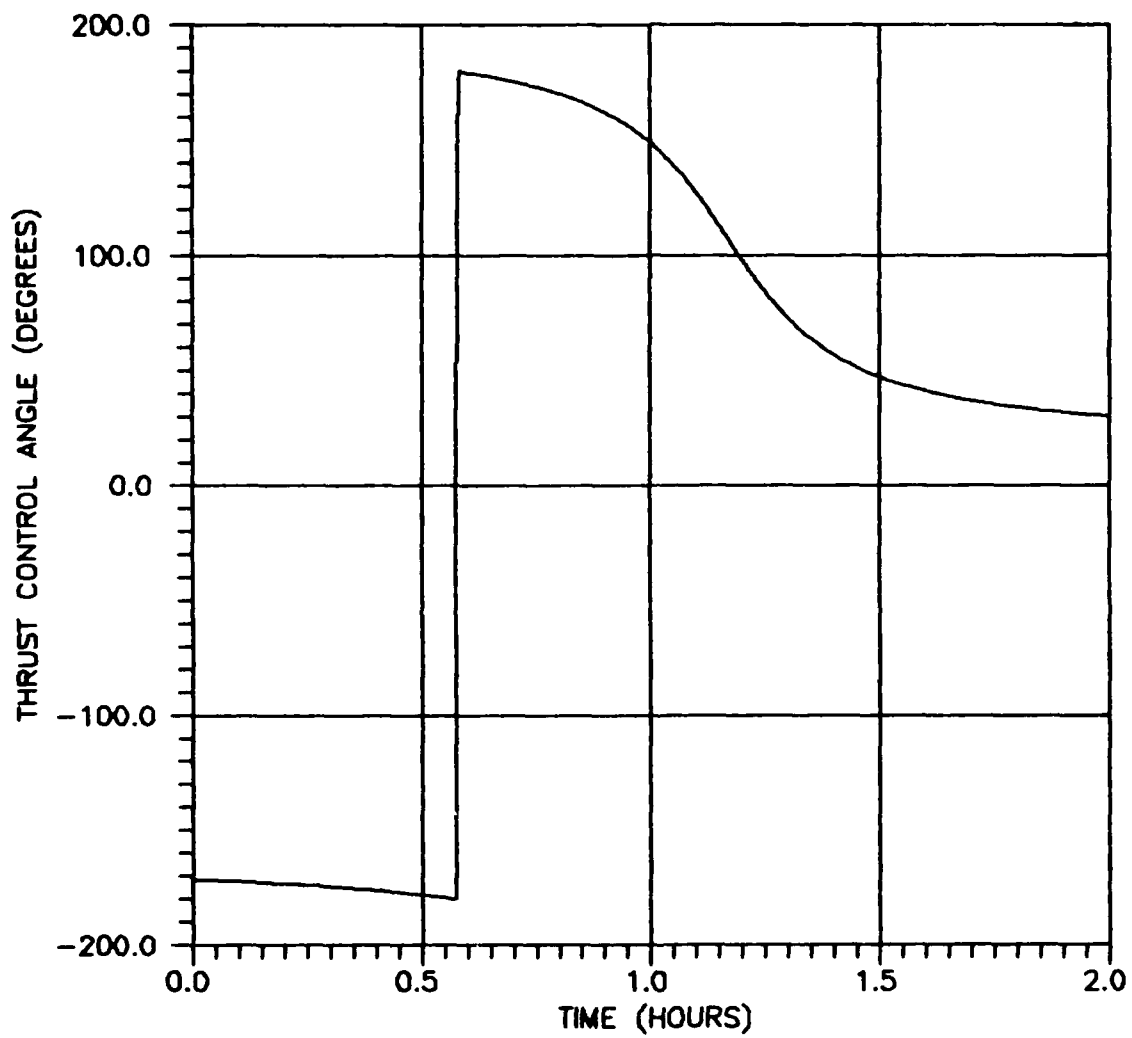
Figure 6. Thrust Control Angle vs Time for 2 Hour Time of Flight to Minimum Radius with Orthogonality Constraint
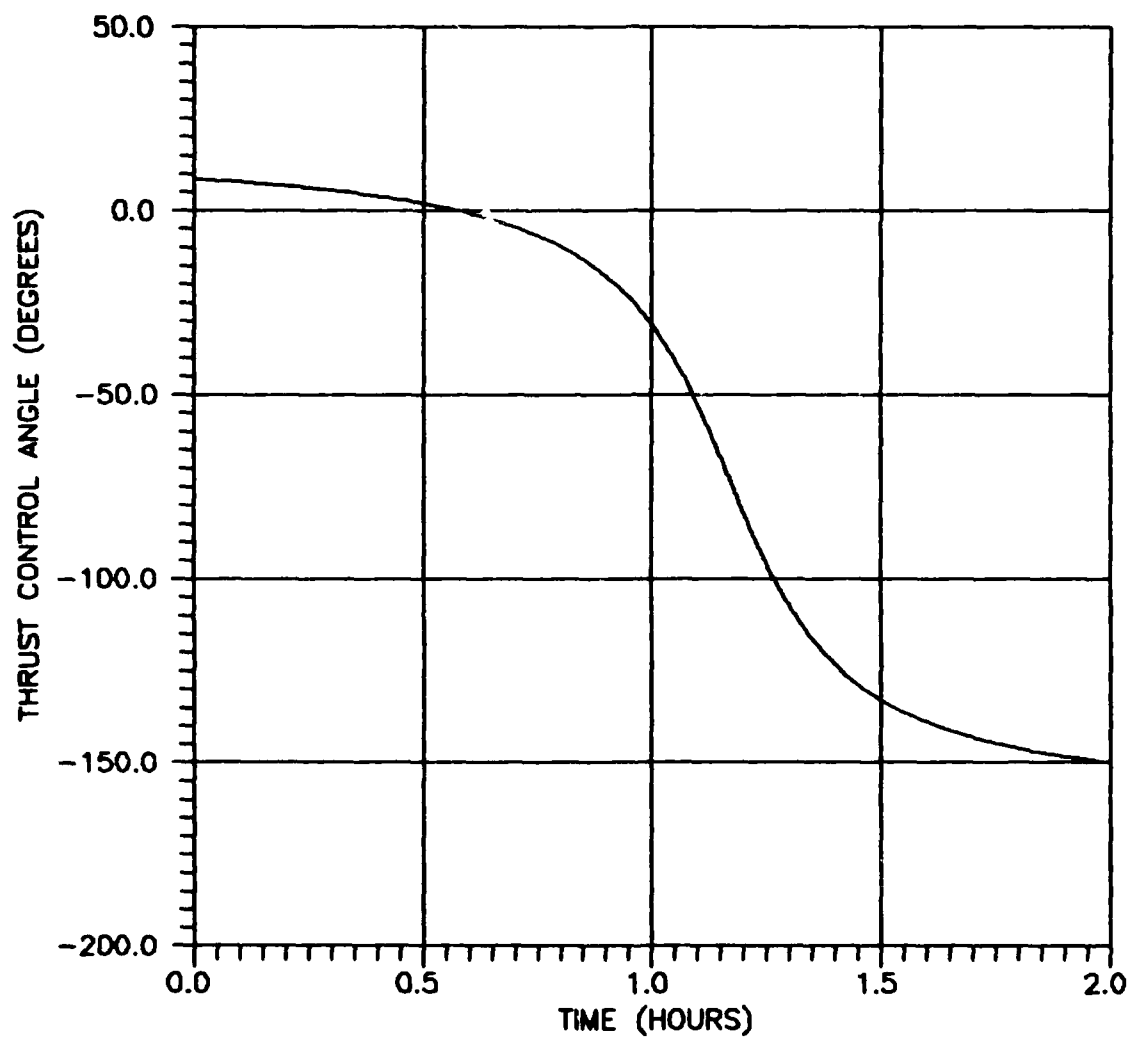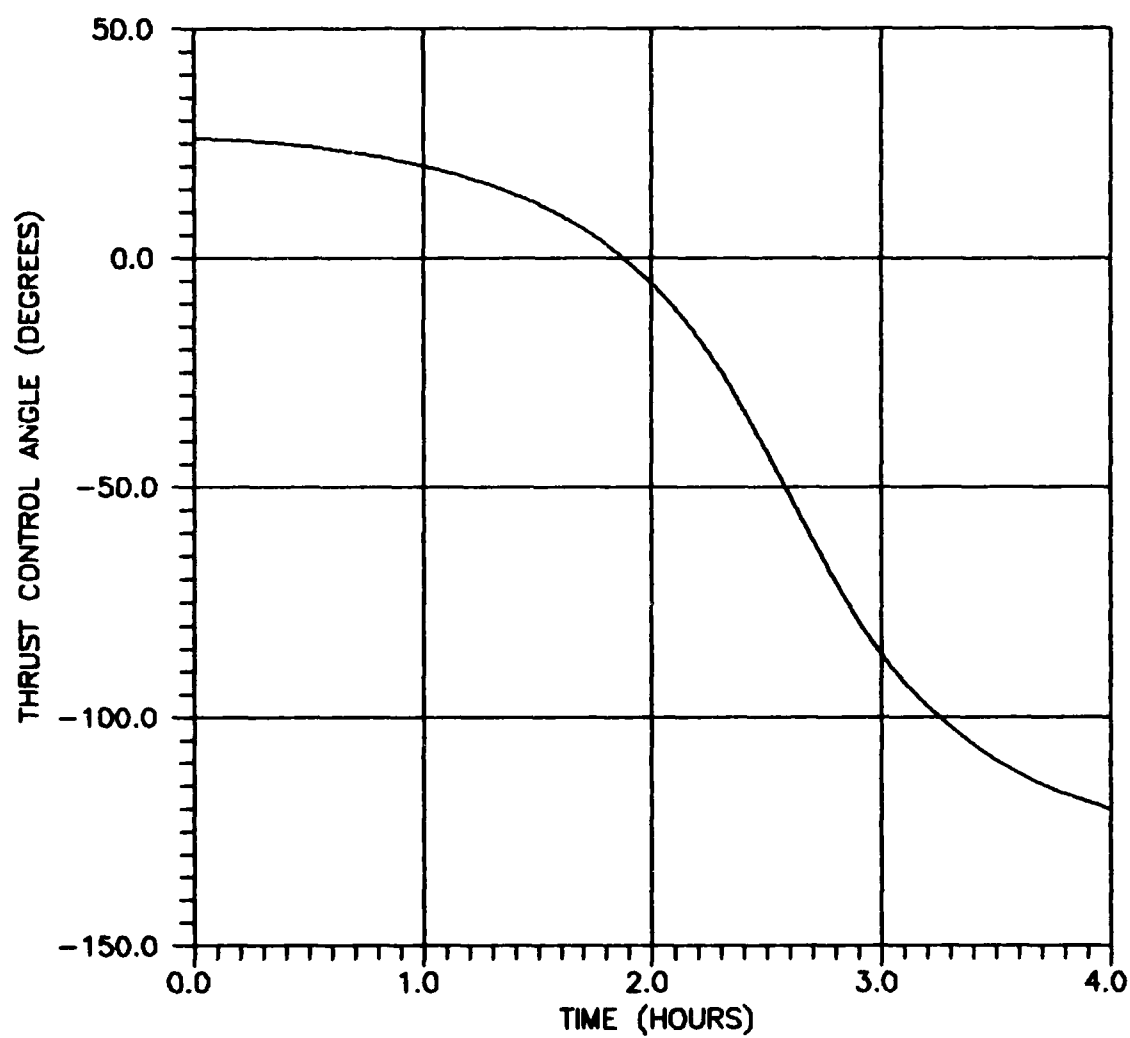
49

Figure 7. Thrust Control Angle vs Time for 4 Hour Time of Flight to Minimum Radius with Orthogonality Constraint

Figure 8.   Thrust Control Angle vs Time for 6 Hour Time of Flight to Minimum Radius with Orthogonality Constraint

51

Table IV. Radial Decrease for Minimum Radius
Evasive Maneuver with Terminal Constraint

Time of Flight (hrs)	Radial Decrease (km)
2	14.1632
4	64.5499
6	72.0168

The final position and velocity states for the constrained

minimum radius maneuver are given in Tables V and VI.

Table V. Terminal Position States for Minimum Radius
Evasive Maneuver with Terminal Constraint

Time of Flight (hrs)	x (km)	y (km)
2	36562.9713	21124.9903
4	21204.5345	36562.7162
6	0.0	42169.1057

Table VI. Terminal Velocity States for Minimum Radius
Evasive Maneuver with Terminal Constraint

Time of Flight (hrs)	u (km/s)	v (km/s)
2	-1.5384	2.6626
4	-2.6705	1.5356
6	-3.0747	0.0

Evasive Maneuver with no Terminal Constraint. The

thrust angle profiles with time for the two, four and six

hour time of flight maneuvers to a maximum orbit radius

without terminal constraint are shown in Figures 9, 10 and

ll, respectively. Due to the lack of the constraint-imposed
shaping effect, the control histories differ significantly
from those of the maneuver enforcing the terminal
orthogonality constraint. Note that the thrust control
angle is confined to thrusting nearly in the radial
direction over the entire maneuver for the two hour and four
hour times of flight. During the six hour time of flight,
however, the thrust angle is directed into the second
quadrant, towards a terminal position again on the +y-axis.
Additionally, the two and four hour time of flight maneuvers
again show an increased orbit period at their termination,
while orbit drift is eliminated over the six hour time of
flight maneuver. The effect of the terminal position upon
the radial increases in distance obtained is similar to that
of the maneuver with the terminal orthogonality constraint,
but the target spacecraft travels a much greater radial
distance, as Table VII shows.

Table VII. Radial Increase for Maximum Radius
Evasive Maneuver with no Terminal Constraint

Time of Flight (hrs)	Radial Increase (km)
2	26.5151
4	116.4321
6	259.0089

Tables VIII and IX illustrate the terminal orientation of
the target craft upon completion of the unconstrained

53

Figure 9. Thrust Control Angle vs Time for 2 Hour Time of Flight to Maximum Radius with no Terminal Constraint
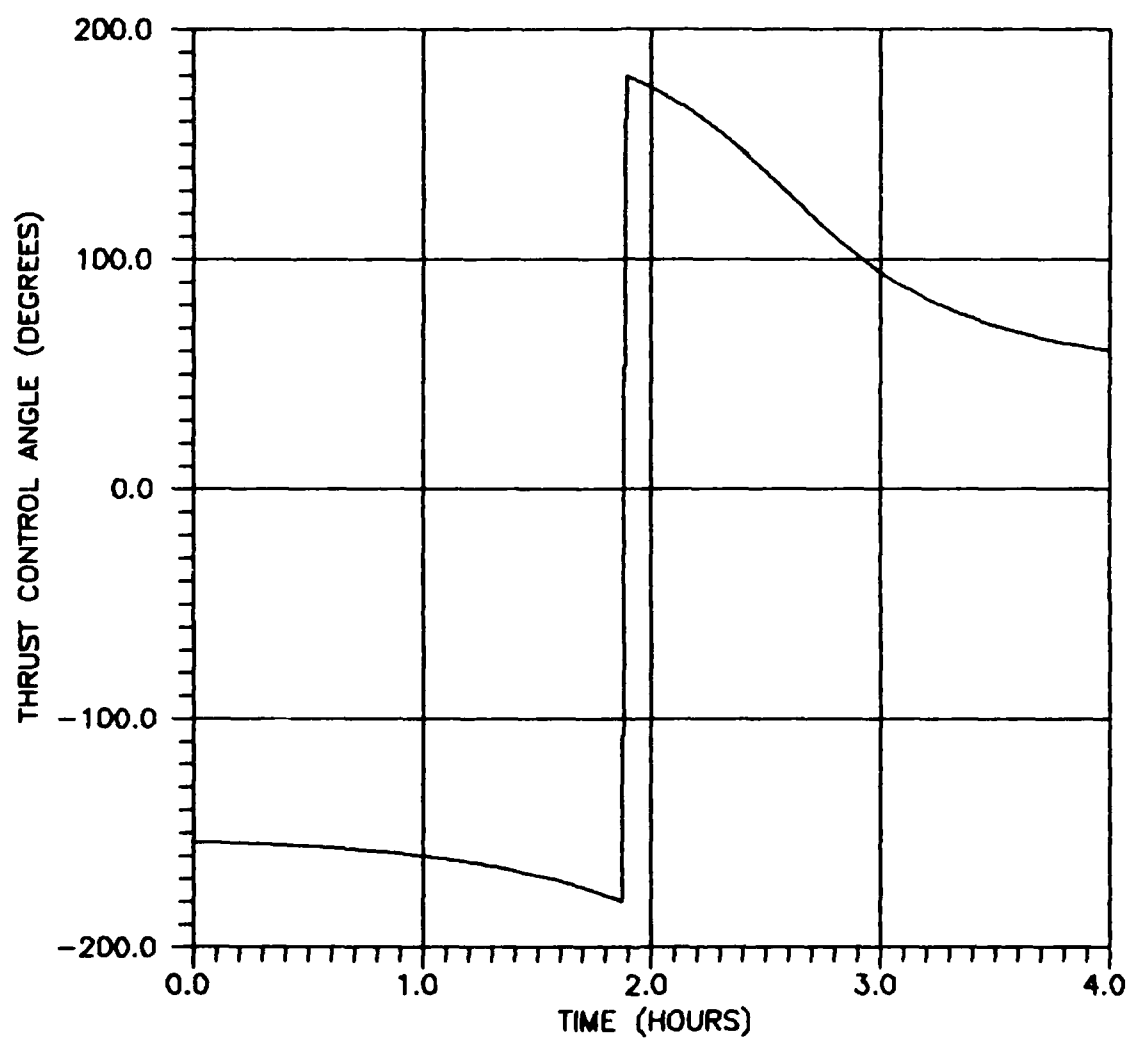
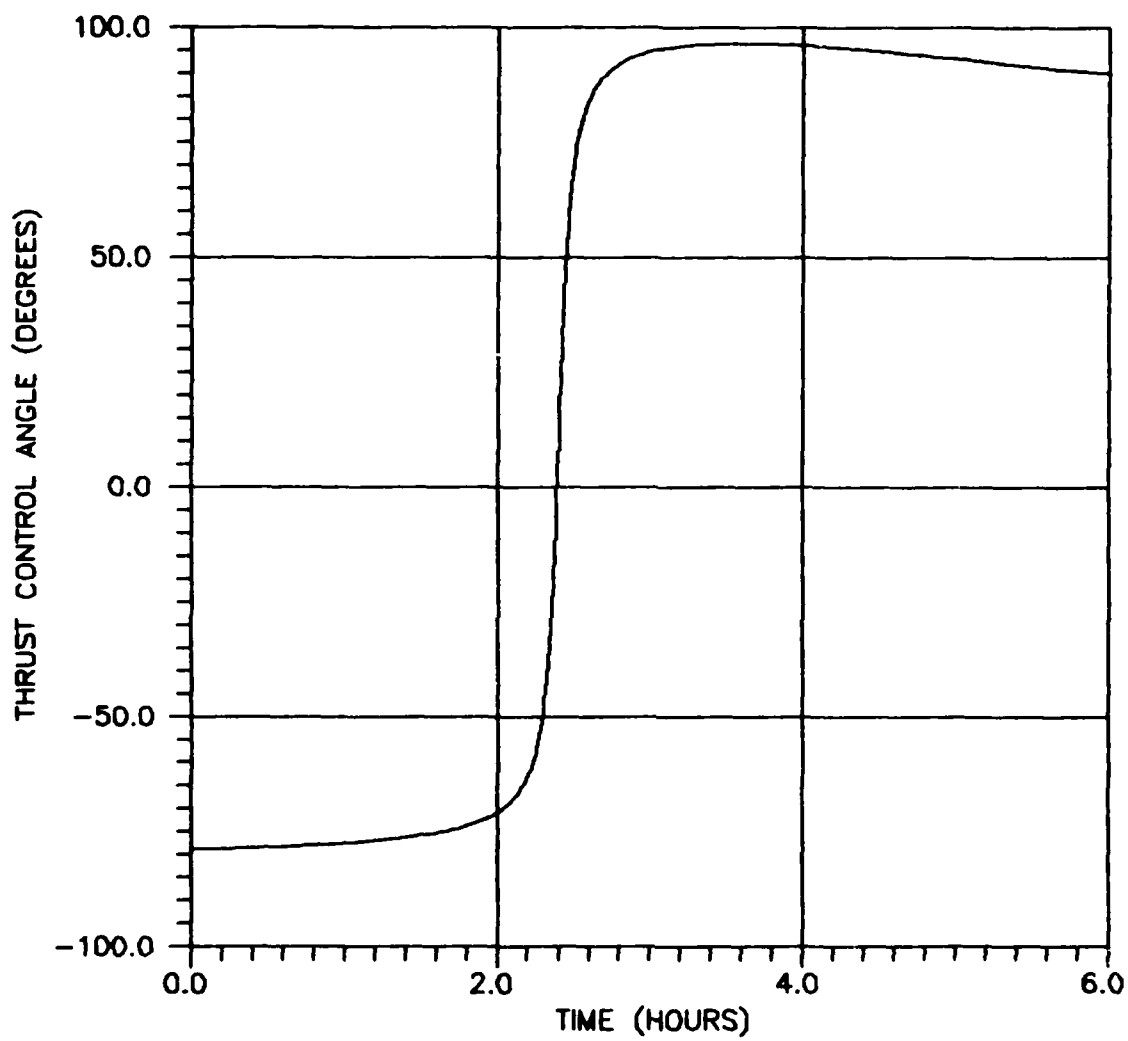Figure 10.   Thrust Control Angle vs Time for 4 Hour Time of Flight to Maximum Radius with no Terminal Constraint

Figure 11. Thrust Control Angle vs Time for 6 Hour Time of Flight to Maximum Radius with no Terminal Constraint

maximum radius maneuver. Note the orientation of the
spacecraft velocity vector in the radially outward
direction.

Table VIII. Terminal Position States for Maximum Radius
Evasive Maneuver with no Terminal Constraint

Time of Flight (hrs)	x (km)	y (km)
2	36605.1947	21133.2181
4	21194.0656	36673.8873
6	0.0	42500.1314

Table IX. Terminal Velocity States for Maximum Radius
Evasive Maneuver with no Terminal Constraint

Time of Flight (hrs)	u (km/s)	v (km/s)
2	-1.5292	2.6640
4	-2.6488	1.5513
6	-3.0710	0.0323

The corresponding control histories for the two, four
and six hour time of flight maneuvers to a minimum radius
with no constraint at the final time are illustrated in
Figures 12, 13 and 14. Again, for each time of flight, the
thrust angle profile is nearly identical to its maximum
radius counterpart, but shifted by 180 degrees. The
resulting changes in radial distance are then only in a
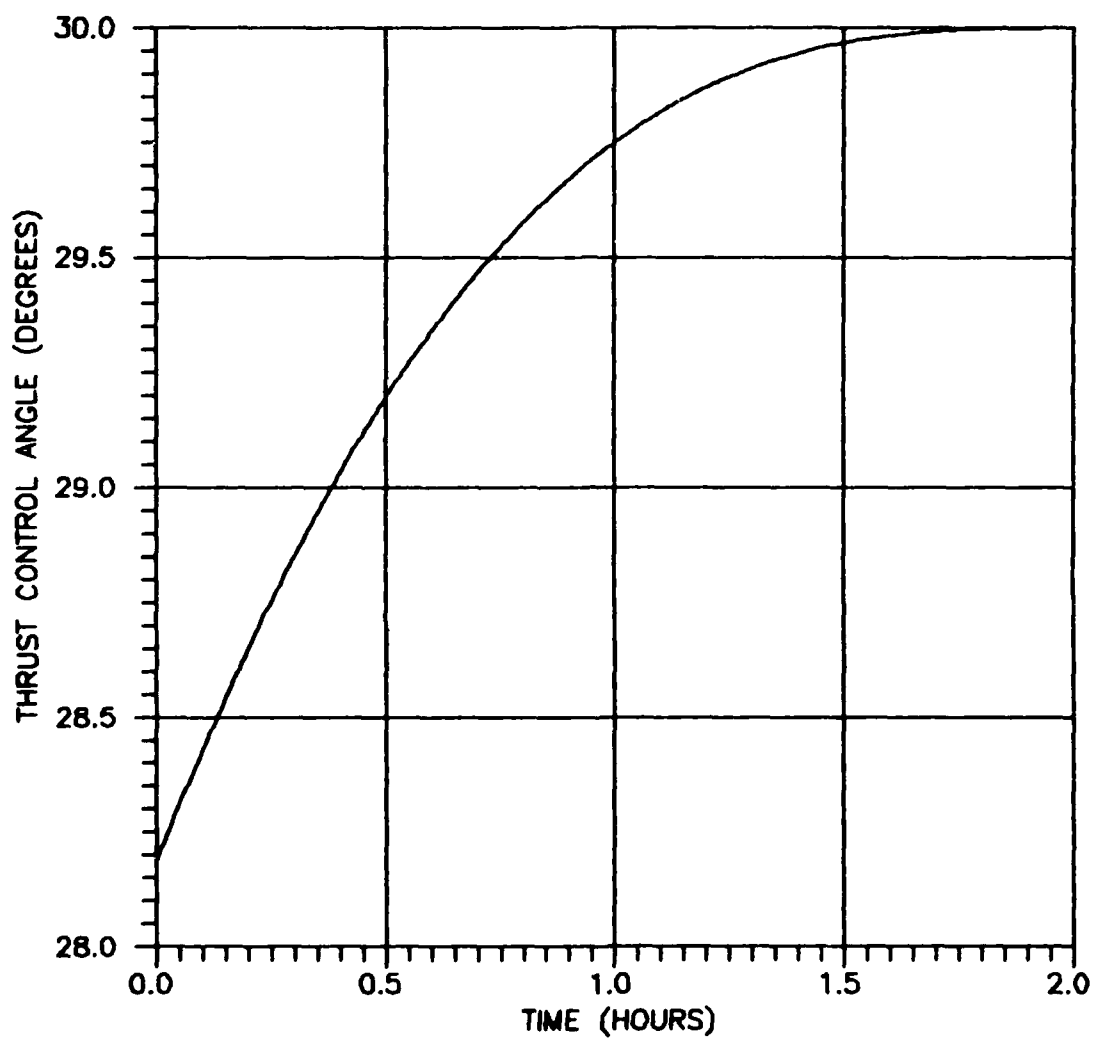radially opposite direction, as shown in Table X.
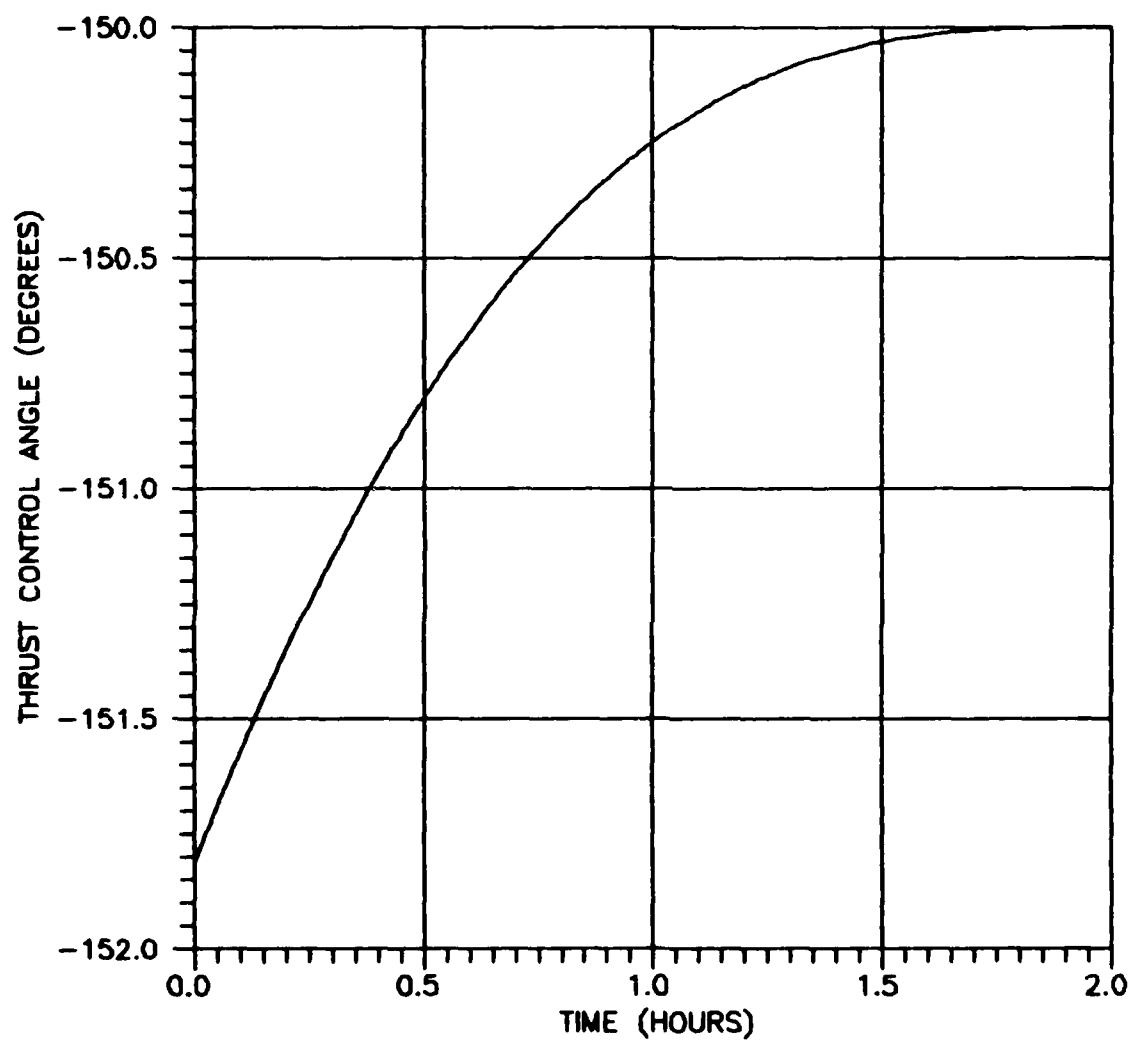
Figure 12.   Thrust Control Angle vs Time for 2 Hour Time of
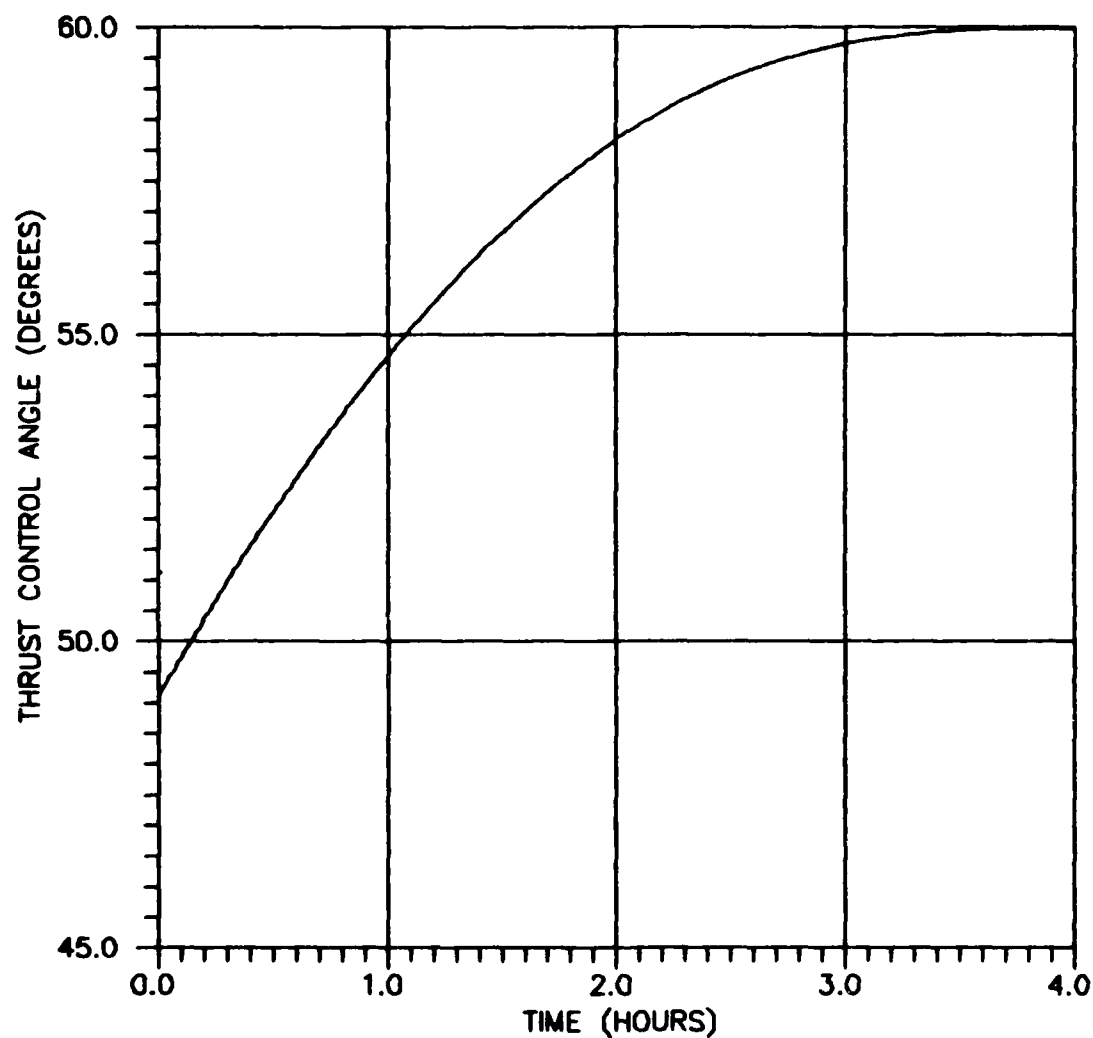Flight to Minimum Radius with no Terminal Constraint
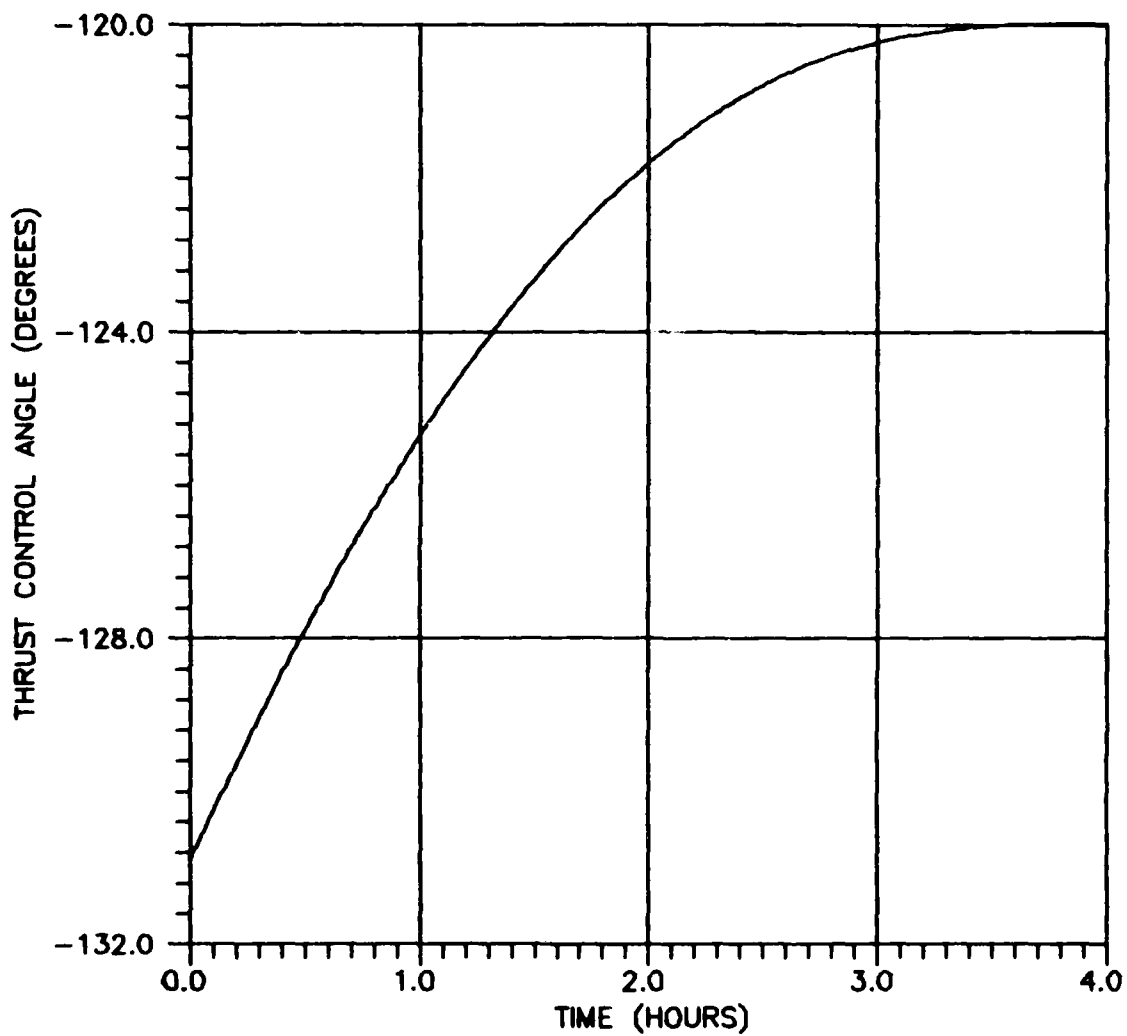
Figure 13. Thrust Control Angle vs Time for 4 Hour Time of
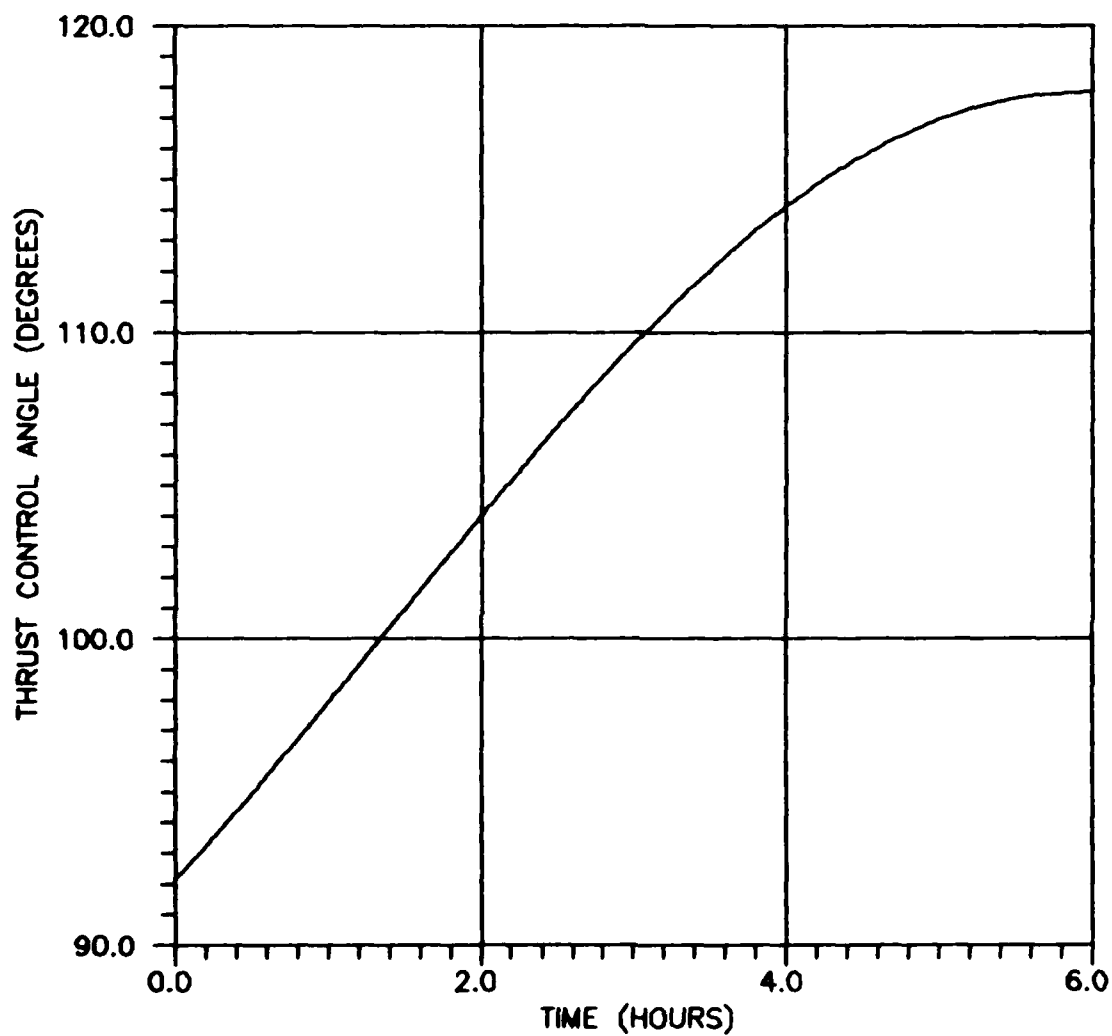Flight to Minimum Radius with no Terminal Constraint
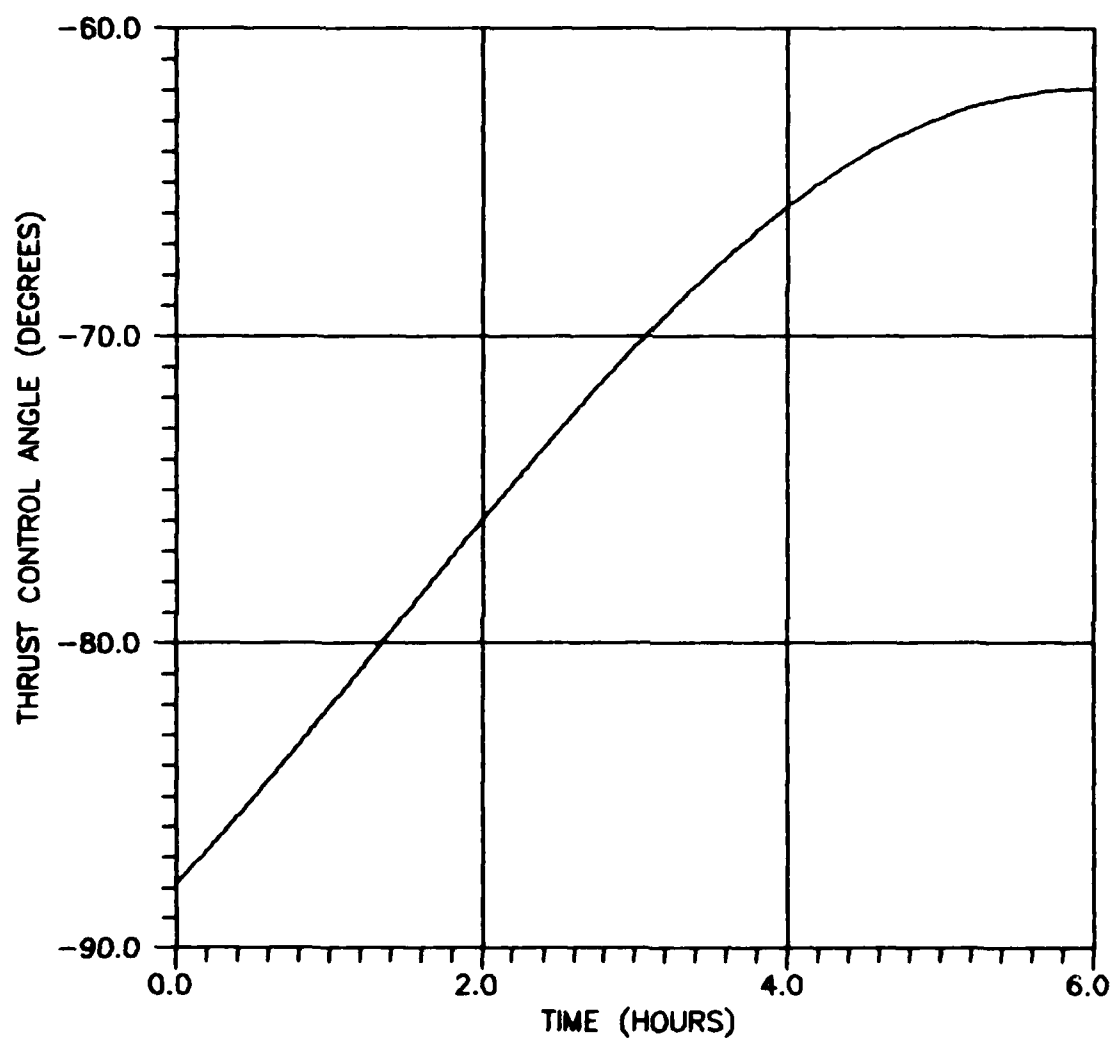
Figure 14. Thrust Control Angle vs Time for 6 Hour Time of Flight to Minimum Radius with no Terminal Constraint

Table X. Radial Decrease for Minimum Radius
Evasive Maneuver with no Terminal Constraint

Time of Flight (hrs)	Radial Decrease (km)
2	26.4681
4	116.4797
6	259.2153

The final position and velocity states for this evasive
maneuver are given in Tables XI and XII.

Table XI. Terminal Position States for Minimum Radius
Evasive Maneuver with no Terminal Constraint

Time of Flight (hrs)	x (km)	y (km)
2	36558.6342	21107.8968
4	21047.1769	36489.7502
6	0.0	41981.9071

Table XII. Terminal Velocity States for Minimum Radius
Evasive Maneuver with no Terminal Constraint

Time of Flight (hrs)	u (km/s)	v (km/s)
2	-1.5427	2.6566
4	-2.6718	1.5205
6	-3.0728	0.0039

Rendezvous Maneuver. Thrust vector control histories
were generated for minimum time rendezvous maneuvers with an
initial position at the terminal point of the maximum radius
evasive maneuvers with the orthogonality constraint.

Figures 15, 16 and 17 show the control angle profiles for
the rendezvous from the two hour, four hour and six hour
termination points, respectively. For all rendezvous
maneuvers, the thrust control angle is nearly constant for
long periods of time, with the control switching direction
by 180 degrees at approximately the sixty percent time point
of the maneuver. Although the control angle is not bounded
in the problem formulation, the numerical solution yields a
control angle region bounded approximately by -30 and 160
degrees for the rendezvous from the two hour evasive
maneuver, 0 and 180 degrees for the return from the four
hour maneuver, and -90 and 90 degrees for the rendezvous
from the six hour maneuver. The penalty for achieving
increased radial distance at the expense of lagging behind
the nominal orbit is evidenced in the time required for
rendezvous from the two hour and four hour time of flight
terminal points, as Table XIII shows.

Table XIII. Time Required to Rendezvous from Evasive
Maneuver with Terminal Constraint

Time of Flight for Evasive Maneuver (hrs)	Rendezvous Time (hrs)
2	3.6104
4	8.0241
6	5.9957
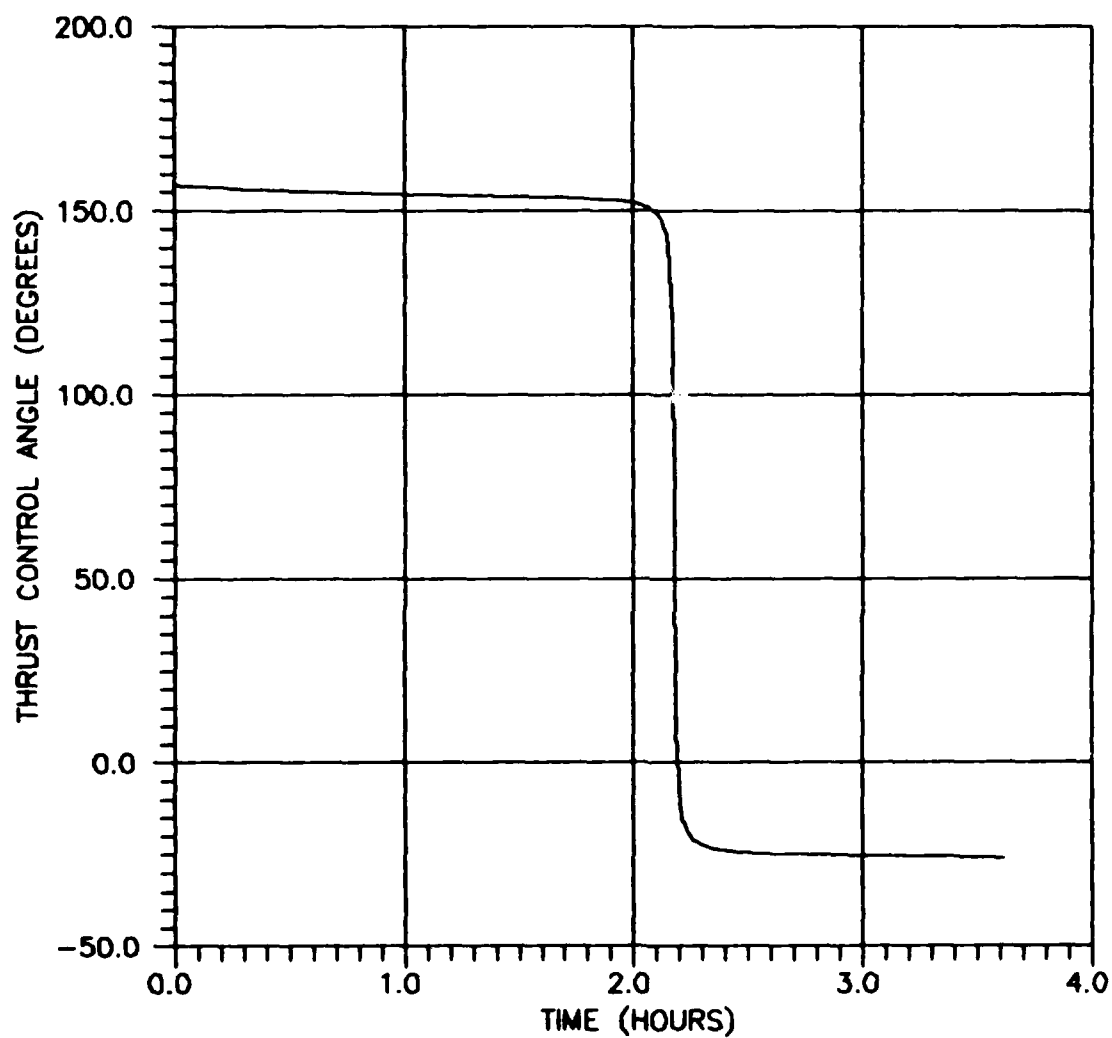
Figure 15. Thrust Control Angle vs Time for Rendezvous from 2 Hr
Time of Flight to Maximum Radius with Orthogonality Constraint
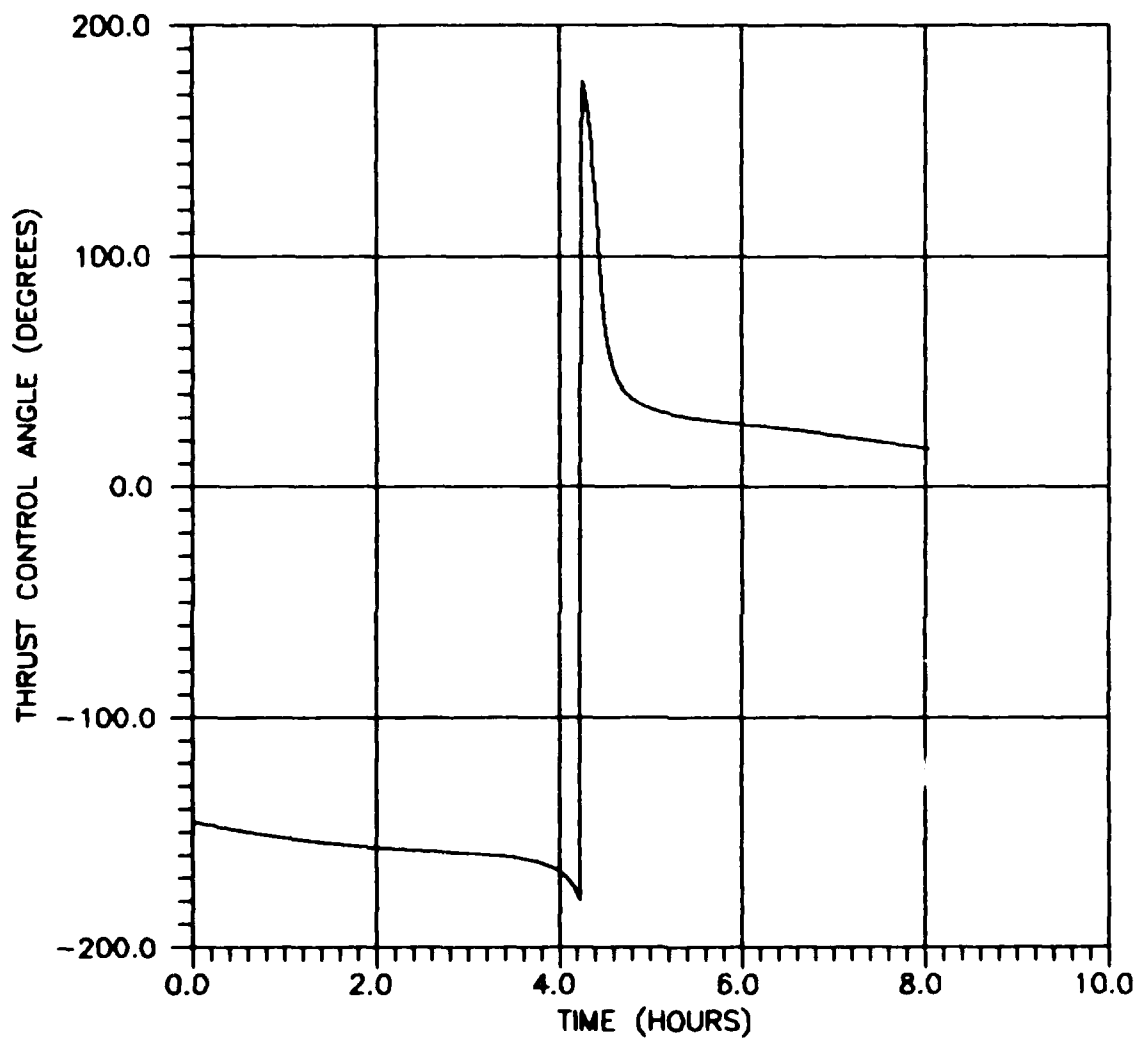
Figure 16. Thrust Control Angle vs Time for Rendezvous from 4 Hr Time of Flight to Maximum Radius with Orthogonality Constraint
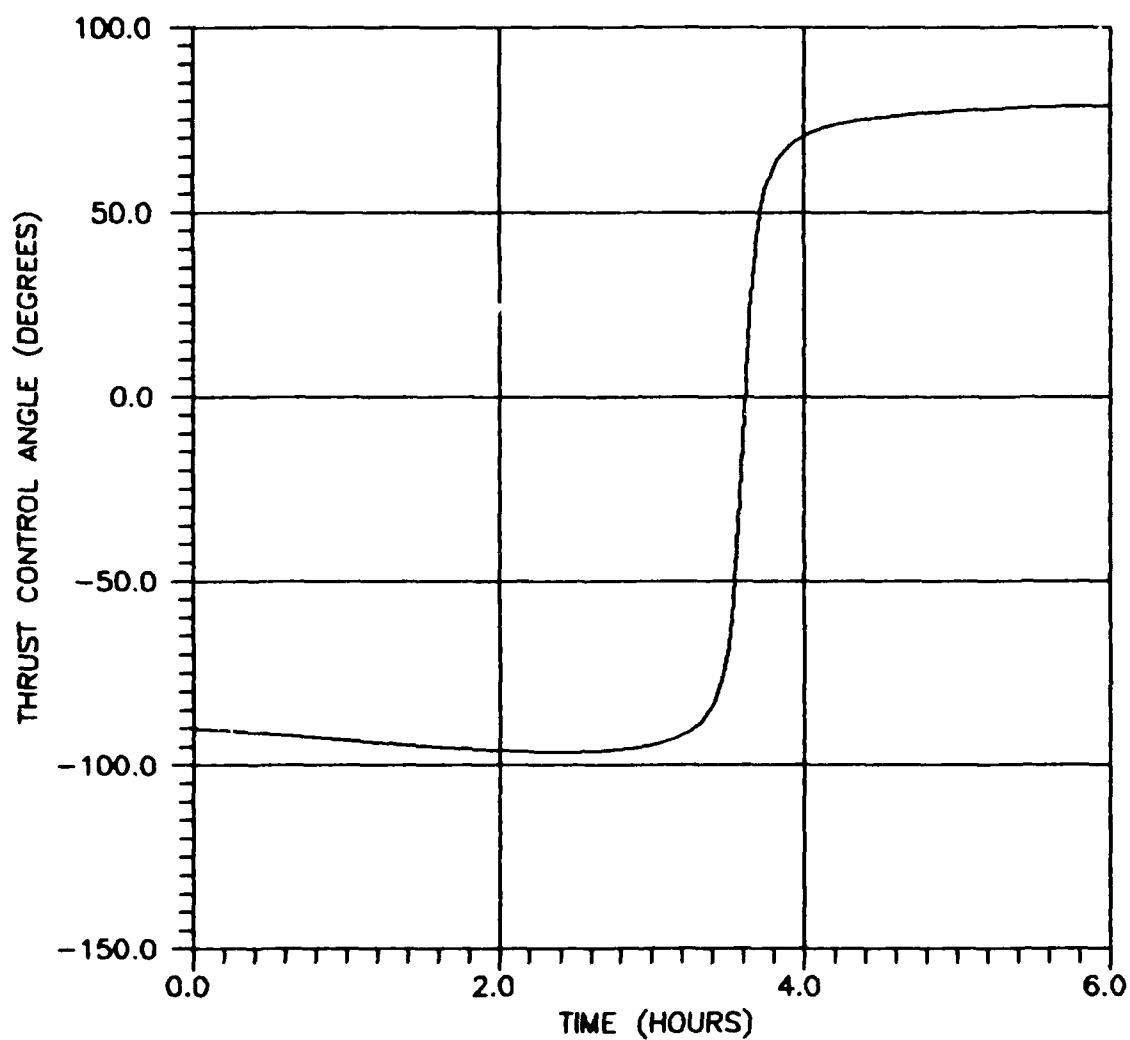
Figure 17.   Thrust Control Angle vs Time for Rendezvous from 6 Hr
Time of Flight to Maximum Radius with Orthogonality Constraint

To verify that the terminal states of the rendezvous maneuver do indeed match those of the nominal orbit, the point of rendezvous is given in Table XIV. Table XV shows the terminal velocity states at the rendezvous point.

Table XIV. Terminal Position States for Rendezvous from Evasive Maneuver with Terminal Constraint

Time of Flight for Evasive Maneuver (hrs)	x (km)	y (km)
2	4301.1276	42021.5792
4	-42238.1810	-261.9727
6	-42241.1149	47.1797

Table XV. Terminal Velocity States for Rendezvous from Evasive Maneuver with Terminal Constraint

Time of Flight for Evasive Maneuver (hrs)	u (km/s)	v (km/s)
2	-3.0559	0.3128
4	0.0191	-3.0716
6	-0.0034	-3.0719

The total amount of time required for a complete evasion and rendezvous maneuver is given in Table XVI. Here the penalty of lagging behind the nominal orbit in order to achieve a larger radial change is seen dramatically. Note that while the maneuvers associated with the 4 hour time of flight and the six hour time of flight evasive maneuvers require approximately the same total flight time, a

trade-off exists between achieving a greater relative radius change during the evasive maneuver and returning more quickly to the nominal orbit.

Table XVI.   Total Time Required for Evasive and Rendezvous Maneuver

Time of Flight for Evasive Maneuver (Hours)	Maneuver Time (Hours)
2	5.6104
4	12.0241
6	11.9957

Rendezvous following any minimum radius evasive maneuver was not a concern, since the interceptor was assumed to be in a direct coasting ascent. The minimum radius trajectory could possibly pass within striking distance of the ascending threat depending upon the size of its lethal radius, which was not specified. However, it is anticipated that a return to the nominal orbit from a minimum orbit radius would require less time since the trajectory would traverse the interior of the nominal orbit.

On the other hand, rendezvous from a maximum radius maneuver with no terminal constraint is of great concern, since this would make apparent the penalty paid in rendezvous time in returning from a much larger radial distance with an unconstrained orientation of the spacecraft velocity vector. Unfortunately, convergence could not be

achieved within the limits of the 8 megabytes of computer memory available; these maneuvers demanded grid sizes in excess of 2342, the upper limit available at this time on the Vax-11/785 system, as indicated by the DVCPR parameter NGRID.

The difficulty posed herein lies not only in the great return distance demanded, but also in an initial orientation of the spacecraft velocity vector in the outward radial direction. In fact, convergence was achieved for rendezvous initiating at the desired x-y position, but with the velocity vector orthogonal to the radius vector. This solution was intended as an input grid for the return maneuver from the unconstrained evasive maneuver with non-orthogonal velocity and radius vectors. In order to achieve the desired solution, the initial velocity vector was then rotated to its non-orthogonal orientation using a continuation scheme with small step size. At most the vector could be rotated sixty-percent towards the desired direction before computer memory limits were exceeded, and even then it was apparent that the rendezvous time required was great in comparison to those cited in Table V.

Minimum Time Intercept Maneuver. The maximum radius evasive maneuvers were also considered in the context of a minimum time intercept of a specified radius, with and without a terminal orthogonality constraint. The resulting

state and control histories duplicated those of the maximum

radius maneuvers, thus verifying the solutions.

Costate Trajectories

As discussed in Chapter VI, the costate trajectories

vary greatly depending upon the initial grid input to the

problem solver DVCPR. Figures 18 through 47 evidence this

behavior, as the x-y and u-v costate trajectories show only

limited similarity in their time histories, even for the

same maneuver over a different time of flight. The

exceptions herein are the costate trajectories associated

with minimum orbit radius maneuvers, shown in Figures 24

through 29 and 36 through 41 for constrained and

unconstrained maneuvers, respectively. These trajectories

are merely reversed in sign from their maximum radius

counterparts, as the problem development suggests.

Additionally, the u-v costate histories for all

maneuvers without constraint clearly satisfy the boundary

conditions requiring these costates to pass through zero at

the final time. For all maneuvers, the costate trajectories

are smooth and continuous over time, as required by

Euler-Lagrange theory.

Although the costate trajectories show only limited

trends towards similar histories, they can be fit quite

accurately with appropriate quadratics. Tables XVII through

XIX give the quadratic curvefits for x-y and u-v costate

trajectories for each maximum radius and rendezvous

maneuver, along with the corresponding correlation coefficients. Note that curvefits on the coefficients for minimum radius maneuvers are merely the negative of the maximum radius curvefits. The purpose in listing these equations and their associated plots is to aid the future user in constructing an input grid which will readily allow convergence. In each equation, the time considered is in hours.

Figure 18. X and Y Costates for 2 Hour Time of Flight to
Maximum Radius with Orthogonality Constraint at Final Time

71

Figure 19. U and V Costates for 2 Hour Time of Flight to
Maximum Radius with Orthogonality Constraint at Final Time

Figure 20. X and Y Costates for 4 Hour Time of Flight to Maximum Radius with Orthogonality Constraint at Final Time

73
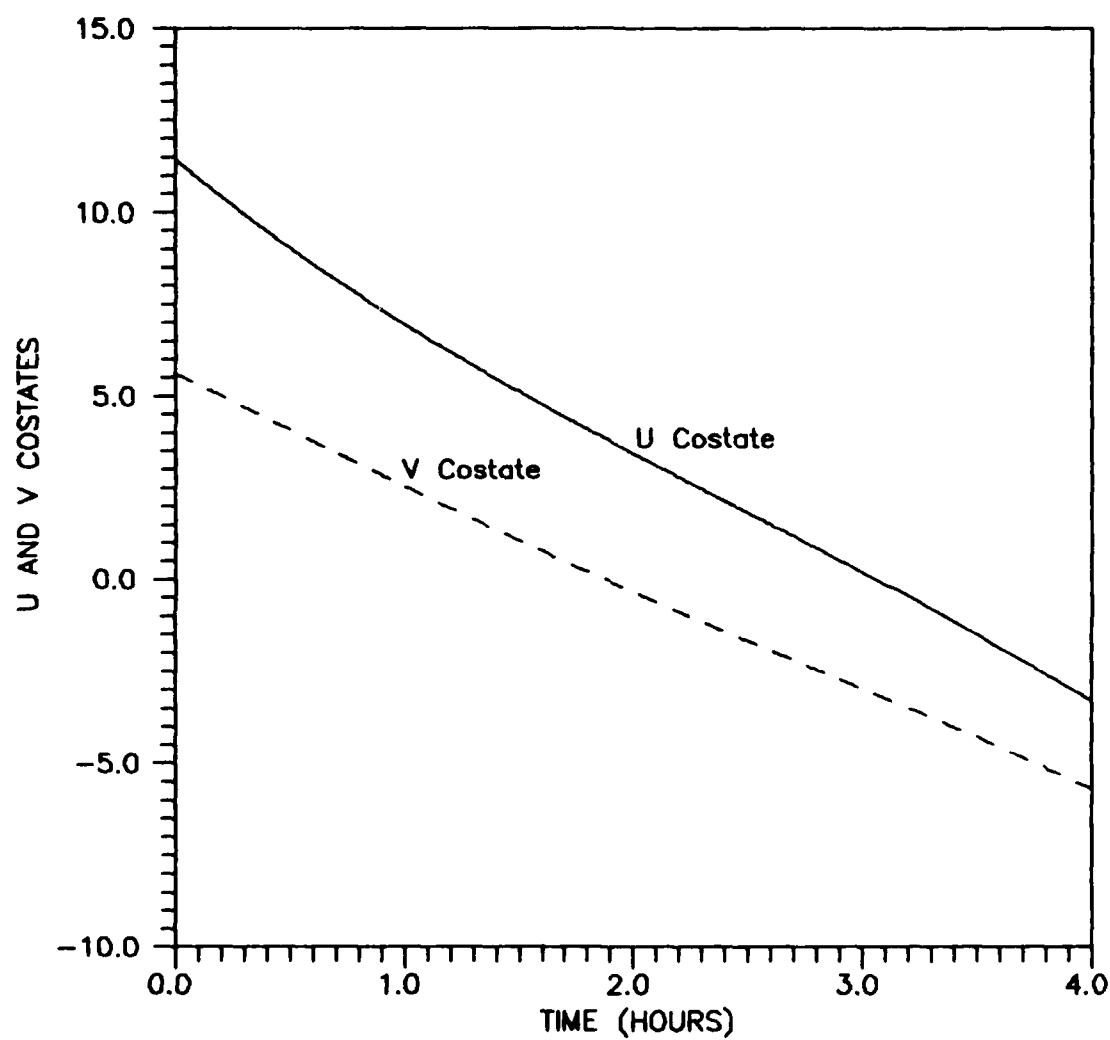
Figure 21.   U and V Costates for 4 Hour Time of Flight to
Maximum Radius with Orthogonality Constraint at Final Time

Figure 22.   X and Y Costates for 6 Hour Time of Flight to
Maximum Radius with Orthogonality Constraint at Final Time

Figure 23. U and V Costates for 6 Hour Time of Flight to
Maximum Radius with Orthogonality Constraint at Final Time
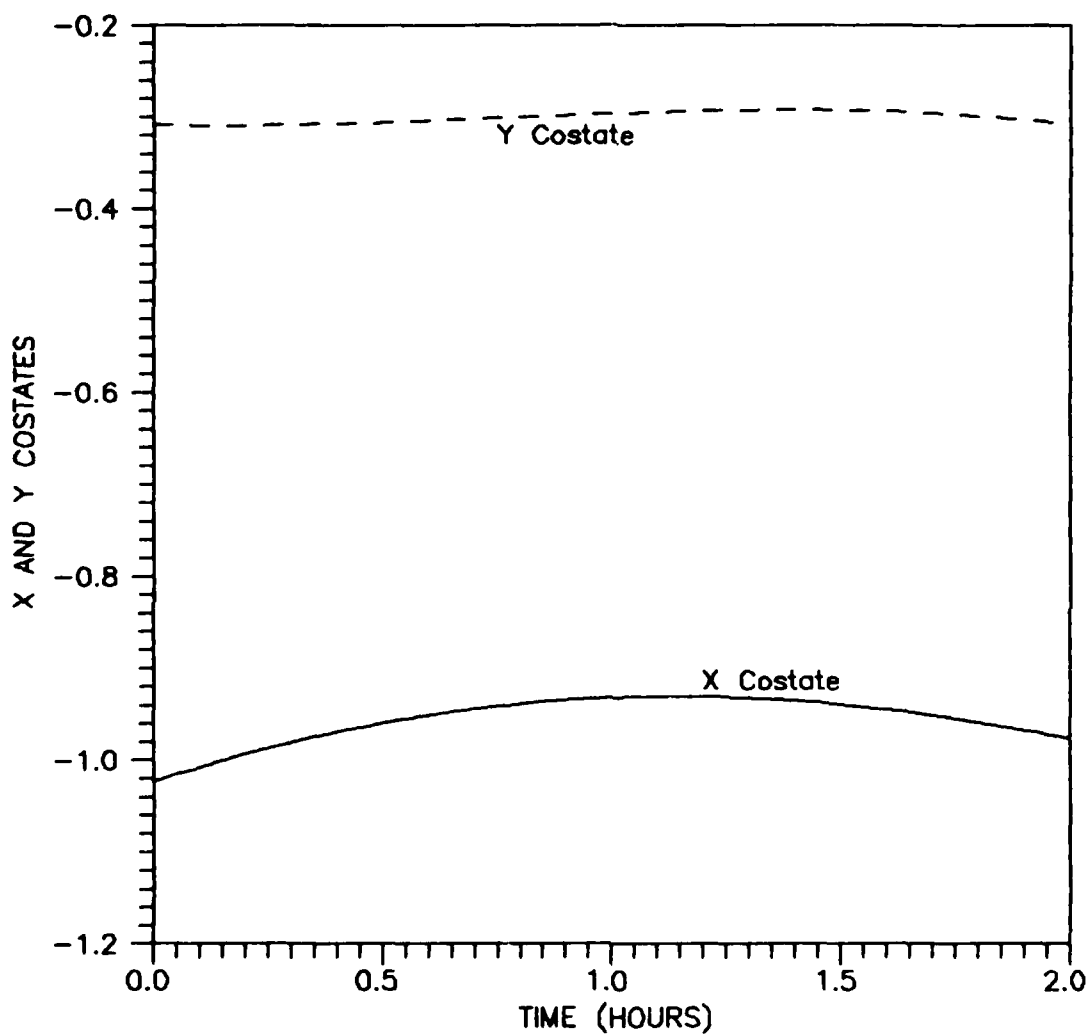
Figure 24. X and Y Costates for 2 Hour Time of Flight to
Minimum Radius with Orthogonality Constraint at Final Time

Figure 25. U and V Costates for 2 Hour Time of Flight to
Mimimum Radius with Orthogonality Constraint at Final Time
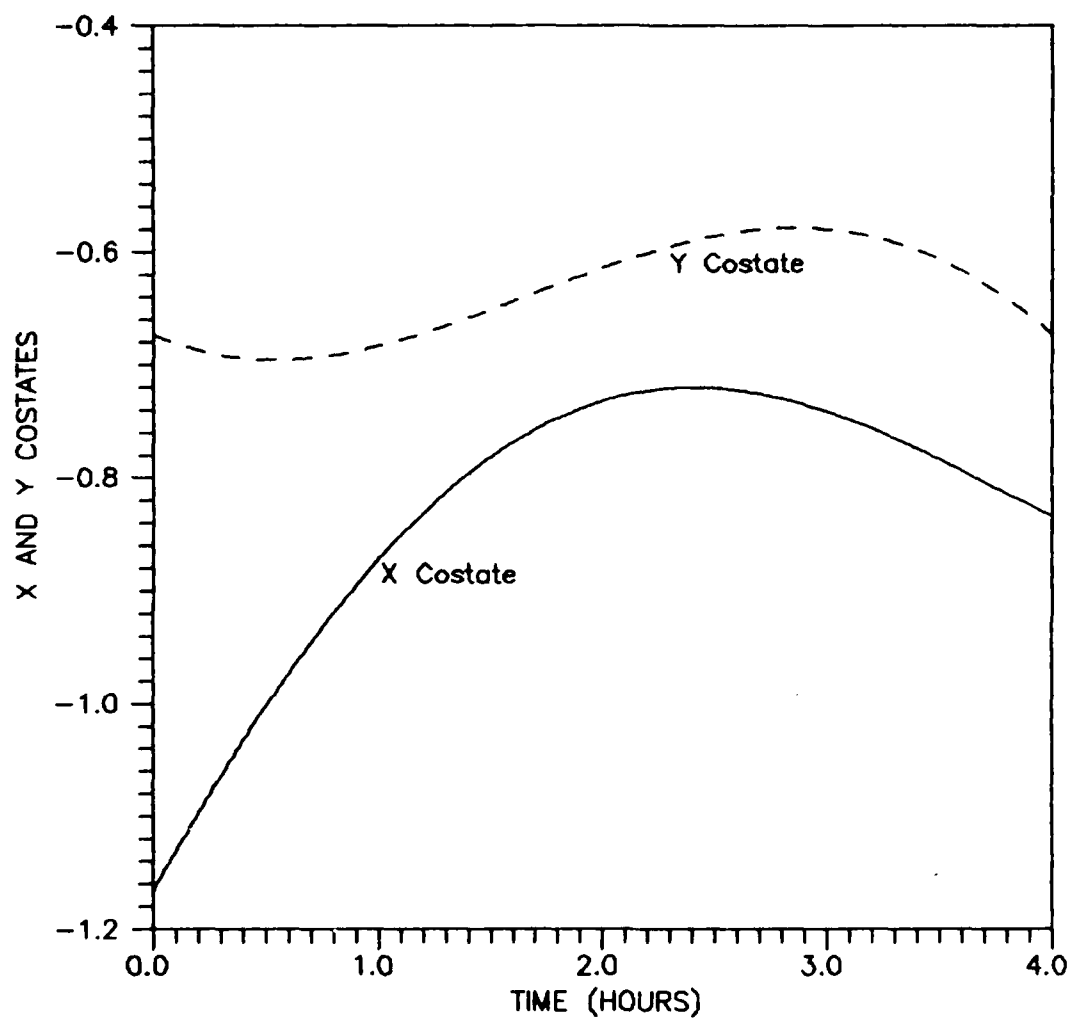
Figure 26. X and Y Costates for 4 Hour Time of Flight to Minimum Radius with Orthogonality Constraint at Final Time

79

Figure 27. U and V Costates for 4 Hour Time of Flight to
Minimum Radius with Orthogonality Constraint at Final Time
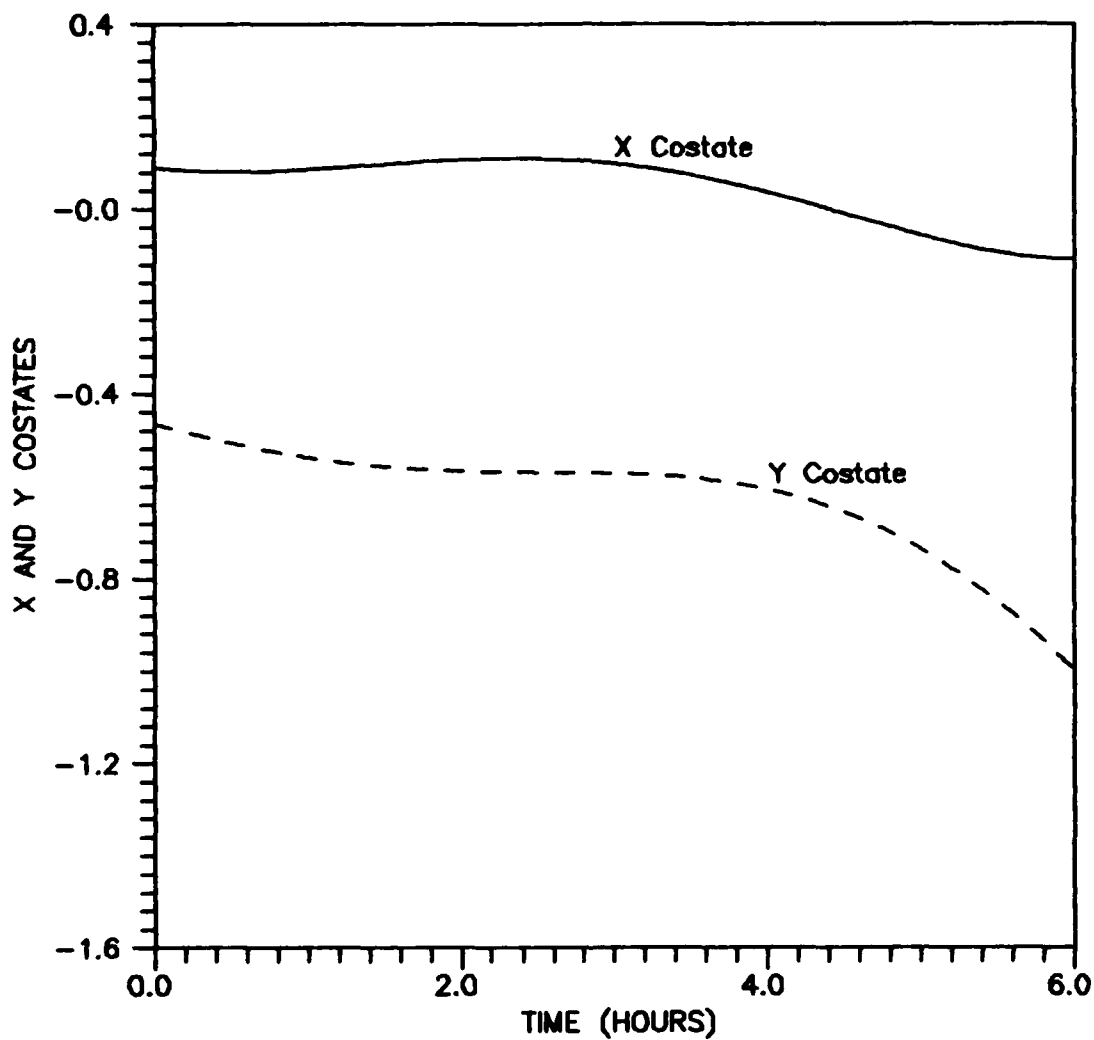
Figure 28.   X and Y Costates for 6 Hour Time of Flight to
Minimum Radius with Orthogonality Constraint at Final Time

81
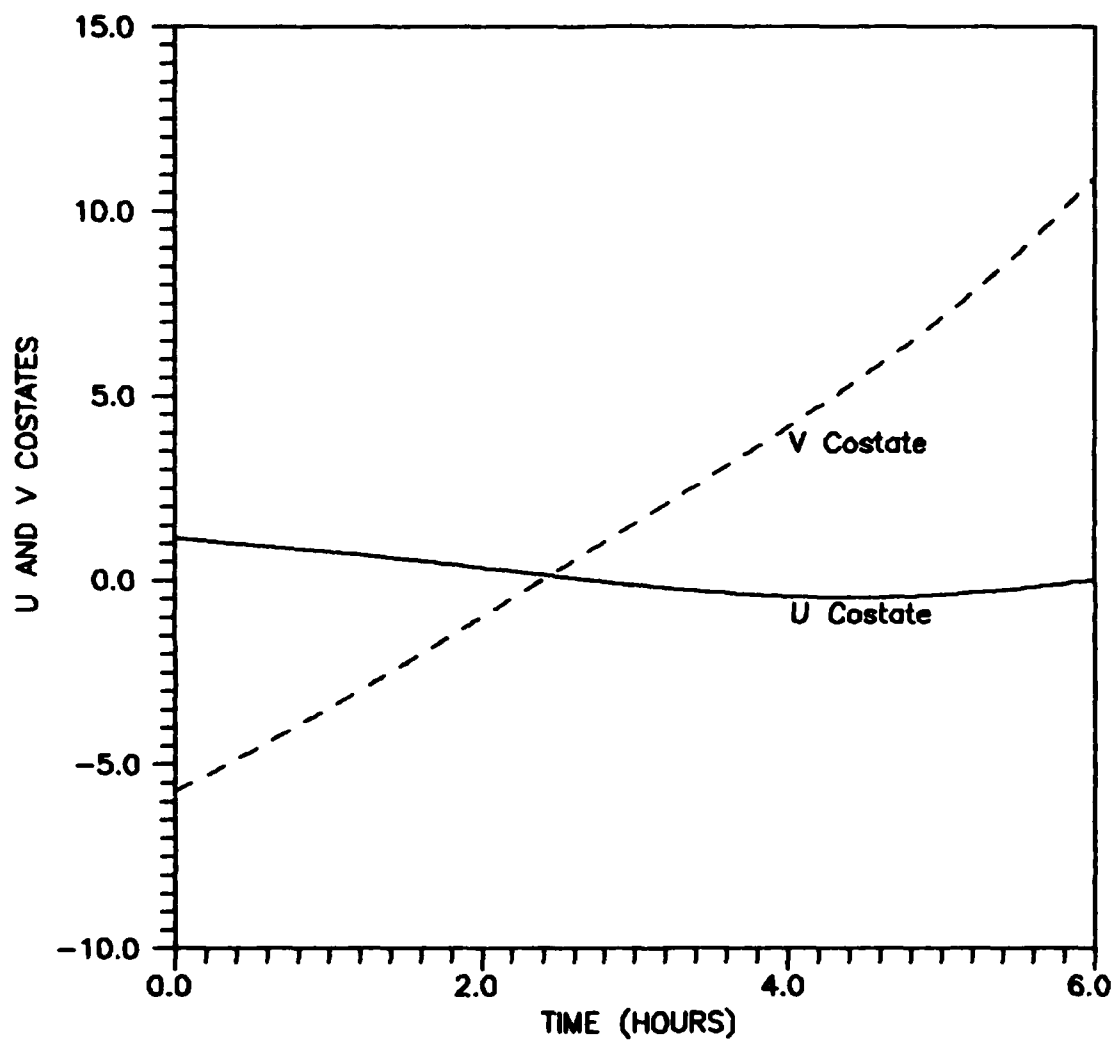
Figure 29.   U and V Costates for 6 Hour Time of Flight to
Minimum Radius with Orthogonality Constraint at Final Time
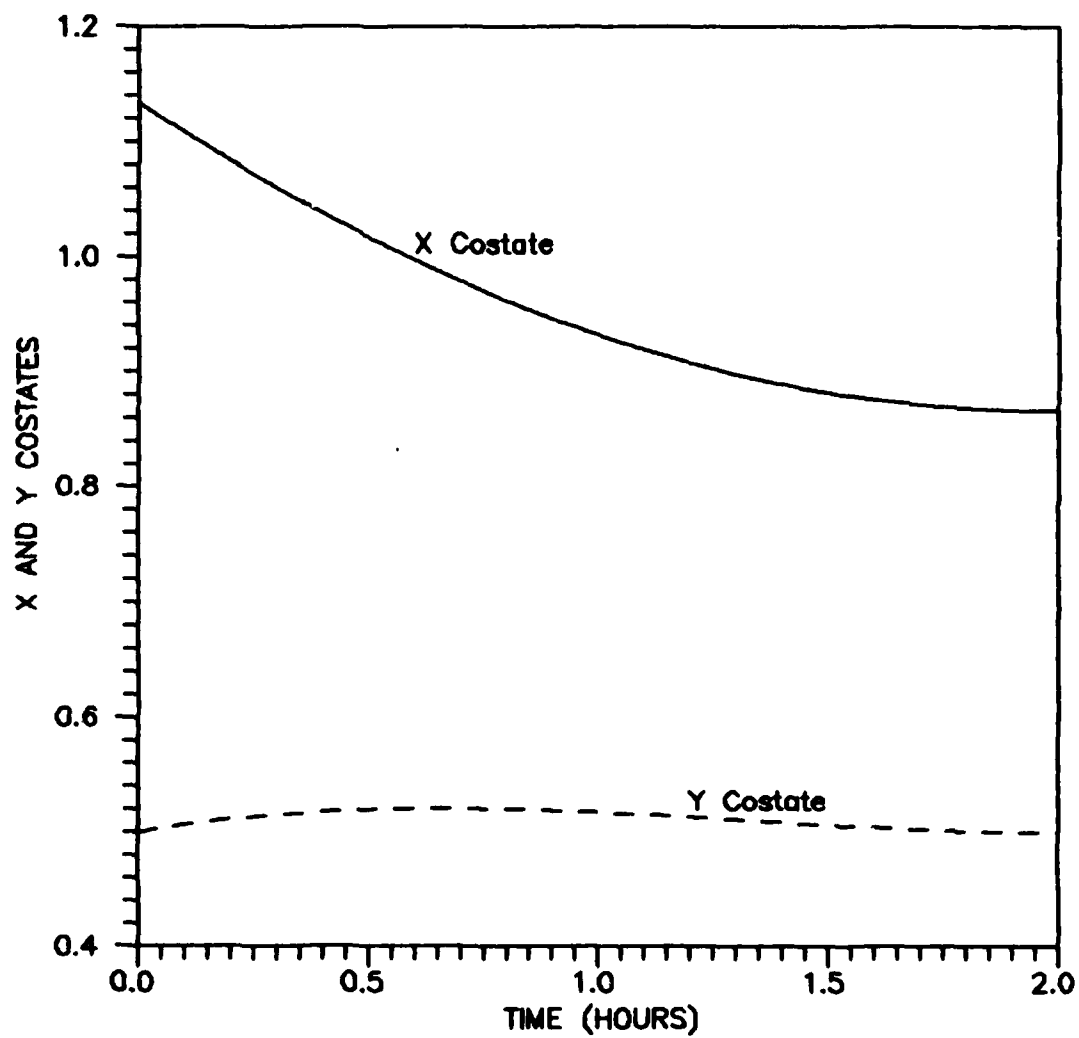
Figure 30.   X and Y Costates for 2 Hour Time of Flight to
Maximum Radius with no Terminal Constraint
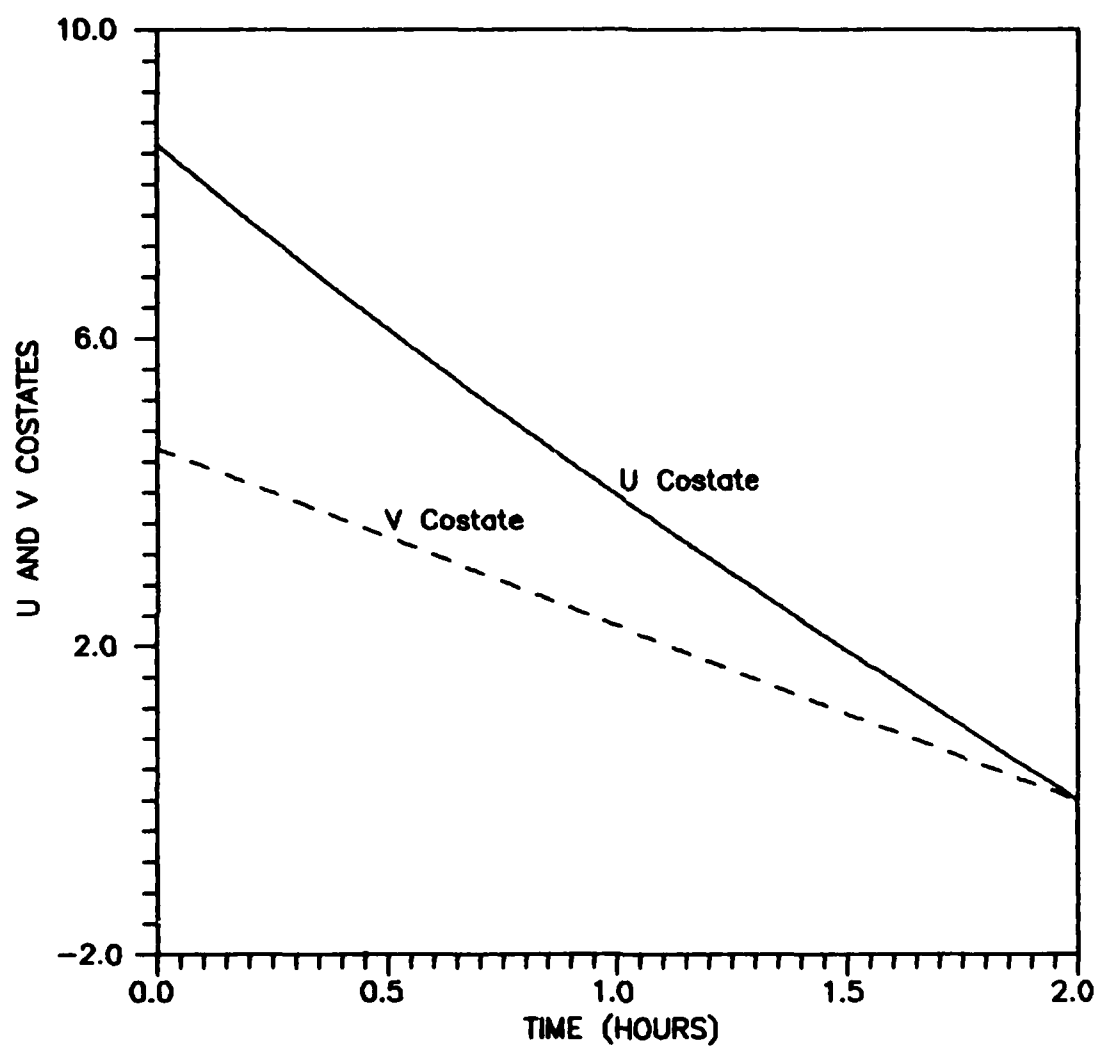
Figure 31. U and V Costates for 2 Hour Time of Flight to Maximum Radius with no Terminal Constraint
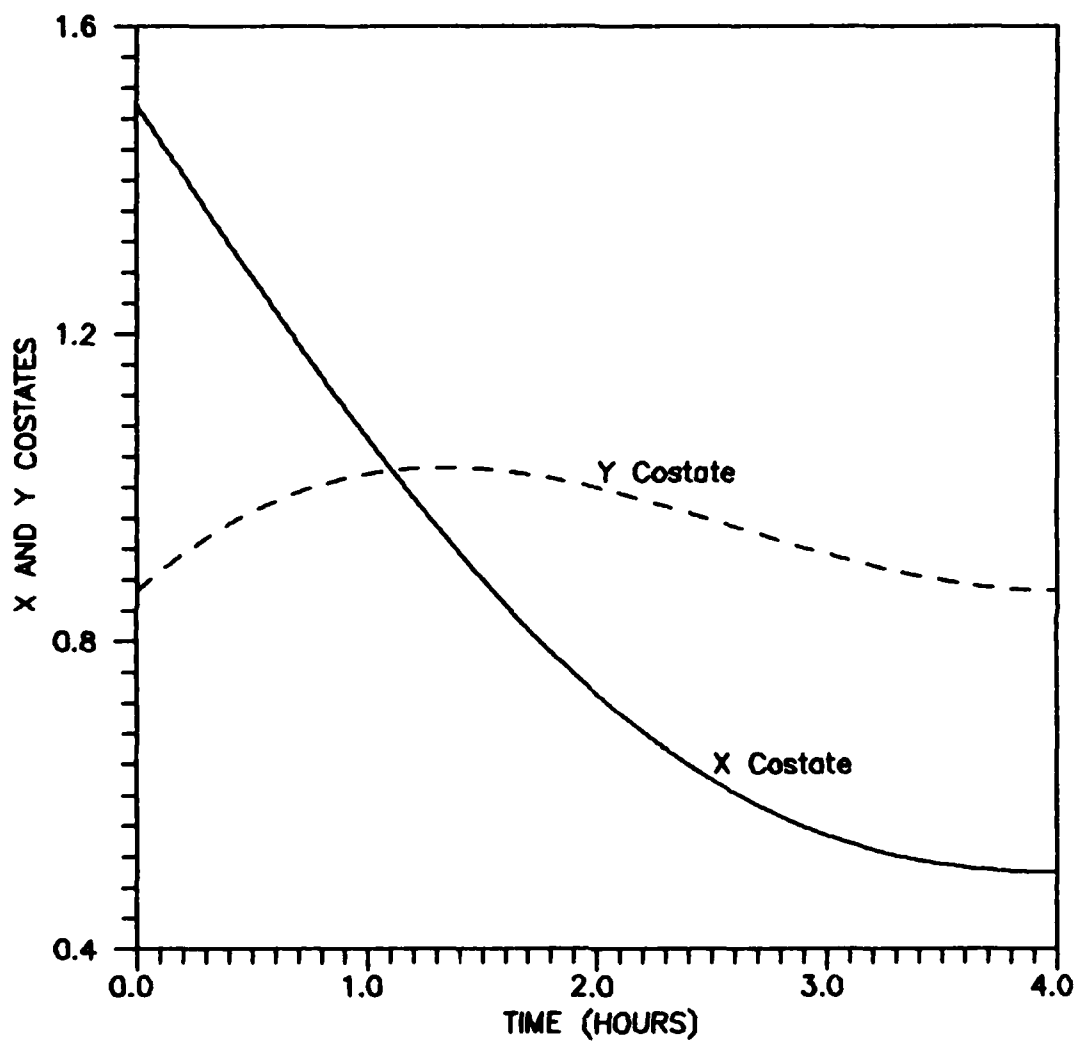
Figure 32. X and Y Costates for 4 Hour Time of Flight to
Maximum Radius with no Terminal Constraint
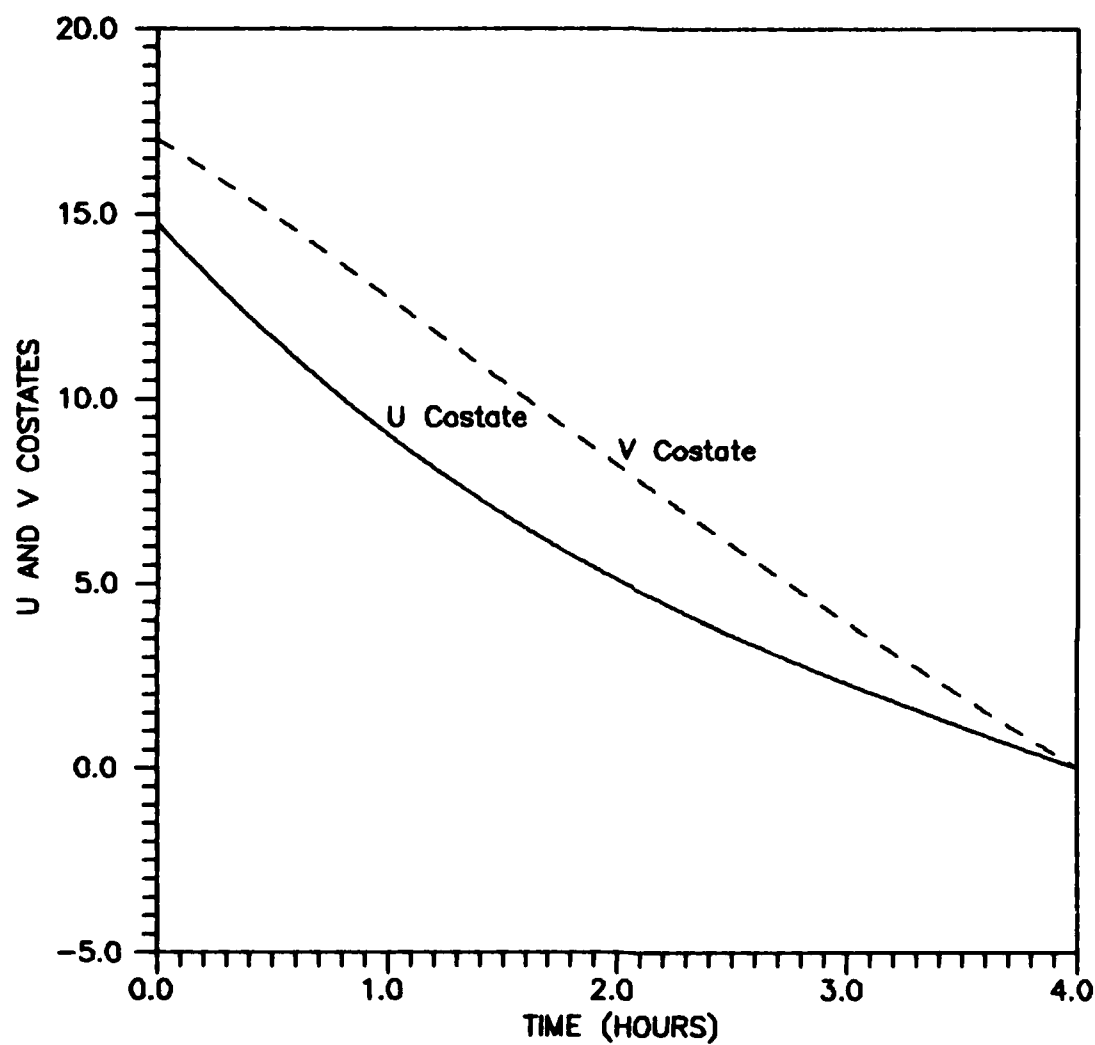
Figure 33. U and V Costates for 4 Hour Time of Flight to
Maximum Radius with no Terminal Constraint
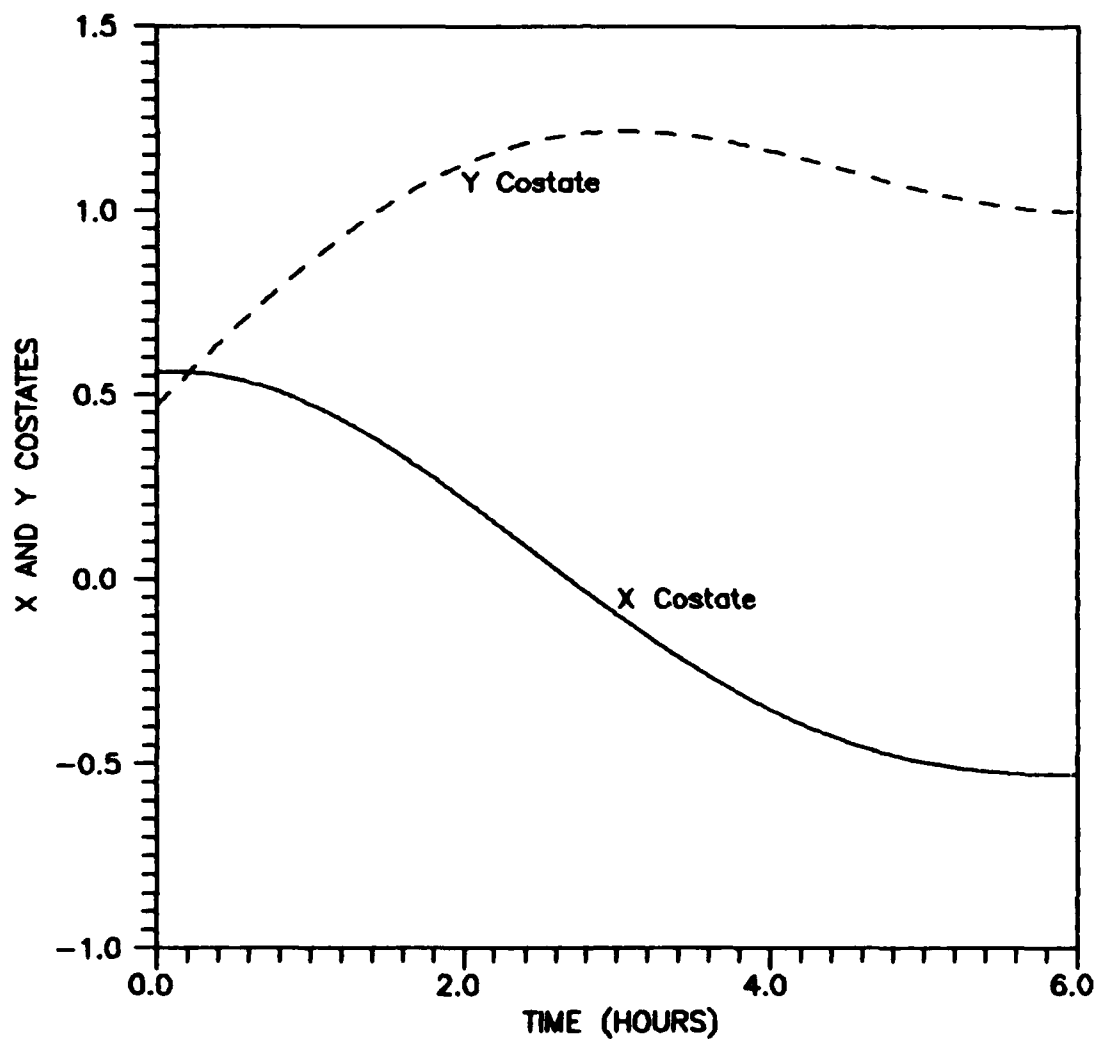
Figure 34. X and Y Costates for 6 Hour Time of Flight to Maximum Radius with no Terminal Constraint
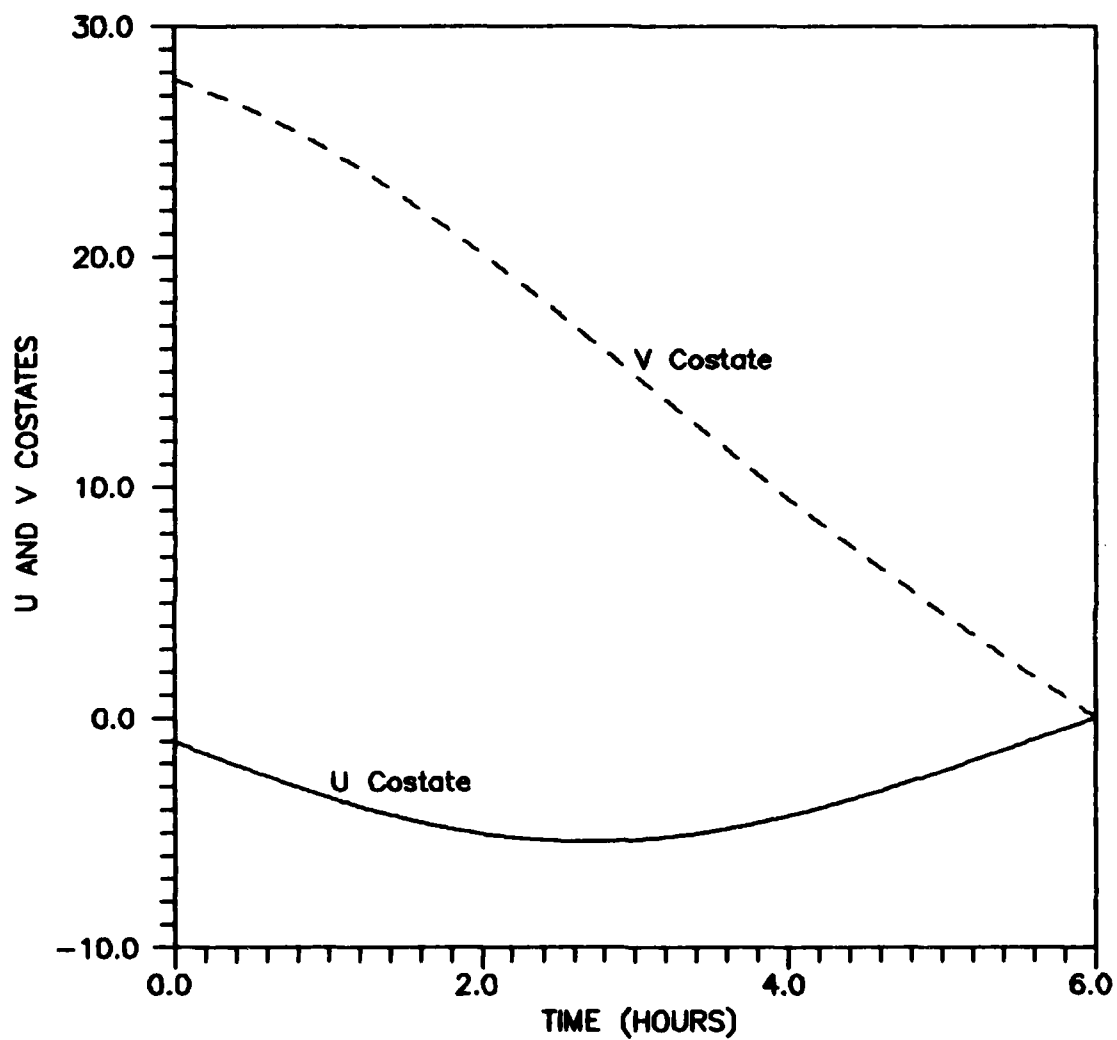
Figure 35. U and V Costates for 6 Hour Time of Flight to
Maximum Radius with no Terminal Constraint
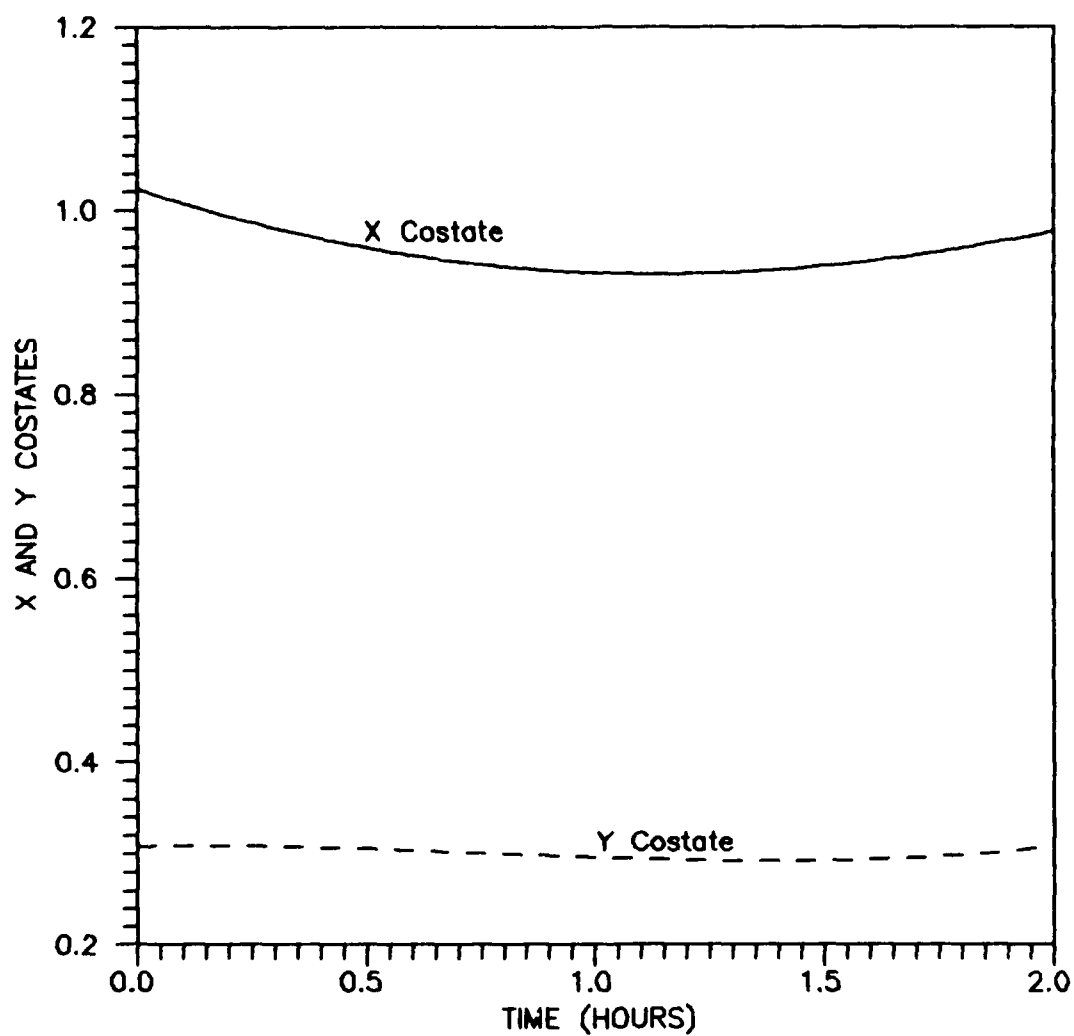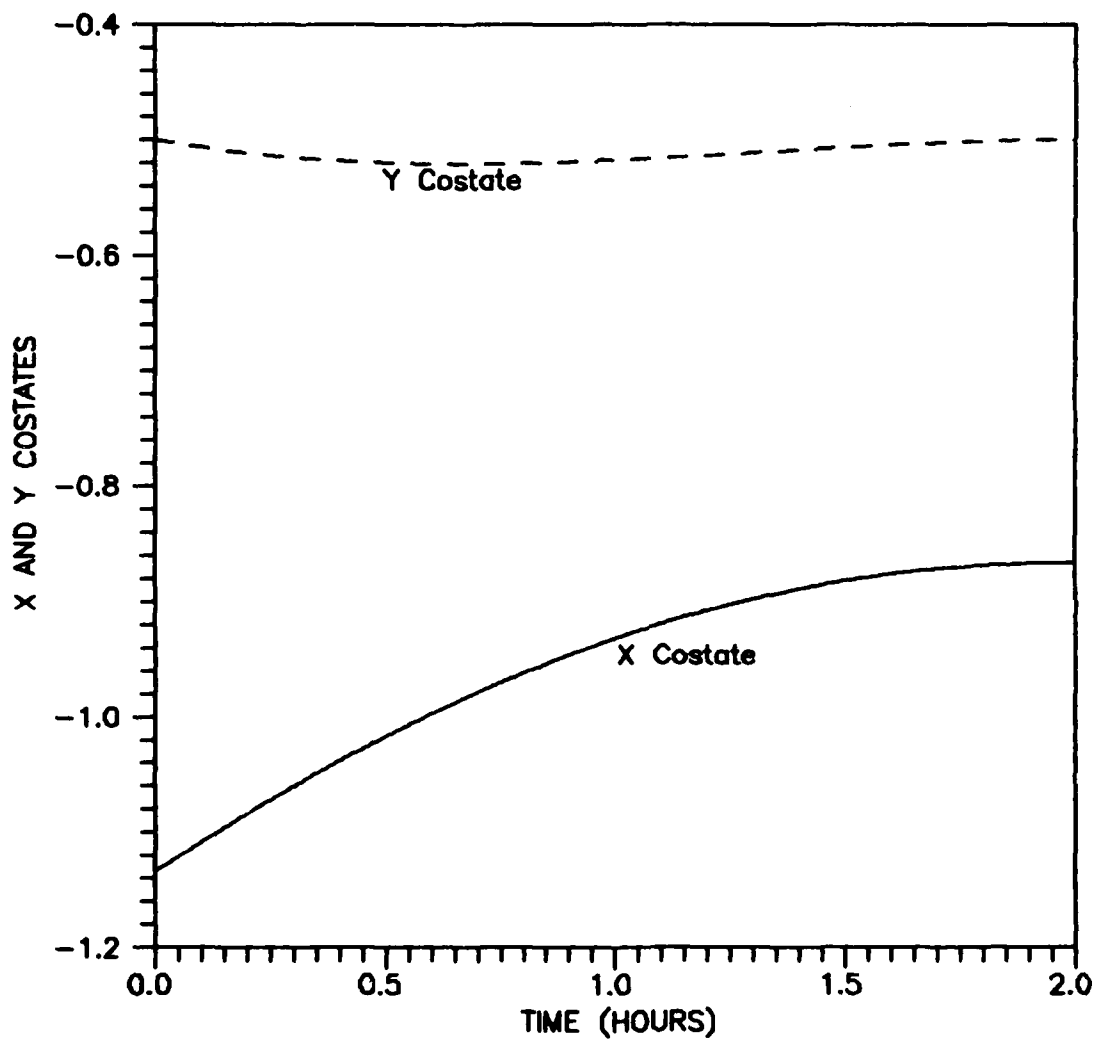
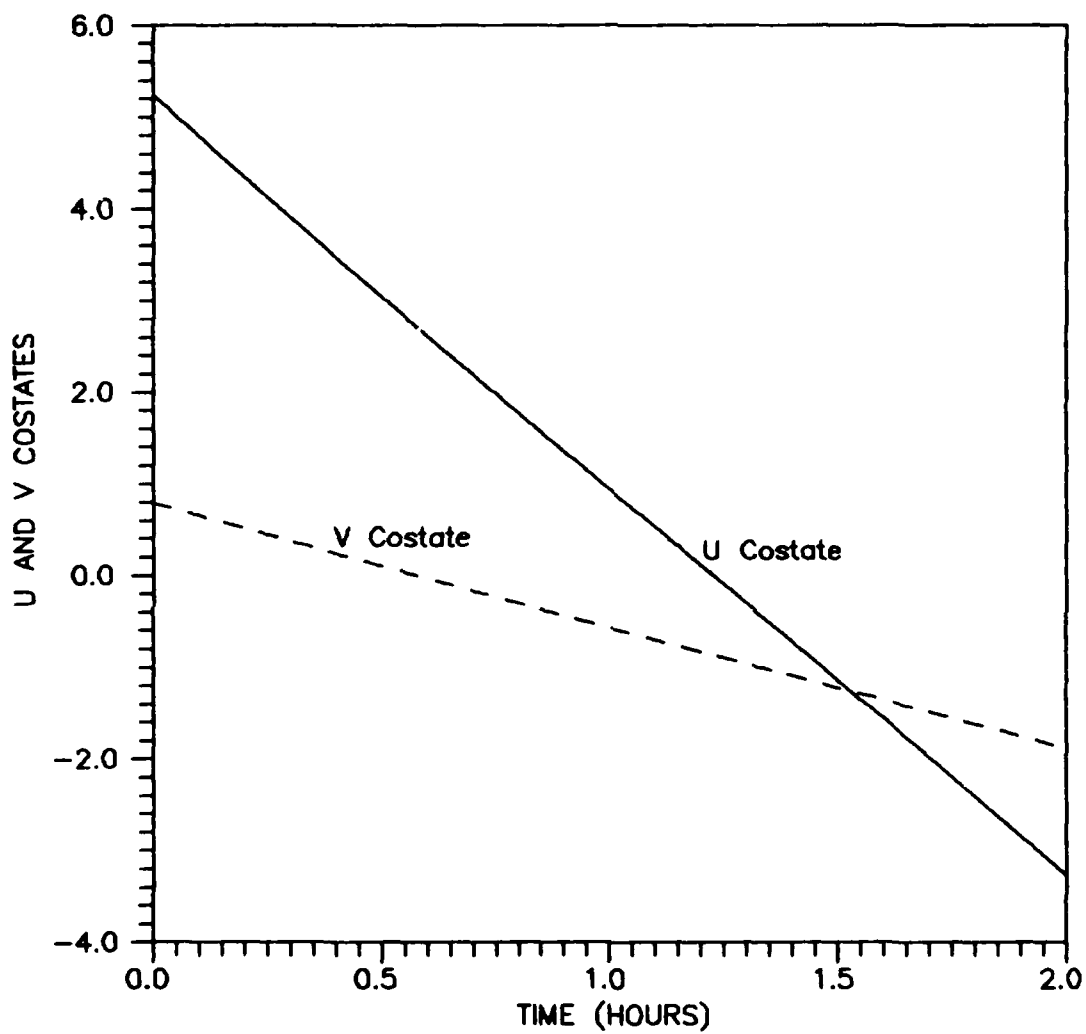Figure 36. X and Y Costates for 2 Hour Time of Flight to
Minimum Radius with no Terminal Constraint
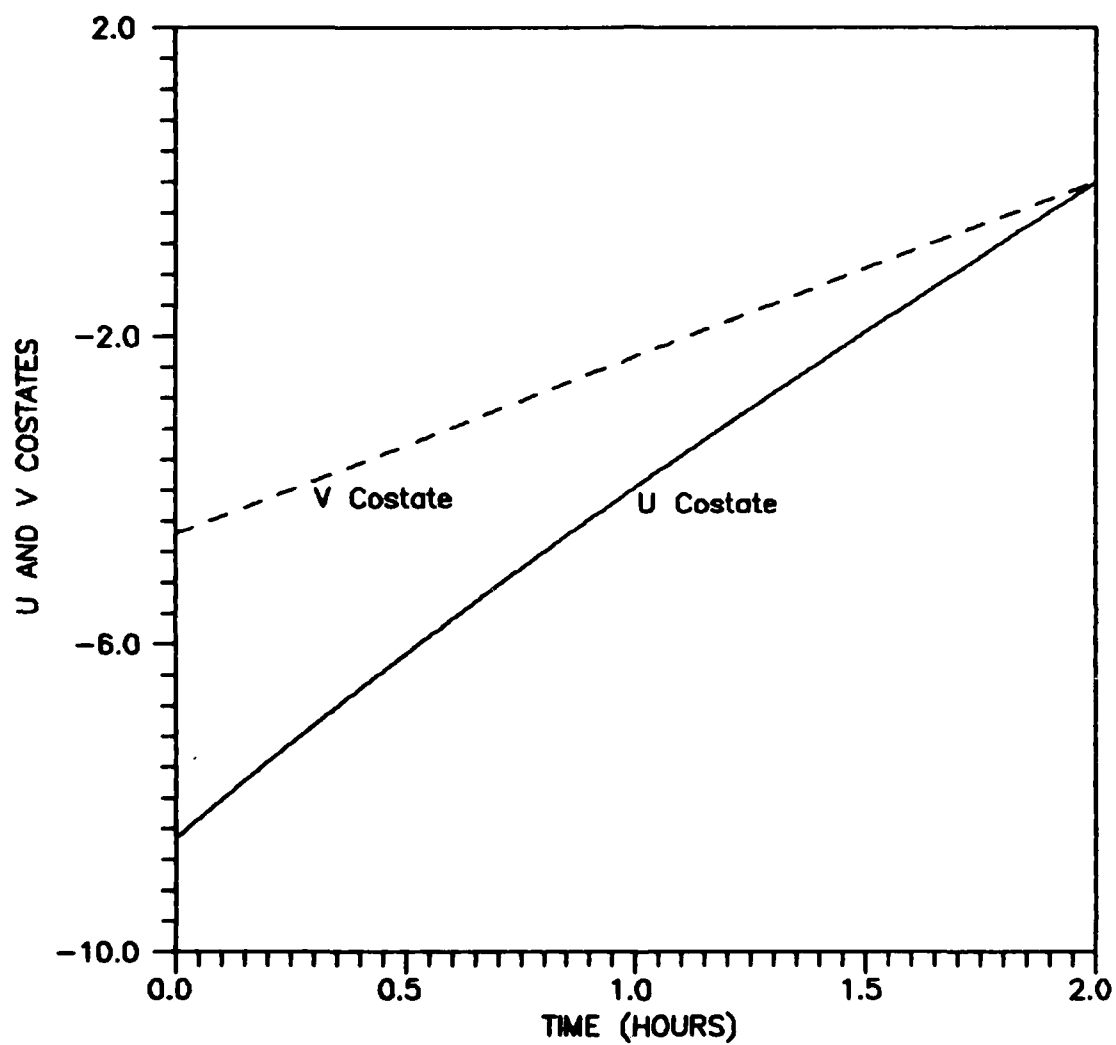
Figure 37. U and V Costates for 2 Hour Time of Flight to Minimum Radius with no Terminal Constraint
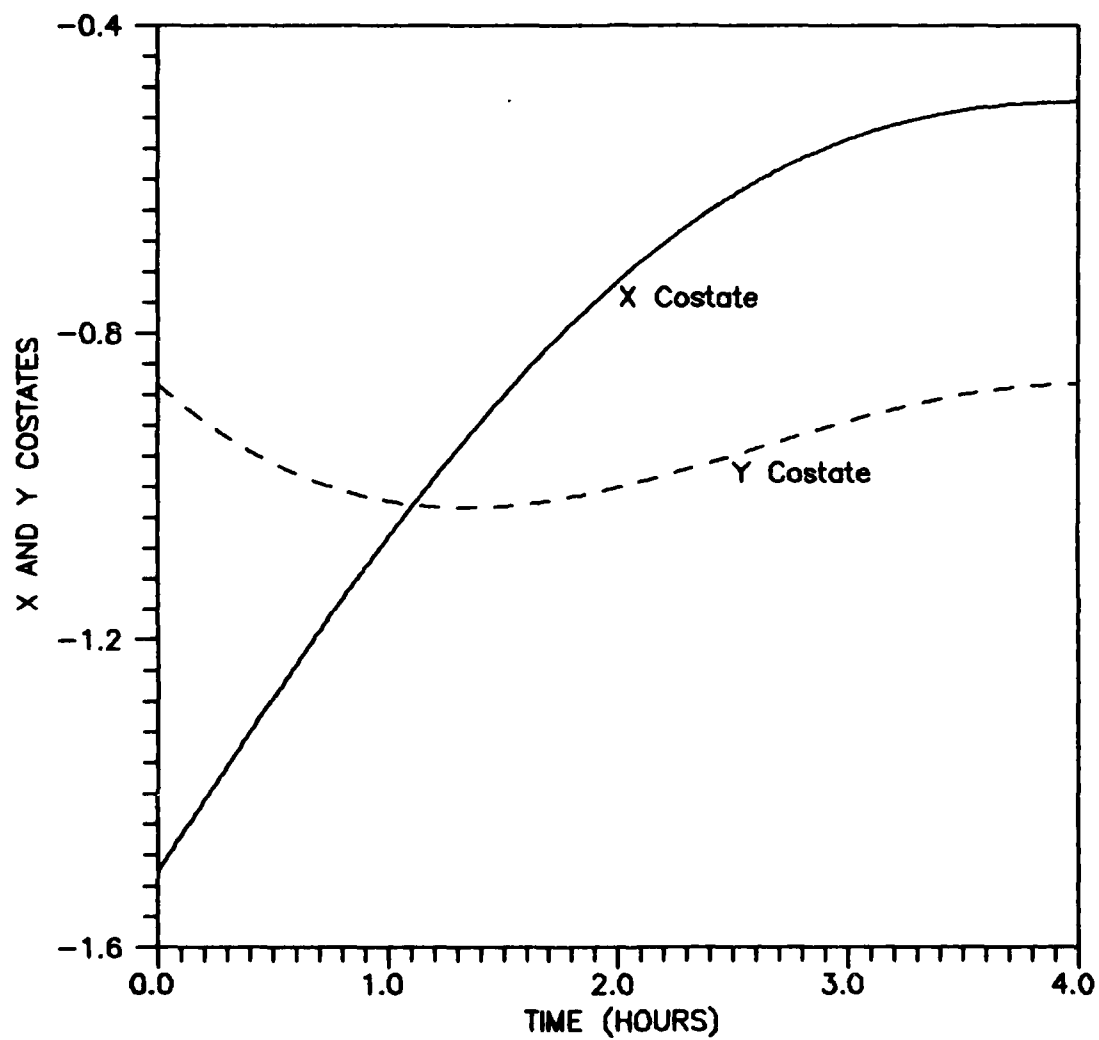
Figure 38. X and Y Costates for 4 Hour Time of Flight to
Minimum Radius with no Terminal Constraint

91
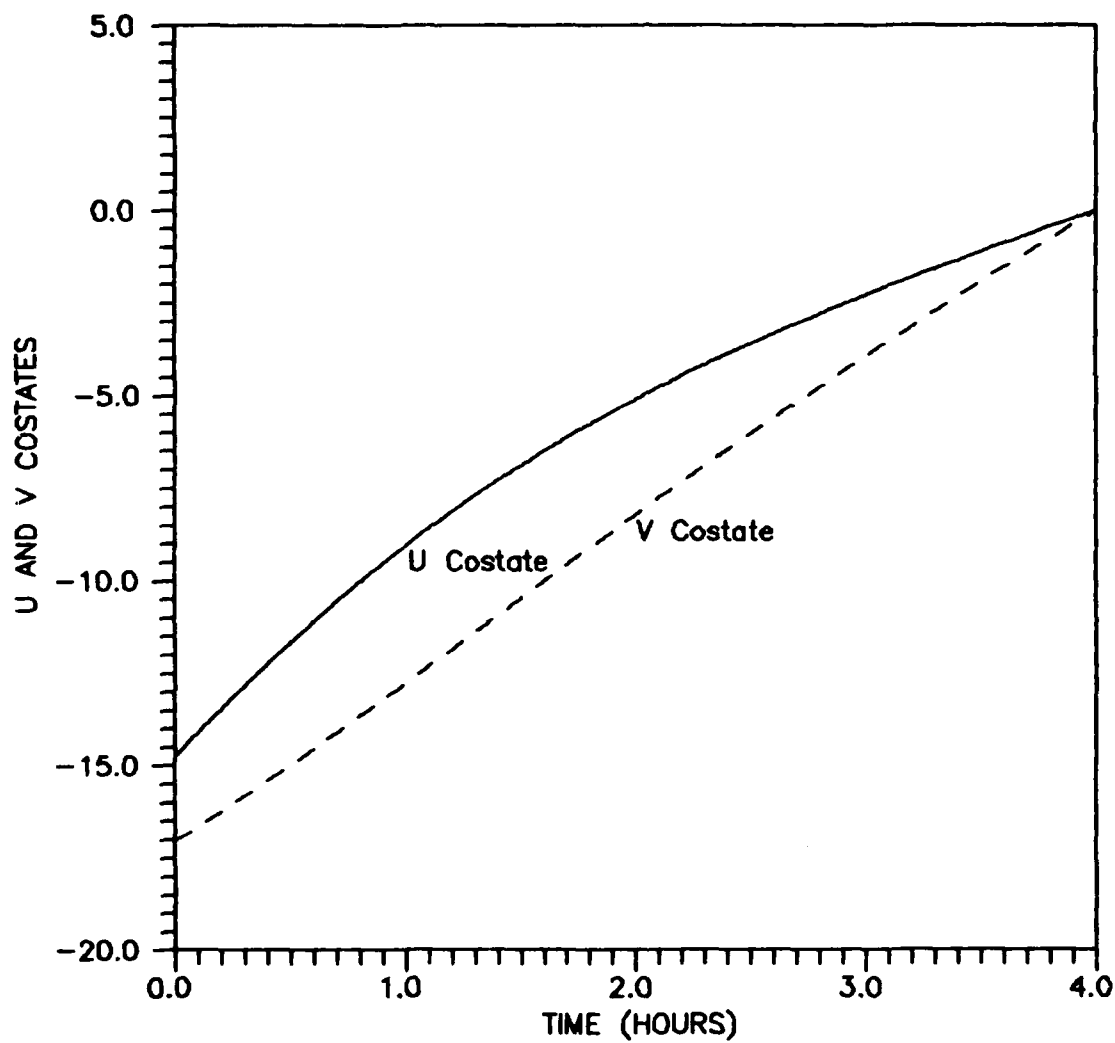
Figure 39. U and V Costates for 4 Hour Time of Flight to Minimum Radius with no Terminal Constraint
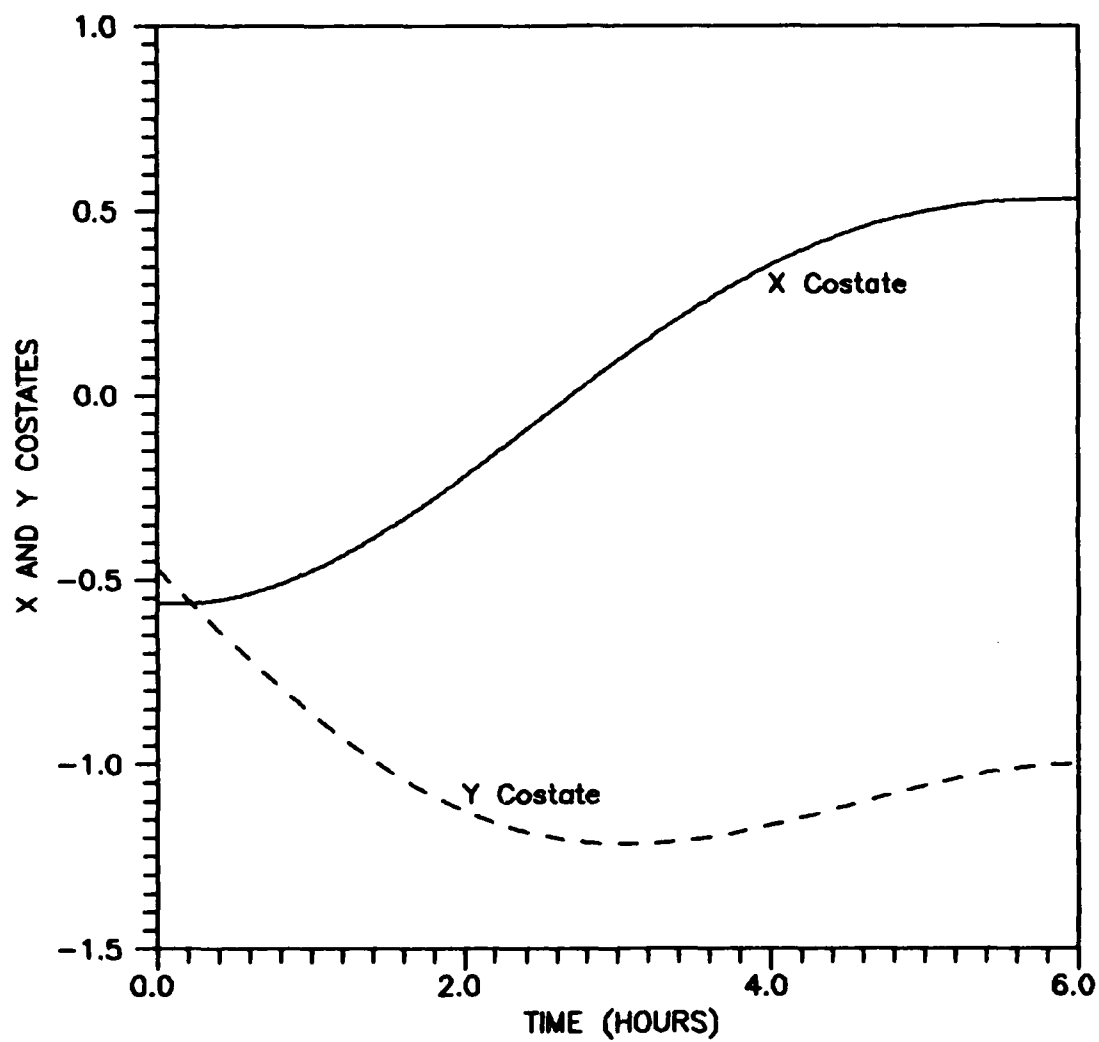
Figure 40. X and Y Costates for 6 Hour Time of Flight to Minimum Radius with no Terminal Constraint
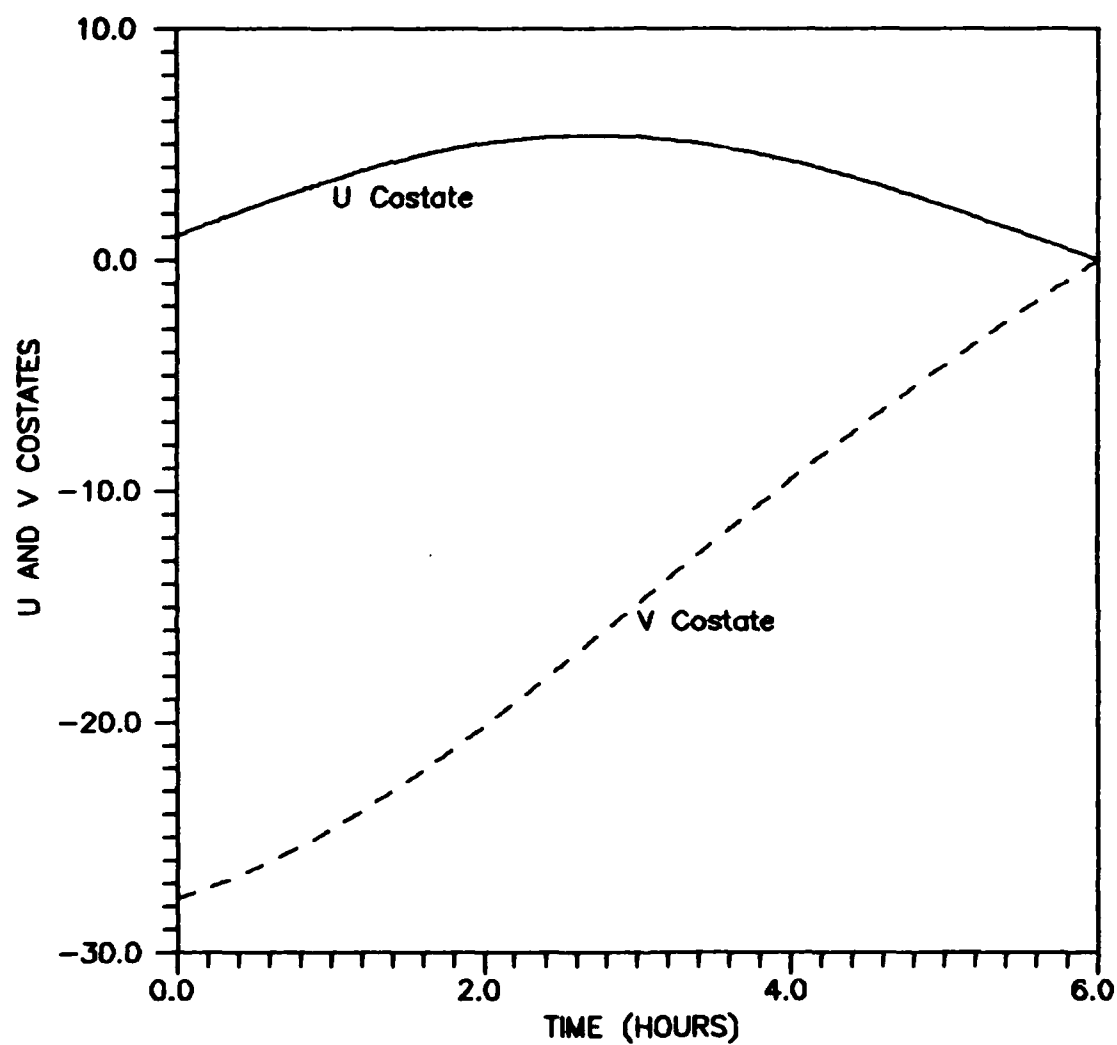
Figure 41. U and V Costates for 6 Hour Time of Flight to
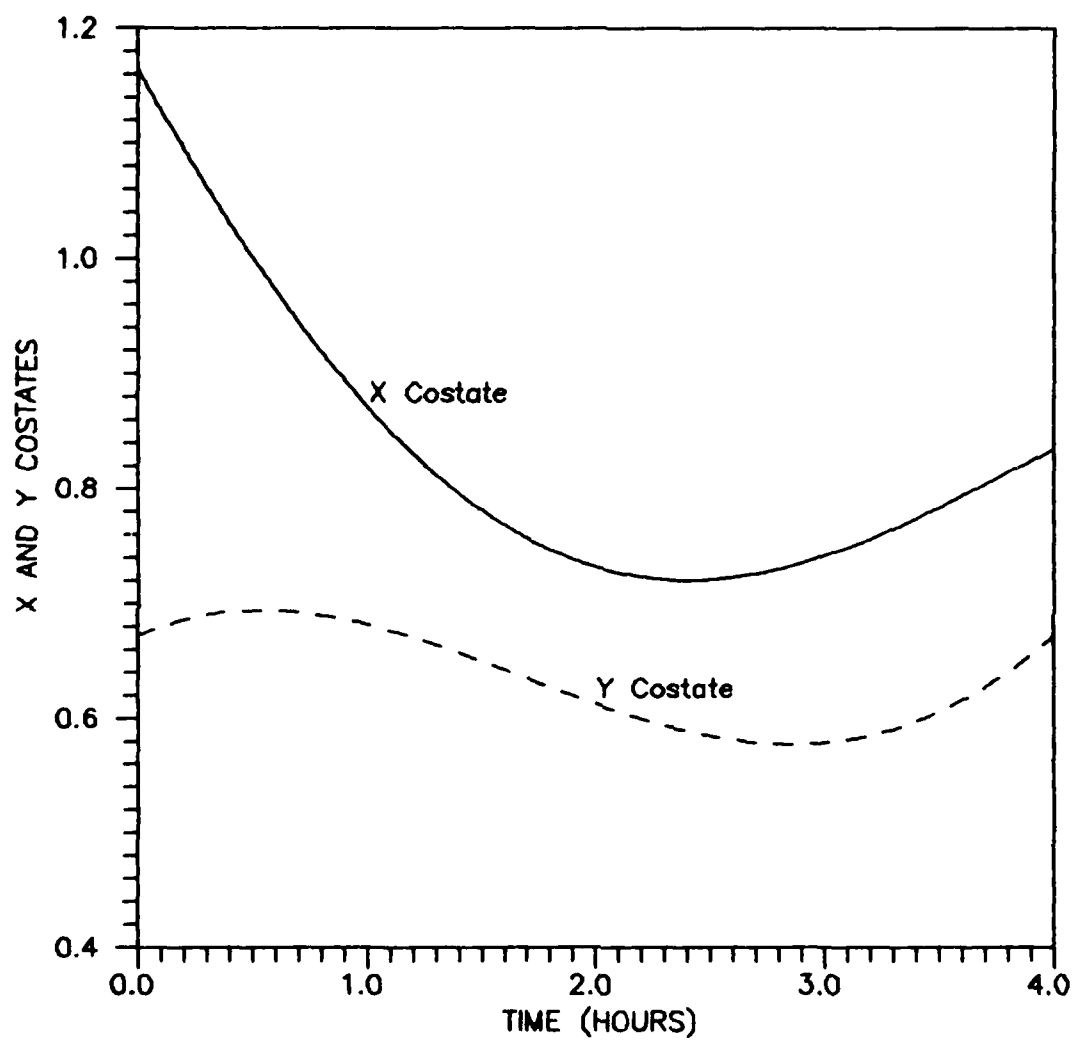Minimum Radius with no Terminal Constraint

94
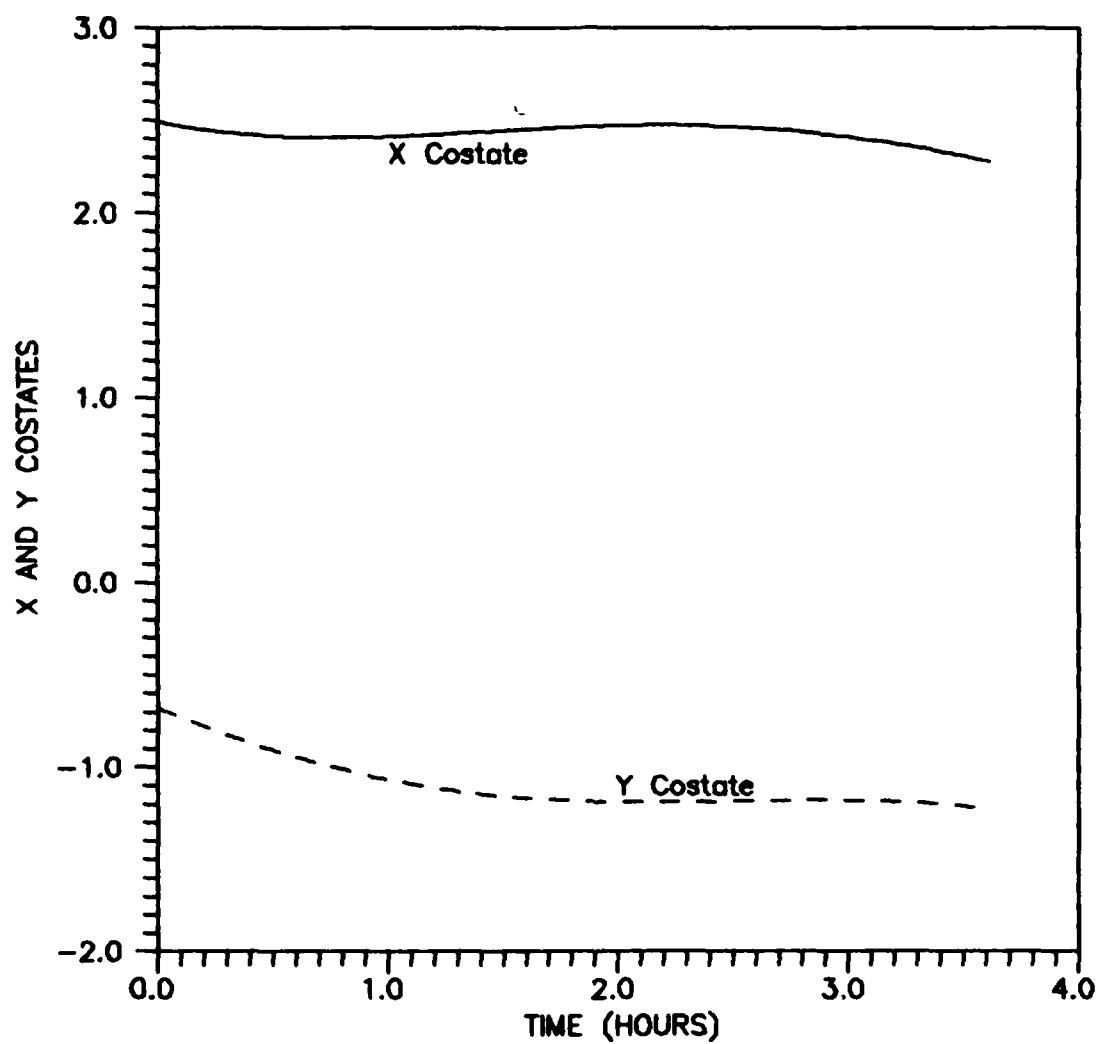
Figure 42.   X and Y Costates for Rendezvous from 2 Hour Time
of Flight to Maximum Radius with Orthogonality Constraint
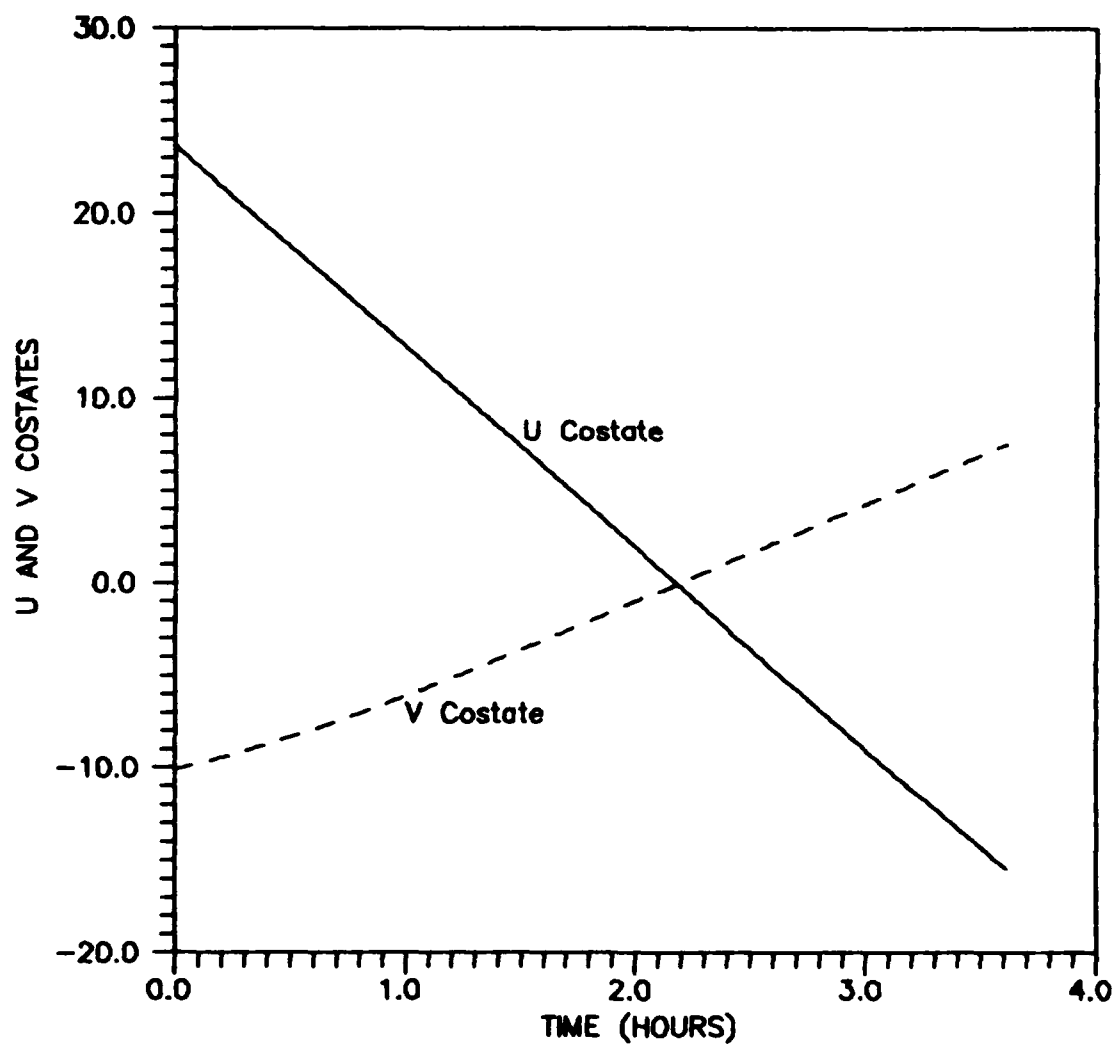
Figure 43. U and V Costates for Rendezvous from 2 Hour Time
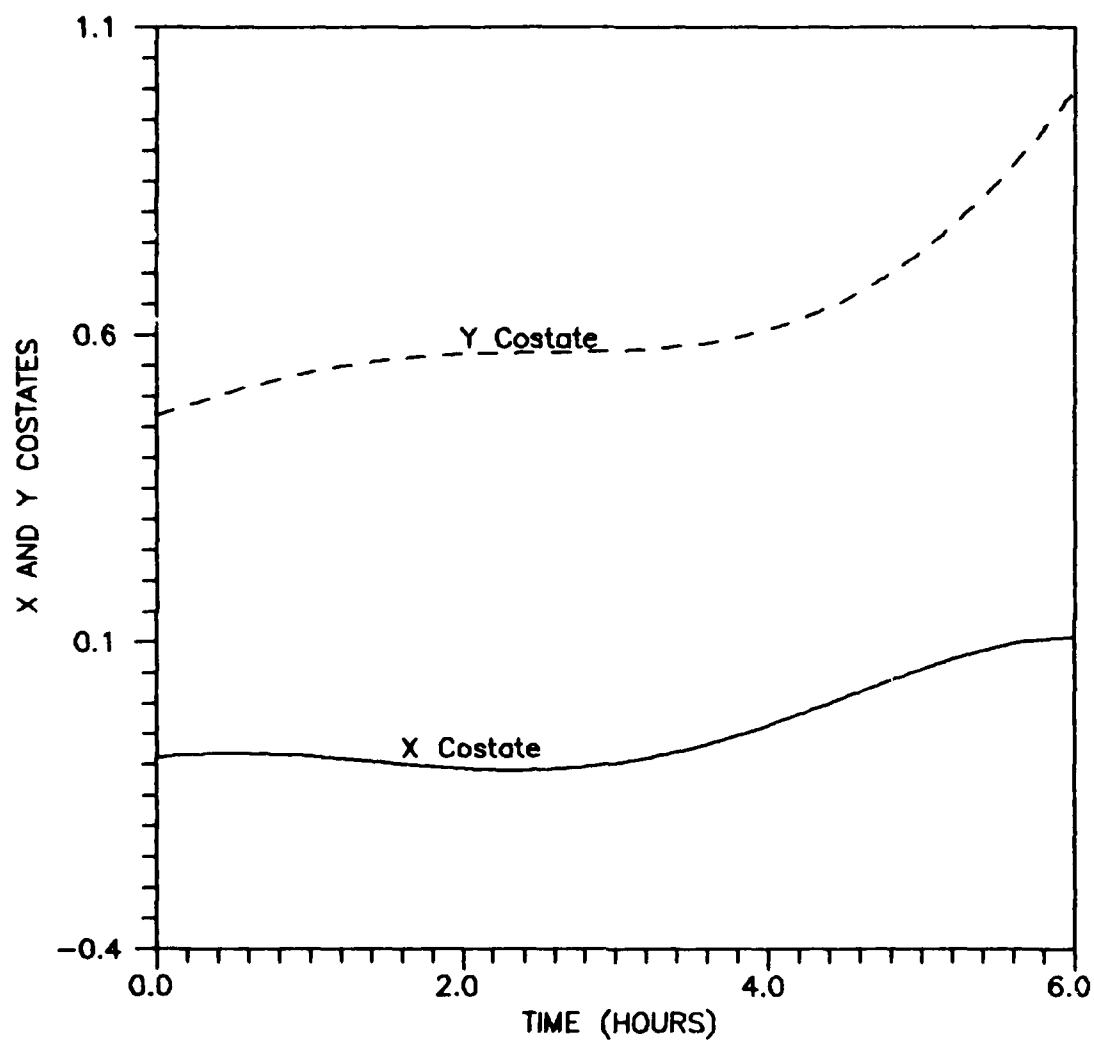of Flight to Maximum Radius with Orthogonality Constraint

96
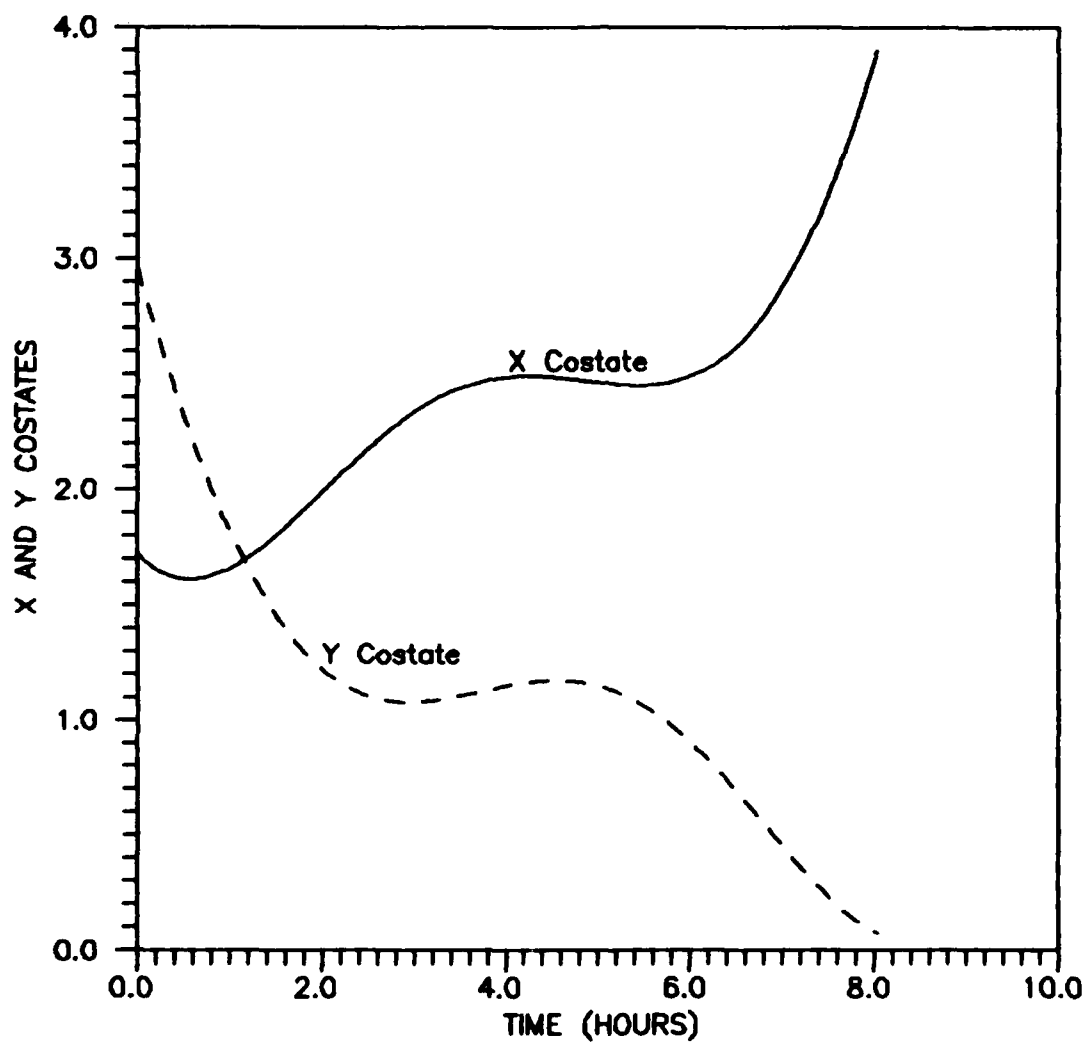
Figure 44. X and Y Costates for Rendezvous from 4 Hour Time
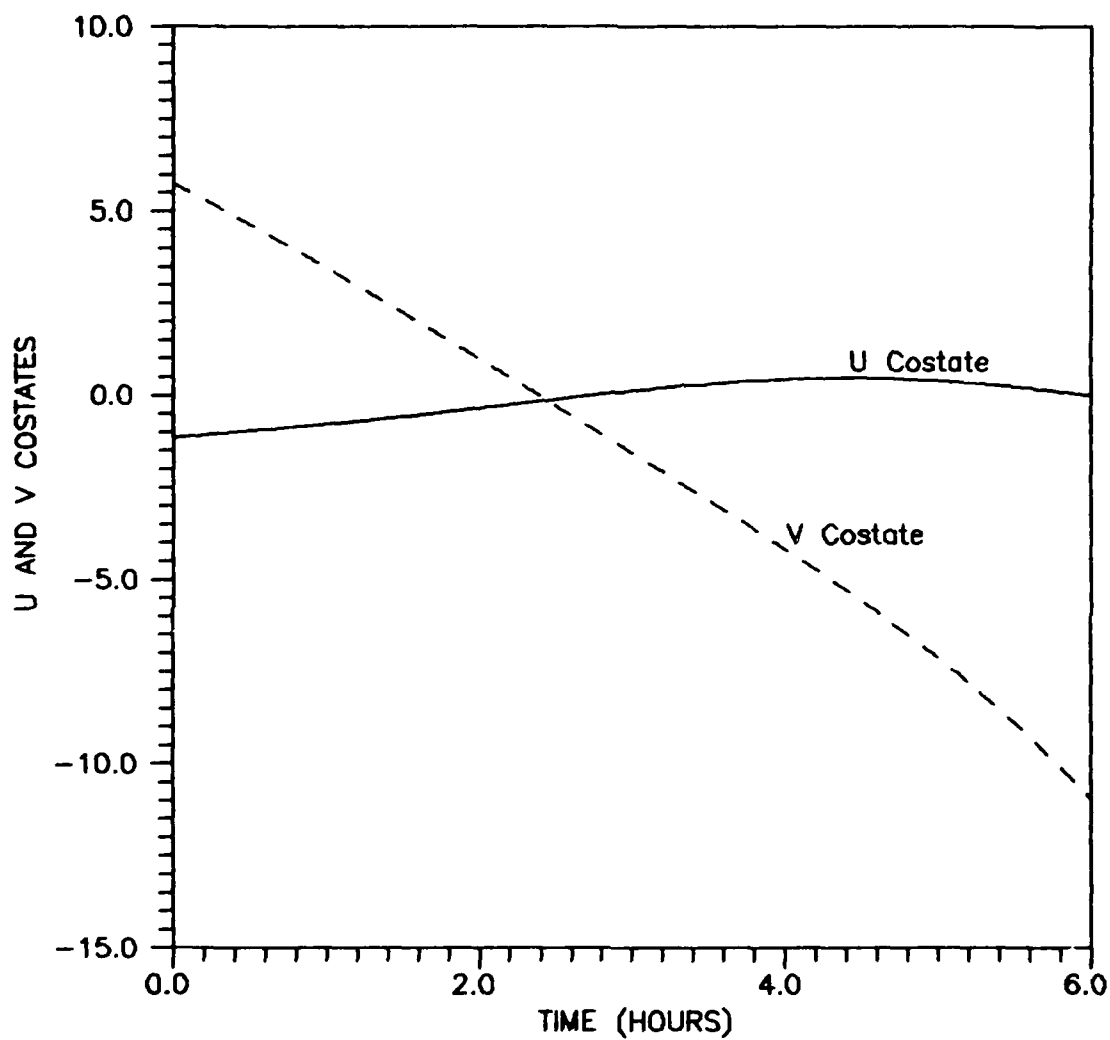of Flight to Maximum Radius with Orthogonality Constraint
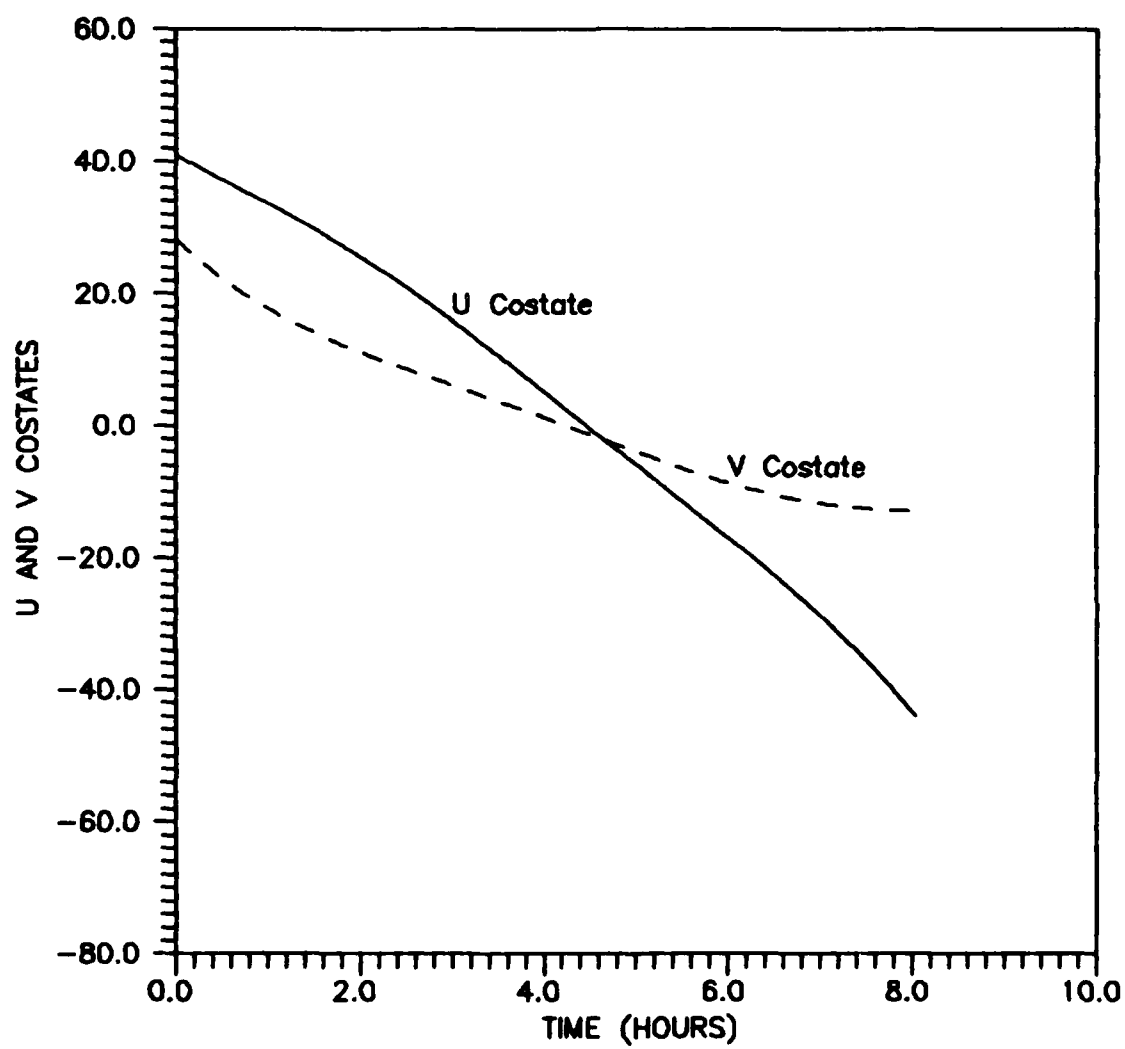
Figure 45. U and V Costates for Rendezvous from 4 Hour Time of Flight to Maximum Radius with Orthogonality Constraint
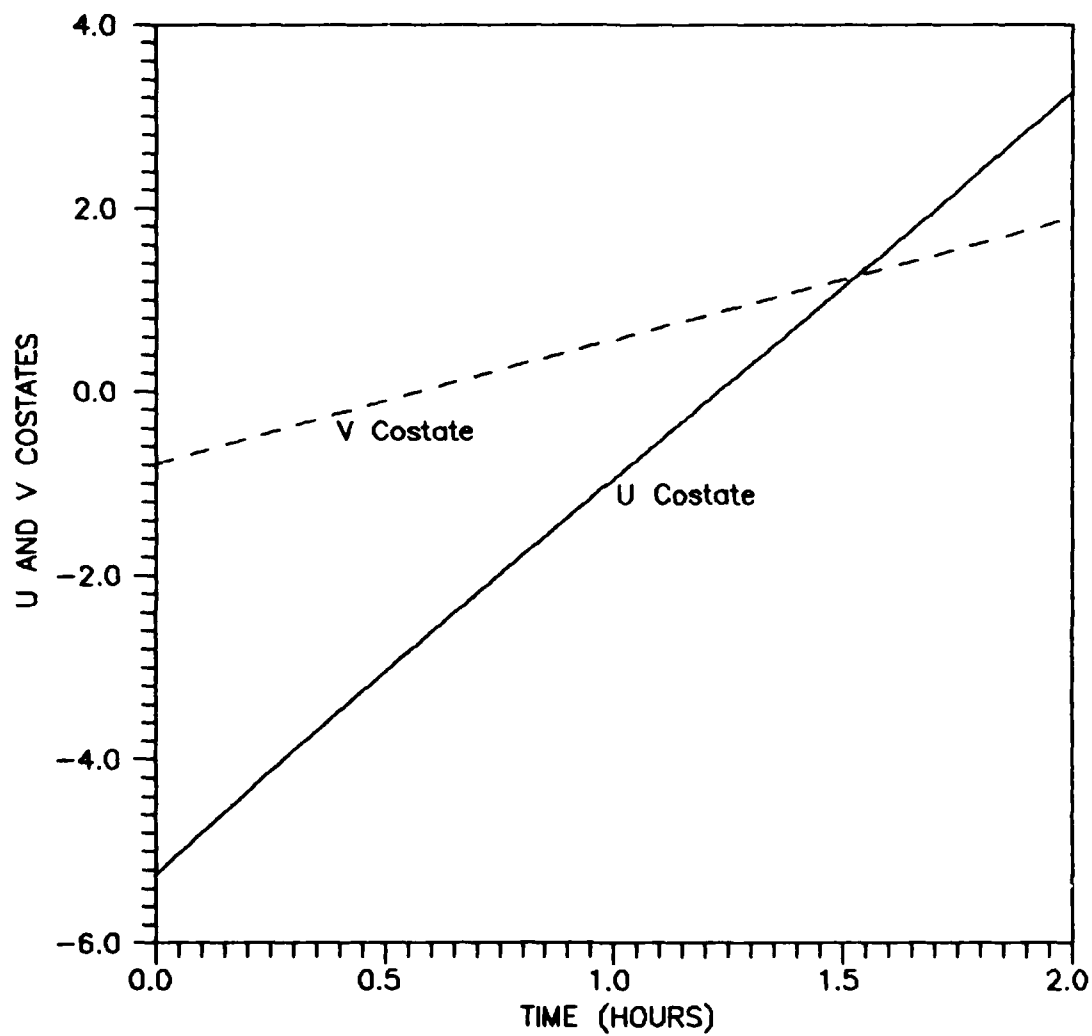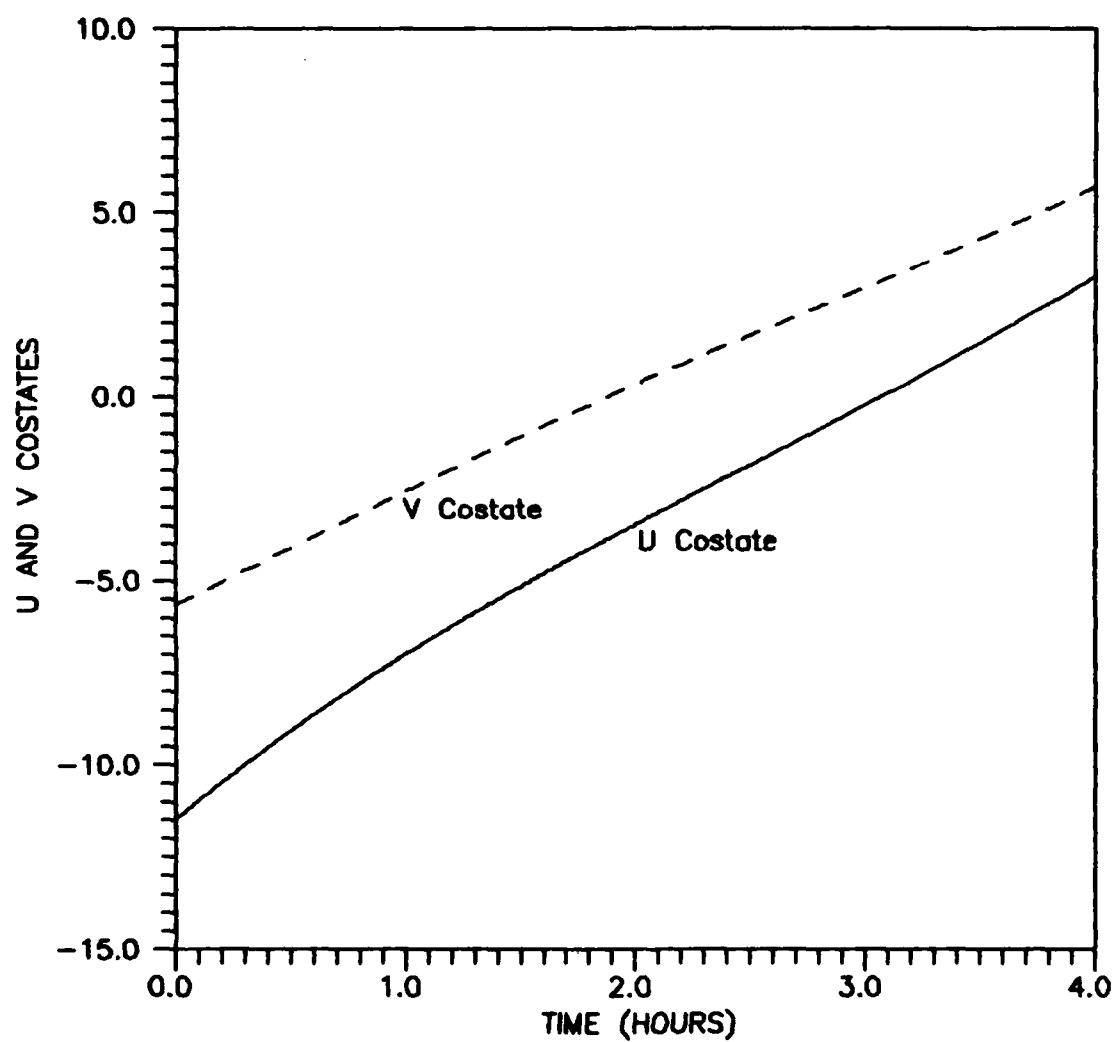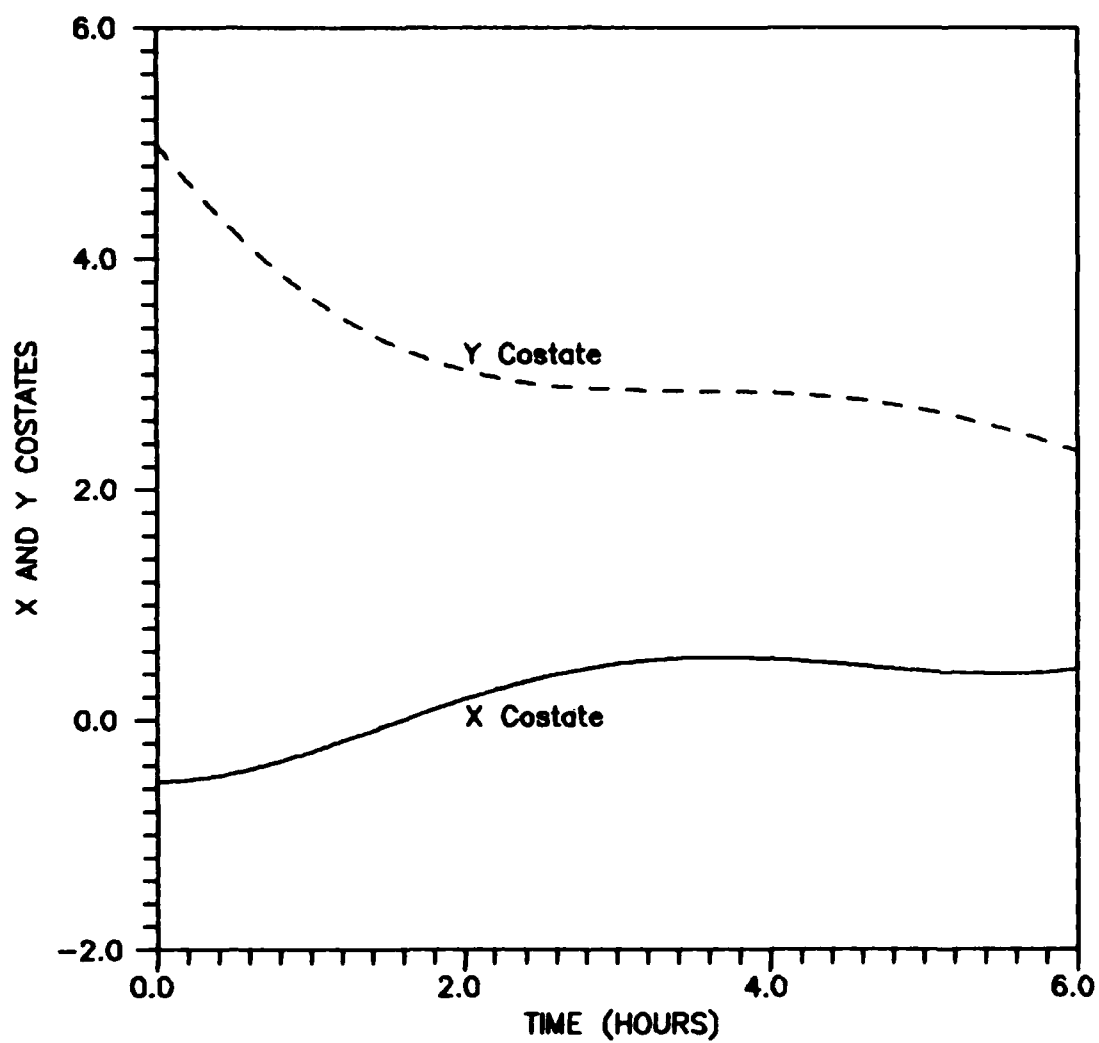
Figure 46. X and Y Costates for Rendezvous from 6 Hour Time
of Flight to Maximum Radius with Orthogonality Constraint

99
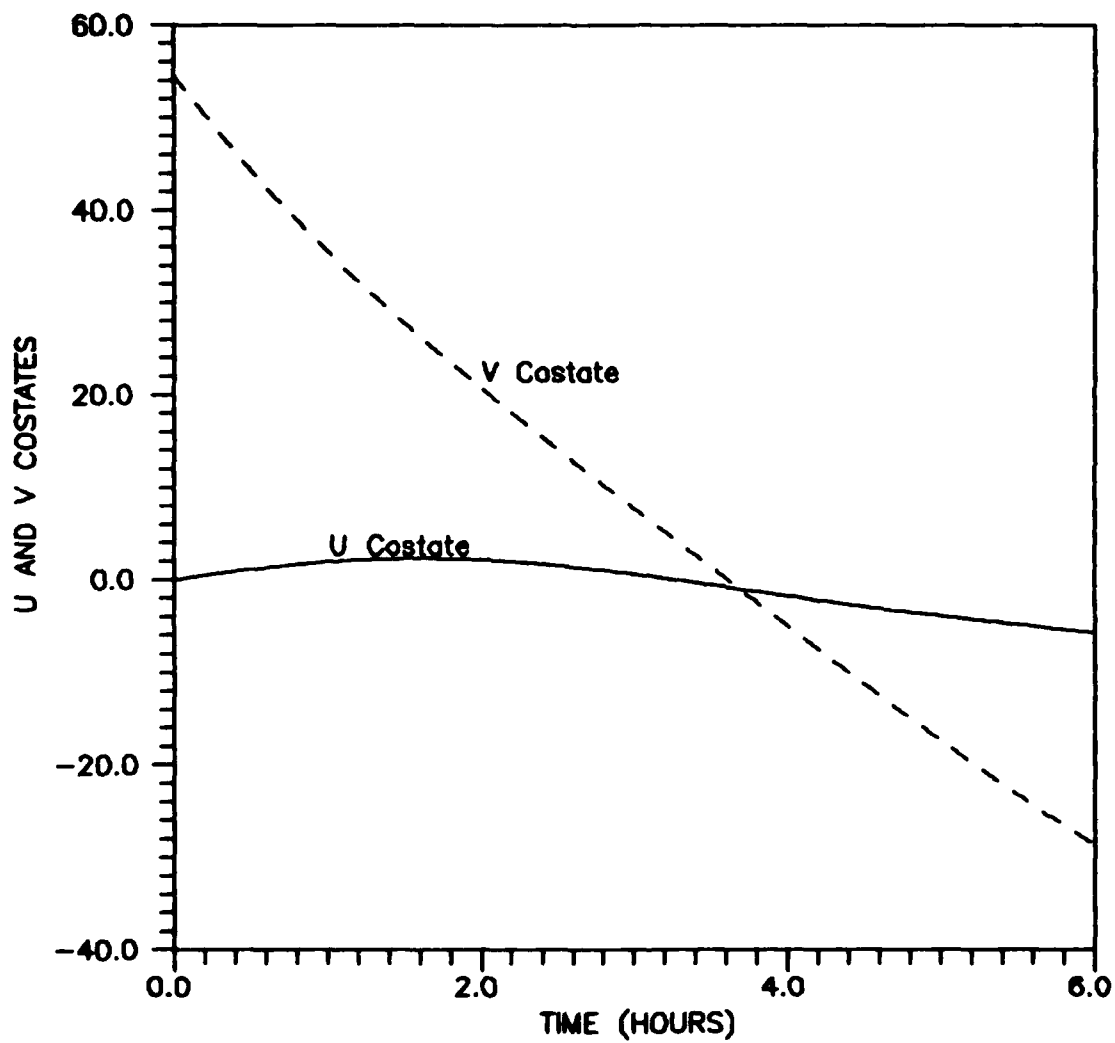
Figure 47. U and V Costates for Rendezvous from 6 Hour Time of Flight to Maximum Radius with Orthogonality Constraint

100

Table XVII. Costate Quadratic Fits for Maximum Radius
Maneuver with Terminal Constraint

TOF (Hrs)	Costate	Equation	Correlation
2	λ_x	$1.022 - .1590t + .0687t^2$	0.9996
	λ_y	$.3149 - .0305t + .0116t^2$	0.8279
	λ_u	$5.210 - 4.318t + .0502t^2$	1.0000
	λ_v	$.7880 - 1.379t + .0235t^2$	1.0000
4	λ_x	$1.157 - .3487t + .0689t^2$	0.9971
	λ_y	$.7275 - .0858t + .0143t^2$	0.7674
	λ_u	$11.11 - 4.186t + .1610t^2$	0.9989
	λ_v	$5.635 - 3.154t + .0897t^2$	0.9999
6	λ_x	$-.0595 - .0540t + .0149t^2$	0.9132
	λ_y	$.4957 + .0351t + .0007t^2$	0.7674
	λ_u	$-1.221 - .4993t + .0240t^2$	0.9904
	λ_v	$5.798 - 2.294t - .0520t^2$	0.9999

Table XVIII. Costate Quadratic Fits for Maximum Radius Maneuver with no Terminal Constraint

TOF (Hrs)	Costate	Equation	Correlation
2	λ_x	$1.135-.2717t+.0685t^2$	1.0000
	λ_y	$.5067-.0290t+.0182t^2$	0.8308
	λ_u	$8.483-4.828t+0.304t^2$	1.0000
	λ_v	$4.568-2.298t+0.000t^2$	1.0000
4	λ_x	$1.518-.5288t+.0685t^2$	0.9997
	λ_y	$.9171-.1100t-.0346t^2$	0.8238
	λ_u	$12.83-3.261t-.1224t^2$	0.9715
	λ_v	$17.06-4.369t+0.000t^2$	0.9993
6	λ_x	$.6474-.1980t-.0119t^2$	0.9884
	λ_y	$.4630+.4779t-.0748t^2$	0.9984
	λ_u	$-.8232-3.305t+.6581t^2$	0.9978
	λ_v	$28.19-3.509t-.2829t^2$	0.9986

Table XIX. Costate Quadratic Fits for Minimum Time
Rendezvous Maneuver

TOF (Hrs)	Costate	Equation	Correlation
2	λ_x	$2.401+1.273t-6.702t^2$	0.4041
	λ_y	$-.7299-6.166t+19.48t^2$	0.9678
	λ_u	$23.66-174.9t-2.077t^2$	1.0000
	λ_v	$-10.46+68.54t+56.66t^2$	0.9995
4	λ_x	$1.526+7.684t+11.86t^2$	0.9484
	λ_y	$2.875-42.91t+247.5t^2$	0.9908
	λ_u	$40.70-226.1t-827.2t^2$	0.9999
	λ_v	$26.97-336.8t+973.0t^2$	0.9960
6	λ_x	$-.7234+15.84t-49.65t^2$	0.9774
	λ_y	$4.794-32.28t+125.5t^2$	0.9782
	λ_u	$.2701+58.85t-472.9t^2$	0.9761
	λ_v	$53.06-470.3t+543.1t^2$	0.9991

VIII. Conclusions and Recommendations

Orbital evasive maneuvers enabling a target spacecraft in geosynchronous orbit to evade an interceptor in direct coasting ascent have been examined. A continuous low thrust propulsion system consisting of ten 30 centimeter primary propulsion thrusters propelled the target craft over each avoidance maneuver. The thrust vector control history was determined over time to generate the optimal spaceflight trajectory achieving a maximum change in orbit radius. In the context of optimal control theory, this change in radius was achieved by both maximizing and minimizing the orbit radius of the target spacecraft.

Two strategies were considered for the evasive maneuvers. An orthogonality constraint was first applied at the final time of each maneuver specifying the target spacecraft's terminal velocity as necessarily orthogonal to its terminal radius. The constraint was then removed such that the spacecraft traveled without regard for the final orientation of its velocity vector. When the spacecraft was allowed to travel free of constraint, the terminal thrust control angle became indeterminate. This singularity was resolved by applying L'Hôspital's rule to the bilinear tangent control law, such that the control definition applied to the state equations was changed at the final time of the evasive maneuver.

For both constraint strategies, optimal maximum radius and optimal minimum radius trajectories achieved the same change in orbit radius, but in the opposite direction. As a result of comparing the two classes of maneuvers, it was apparent that a significant penalty was paid in terms of radial distance traveled when a terminal constraint was applied. A second comparison was available in that, in the case of either strategy, change in radius was sacrificed for the elimination of orbit drift to retain the nominal orbit period. As expected, longer time of flight maneuvers yielded greater changes in orbit radius. It must be considered, however, that the time of flight of an implemented maneuver should be as short as possible to maintain a minimum of fuel consumption.

Minimum time intercepts of a specified radius were considered as a means of duplicating the maximum radius evasive maneuvers. The resulting time optimal state and control trajectories were indeed identical to results found earlier, thus verifying the quality of the maximum radius solutions.

Upon completion of the evasive maneuver, the target spacecraft was required to rendezvous with its nominal orbit position. Rendezvous maneuvers could only be completed for maximum radius maneuvers with the terminal orthogonality constraint applied due to computer memory limits. In comparing the maneuvers that were successfully completed, it

For both constraint strategies, optimal maximum radius and optimal minimum radius trajectories achieved the same change in orbit radius, but in the opposite direction. As a result of comparing the two classes of maneuvers, it was apparent that a significant penalty was paid in terms of radial distance traveled when a terminal constraint was applied. A second comparison was available in that, in the case of either strategy, change in radius was sacrificed for the elimination of orbit drift to retain the nominal orbit period. As expected, longer time of flight maneuvers yielded greater changes in orbit radius. It must be considered, however, that the time of flight of an implemented maneuver should be as short as possible to maintain a minimum of fuel consumption.

Minimum time intercepts of a specified radius were considered as a means of duplicating the maximum radius evasive maneuvers. The resulting time optimal state and control trajectories were indeed identical to results found earlier, thus verifying the quality of the maximum radius solutions.

Upon completion of the evasive maneuver, the target spacecraft was required to rendezvous with its nominal orbit position. Rendezvous maneuvers could only be completed for maximum radius maneuvers with the terminal orthogonality constraint applied due to computer memory limits. In comparing the maneuvers that were successfully completed, it

was evident that the time required to rendezvous was, in general, significantly greater than the time of flight of the evasive maneuver. One case was found, however, in which a six hour orbit evasive maneuver enabled an approximately equal time of flight for the rendezvous maneuver. This anomaly was attributed to the position of the target spacecraft at the end of the six hour evasive maneuver, which was on the same radius vector as the nominal orbit as a result of the elimination of orbit drift. Thus, a trade-off was apparent in which the optimal evasive maneuver did not necessarily transition readily to the optimal rendezvous maneuver.

Rendezvous maneuvers following minimum radius evasive maneuvers were not a concern since the evasive trajectory may tend to pass through a lethal radius centered on an ascending interceptor, depending upon the interceptor's particular characteristics. It was anticipated, however, that these maneuvers would consume less time than the return maneuvers from maximum radius evasions due to their shorter path length.

The optimal rendezvous trajectory from the evasive maneuvers with no terminal constraint could not be determined by numerical methods due to memory limits on the computer system used. It was anticipated, however, that the return from a position with an unconstrained velocity vector would require significantly more time than that from an

orientation determined by the orthogonality constraint.

In order to resolve the intercept-rendezvous problem completely in terms of total minimum fuel expended, the numerical solution for the return maneuver from an unconstrained evasive maneuver must be determined on a computer system with greater memory capacity. Current plans include adapting the associated two point boundary value problem solution on the ASD Cyber system.

The development and solutions herein are precursors to modeling a target spacecraft in three dimensions. Various dynamics of the interceptor may also be considered, such that the threat is itself maneuvering. The formulation of the optimal control problem would then maximize the distance between the threat and the target spacecraft at the nominal intercept time, where the states would be given in terms of the vector from interceptor to target and its first time derivative. Such a description of the two point boundary value problem would determine if out of plane maneuvers are potentially more optimal than those in plane. These studies could yield practical results pertinent to future spacecraft mission planning and the increasingly relevant intercept avoidance problem.

Appendix A: <u>Subroutines</u> <u>FCNI</u>, <u>FCNJ</u> <u>and</u> <u>FCNB</u> <u>for Maximum</u>
<u>Radius Evasive Maneuver with Orthogonality Constraint</u>

```
      SUBROUTINE FCNI(N,T,X,XP)
      DOUBLE PRECISION T,X(N),XP(N),MU,R,R3,R5,B,D,TH,MO,MD,
     *   DSC
      INTEGER N
      COMMON /A/ MU /B/ TH,MO,MD
      R=DSQRT(X(1)**2+X(2)**2)
      B=TH/(MO-MD*T)
      DSC=DSQRT(X(7)**2+X(8)**2)
      D=X(7)*X(1)+X(8)*X(2)
      R3=R**3
      R5=R**5
      XP(1)=X(3)
      XP(2)=X(4)
      XP(3)=-MU*X(1)/R3+B*X(7)/DSC
      XP(4)=-MU*X(2)/R3+B*X(8)/DSC
      XP(5)=MU*(X(7)/R3-3.0d+00*D*X(1)/R5)
      XP(6)=MU*(X(8)/R3-3.0d+00*D*X(2)/R5)
      XP(7)=-X(5)
      XP(8)=-X(6)
      RETURN
      END
*
*******************************************************************
*
      SUBROUTINE FCNJ(N,T,X,PD)
      DOUBLE PRECISION T,X(N),PD(N,N),MU,R,R3,R5,R7,B,D,TH,
     *   MO,MD,E,F,G,DSC
      INTEGER N
      COMMON /A/ MU /B/ TH,MO,MD
      R=DSQRT(X(1)**2+X(2)**2)
      B=TH/(MO-MD*T)
      R3=R**3
      R5=R**5
      R7=R**7
      DSC=DSQRT(X(7)**2+X(8)**2)
      D=X(7)*X(1)+X(8)*X(2)
      E=X(7)*X(2)+X(8)*X(1)
      F=3.0d+00*X(7)*X(1)+X(8)*X(2)
      G=3.0d+00*X(8)*X(2)+X(7)*X(1)

      PD(1,1)=0.0
      PD(1,2)=0.0
      PD(1,3)=1.00d+00
      PD(1,4)=0.0
      PD(1,5)=0.0
      PD(1,6)=0.0
      PD(1,7)=0.0
      PD(1,8)=0.0
```

108

```
PD(2,1)=0.0
PD(2,2)=0.0
PD(2,3)=0.0
PD(2,4)=1.0d+00
PD(2,5)=0.0
PD(2,6)=0.0
PD(2,7)=0.0
PD(2,8)=0.0

PD(3,1)=MU*(-1.0d+00/R3+3.0d+00*X(1)**2/R5)
PD(3,2)=3.00d+00*MU*X(1)*X(2)/R5
PD(3,3)=0.0
PD(3,4)=0.0
PD(3,5)=0.0
PD(3,6)=0.0
PD(3,7)=B*X(8)**2/DSC**3
PD(3,8)=-B*X(7)*X(8)/DSC**3

PD(4,1)=PD(3,2)
PD(4,2)=MU*(-1.0d+00/R3+3.0d+00*X(2)**2/R5)
PD(4,3)=0.0
PD(4,4)=0.0
PD(4,5)=0.0
PD(4,6)=0.0
PD(4,7)=PD(3,8)
PD(4,8)=B*X(7)**2/DSC**3

PD(5,1)=MU*(-3.0d+00*F/R5+15.0d+00*X(1)**2*D/R7)
PD(5,2)=MU*(-3.0d+00*E/R5+15.0d+00*X(1)*X(2)*D/R7)
PD(5,3)=0.0
PD(5,4)=0.0
PD(5,5)=0.0
PD(5,6)=0.0
PD(5,7)=-PD(3,1)
PD(5,8)=-PD(3,2)

PD(6,1)=PD(5,2)
PD(6,2)=MU*(-3.0d+00*G/R5+15.0d+00*X(2)**2*D/R7)
PD(6,3)=0.0
PD(6,4)=0.0
PD(6,5)=0.0
PD(6,6)=0.0
PD(6,7)=PD(5,8)
PD(6,8)=-PD(4,2)

PD(7,1)=0.0
PD(7,2)=0.0
PD(7,3)=0.0
PD(7,4)=0.0
PD(7,5)=-1.0d+00
PD(7,6)=0.0
```

```
          PD(7,7)=0.0
          PD(7,8)=0.0

          PD(8,1)=0.0
          PD(8,2)=0.0
          PD(8,3)=0.0
          PD(8,4)=0.0
          PD(8,5)=0.0
          PD(8,6)=-1.0d+00
          PD(8,7)=0.0
          PD(8,8)=0.0

          RETURN
          END
*
***************************************************************
*
          SUBROUTINE FCNB(N,XA,XB,F)
          DOUBLE PRECISION XA(N),XB(N),F(N),KS,KM,RB
          INTEGER N
          COMMON /CONV/ KM,KS
          RB=DSQRT(XB(1)**2+XB(2)**2)
          F(1)=XA(1)-KM
          F(2)=XA(2)
          F(3)=XA(3)
          F(4)=XA(4)-KS
          F(5)=XB(1)*XB(3)+XB(2)*XB(4)
          F(6)=XB(5)*XB(1)-XB(1)**2/RB-XB(7)*XB(3)
          F(7)=XB(6)*XB(2)-XB(2)**2/RB-XB(8)*XB(4)
          F(8)=XB(8)*XB(1)-XB(7)*XB(2)
          RETURN
          END
```

110

Appendix B: Subroutines FCMI, FCMJ and FCMB for Maximum
Radius Maneuver with no Terminal Constraint

```
      SUBROUTINE FCMI(N,T,X,XP)
      DOUBLE PRECISION T,X(N),XP(N),MU,R,R3,R5,B,D,TH,MO,MD,
     *  DSC
      INTEGER N
      COMMON /A/ MU /B/ TH,MO,MD
      B=TH/(MO-MD*T)
      DSC=DSQRT(X(7)**2+X(8)**2)
      D=X(7)*X(1)+X(8)*X(2)
      R3=R**3
      R5=R**5
      XP(1)=X(3)
      XP(2)=X(4)
      IF (DSC .NE. 0.0d+00) THEN
      XP(3)=-MU*X(1)/R3+B*X(7)/DSC
      XP(4)=-MU*X(2)/R3+B*X(8)/DSC
      ELSE
      DSC=DSQRT(X(5)**2+X(6)**2)
      XP(3)=-MU*X(1)/R3+B*X(5)/DSC
      XP(4)=-MU*X(2)/R3+B*X(6)/DSC
      ENDIF
      XP(5)=MU*(X(7)/R3-3.0d+00*D*X(1)/R5)
      XP(6)=MU*(X(8)/R3-3.0d+00*D*X(2)/R5)
      XP(7)=-X(5)
      XP(8)=-X(6)
      RETURN
      END
*
****************************************************************
*
      SUBROUTINE FCMJ(N,T,X,PD)
      DOUBLE PRECISION T,X(N),PD(N,N),MU,R,R3,R5,R7,B,D,TH,
     *  MO,MD,E,F,G,DSC
      INTEGER N
      COMMON /A/ MU /B/ TH,MO,MD
      R=DSQRT(X(1)**2+X(2)**2)
      B=TH/(MO-MD*T)
      R3=R**3
      R5=R**5
      R7=R**7
      DSC=DSQRT(X(7)**2+X(8)**2)
      D=X(7)*X(1)+X(8)*X(2)
      E=X(7)*X(2)+X(8)*X(1)
      F=3.0d+00*X(7)*X(1)+X(8)*X(2)
      G=3.0d+00*X(8)*X(2)+X(7)*X(1)
      IF (DSC .NE. 0.0d+00) THEN

      PD(1,1)=0.0
      PD(1,2)=0.0
```

111

```
        PD(1,3)=1.00d+00
        PD(1,4)=0.0
        PD(1,5)=0.0
        PD(1,6)=0.0
        PD(1,7)=0.0
        PD(1,8)=0.0

        PD(2,1)=0.0
        PD(2,2)=0.0
        PD(2,3)=0.0
        PD(2,4)=1.0d+00
        PD(2,5)=0.0
        PD(2,6)=0.0
        PD(2,7)=0.0
        PD(2,8)=0.0

        PD(3,1)=MU*(-1.0d+00/R3+3.0d+00*X(1)**2/R5)
        PD(3,2)=3.00d+00*MU*X(1)*X(2)/R5
        PD(3,3)=0.0
        PD(3,4)=0.0
        PD(3,5)=0.0
        PD(3,6)=0.0
        PD(3,7)=B*X(8)**2/DSC**3
        PD(3,8)=-B*X(7)*X(8)/DSC**3

        PD(4,1)=PD(3,2)
        PD(4,2)=MU*(-1.0d+00/R3+3.0d+00*X(2)**2/R5)
        PD(4,3)=0.0
        PD(4,4)=0.0
        PD(4,5)=0.0
        PD(4,6)=0.0
        PD(4,7)=PD(3,8)
        PD(4,8)=B*X(7)**2/DSC**3

        PD(5,1)=MU*(-3.0d+00*F/R5+15.0d+00*X(1)**2*D/R7)
        PD(5,2)=MU*(-3.0d+00*E/R5+15.0d+00*X(1)*X(2)*D/R7)
        PD(5,3)=0.0
        PD(5,4)=0.0
        PD(5,5)=0.0
        PD(5,6)=0.0
        PD(5,7)=-PD(3,1)
        PD(5,8)=-PD(3,2)

        PD(6,1)=PD(5,2)
        PD(6,2)=MU*(-3.0d+00*G/R5+15.0d+00*X(2)**2*D/R7)
        PD(6,3)=0.0
        PD(6,4)=0.0
        PD(6,5)=0.0
        PD(6,6)=0.0
        PD(6,7)=PD(5,8)
        PD(6,8)=-PD(4,2)
```

112

```
      PD(7,1)=0.0
      PD(7,2)=0.0
      PD(7,3)=0.0
      PD(7,4)=0.0
      PD(7,5)=-1.0d+00
      PD(7,6)=0.0
      PD(7,7)=0.0
      PD(7,8)=0.0

      PD(8,1)=0.0
      PD(8,2)=0.0
      PD(8,3)=0.0
      PD(8,4)=0.0
      PD(8,5)=0.0
      PD(8,6)=-1.0d+00
      PD(8,7)=0.0
      PD(8,8)=0.0

      ELSE
      DSC=DSQRT(X(5)**2+X(6)**2)

      PD(1,1)=0.0
      PD(1,2)=0.0
      PD(1,3)=1.00d+00
      PD(1,4)=0.0
      PD(1,5)=0.0
      PD(1,6)=0.0
      PD(1,7)=0.0
      PD(1,8)=0.0

      PD(2,1)=0.0
      PD(2,2)=0.0
      PD(2,3)=0.0
      PD(2,4)=1.0d+00
      PD(2,5)=0.0
      PD(2,6)=0.0
      PD(2,7)=0.0
      PD(2,8)=0.0

      PD(3,1)=MU*(-1.0d+00/R3+3.0d+00*X(1)**2/R5)
      PD(3,2)=3.00d+00*MU*X(1)*X(2)/R5
      PD(3,3)=0.0
      PD(3,4)=0.0
      PD(3,7)=0.0
      PD(3,8)=0.0
      PD(3,5)=B*X(6)**2/DSC**3
      PD(3,6)=-B*X(5)*X(6)/DSC**3

      PD(4,1)=PD(3,2)
      PD(4,2)=MU*(-1.0d+00/R3+3.0d+00*X(2)**2/R5)
      PD(4,3)=0.0
      PD(4,4)=0.0
```

113

```fortran
      PD(4,7)=0.0
      PD(4,8)=0.0
      PD(4,5)=PD(3,6)
      PD(4,6)=B*X(5)**2/DSC**3

      PD(5,1)=MU*(-3.0d+00*F/R5+15.0d+00*X(1)**2*D/R7)
      PD(5,2)=MU*(-3.0d+00*E/R5+15.0d+00*X(1)*X(2)*D/R7)
      PD(5,3)=0.0
      PD(5,4)=0.0
      PD(5,5)=0.0
      PD(5,6)=0.0
      PD(5,7)=-PD(3,1)
      PD(5,8)=-PD(3,2)

      PD(6,1)=PD(5,2)
      PD(6,2)=MU*(-3.0d+00*G/R5+15.0d+00*X(2)**2*D/R7)
      PD(6,3)=0.0
      PD(6,4)=0.0
      PD(6,5)=0.0
      PD(6,6)=0.0
      PD(6,7)=PD(5,8)
      PD(6,8)=-PD(4,2)

      PD(7,1)=0.0
      PD(7,2)=0.0
      PD(7,3)=0.0
      PD(7,4)=0.0
      PD(7,5)=-1.0d+00
      PD(7,6)=0.0
      PD(7,7)=0.0
      PD(7,8)=0.0

      PD(8,1)=0.0
      PD(8,2)=0.0
      PD(8,3)=0.0
      PD(8,4)=0.0
      PD(8,5)=0.0
      PD(8,6)=-1.0d+00
      PD(8,7)=0.0
      PD(8,8)=0.0

      ENDIF
      RETURN
      END
*
****************************************************************
*
      SUBROUTINE FCNB(N,XA,XB,F)
      DOUBLE PRECISION XA(N),XB(N),F(N),KS,KM,RB,AL
      INTEGER N
      COMMON /CONV/ KM,KS
      COMMON /CONST/ AL
```

114

```
RB=DSQRT(XB(1)**2+XB(2)**2)
F(1)=XA(1)-XM
F(2)=XA(2)
F(3)=XA(3)
F(4)=XA(4)-KS
F(5)=AL*(XB(1)*XB(3)+XB(2)*XB(4))+(1.0d+00-AL)*XB(7)
F(6)=XB(5)*XB(1)-XB(1)**2/RB-AL*(XB(7)*XB(3))
F(7)=XB(6)*XB(2)-XB(2)**2/RB-AL*(XB(8)*XB(4))
F(8)=AL*(XB(8)*XB(1)-XB(7)*XB(2))+(1.0d+00-AL)*XB(8)
RETURN
END
```

```fortran
      SUBROUTINE FCNI(N,T,X,XP)
      DOUBLE PRECISION T,X(N),XP(N),MU,R,R3,R5,B,D,TH,MO,MD,
     *   DSC
      INTEGER N
      COMMON /ACOM/ MU /BCOM/ TH,MO,MD
      R=DSQRT(X(1)**2+X(2)**2)
      B=TH/(MO-MD*T*X(9))
      DSC=DSQRT(X(7)**2+X(8)**2)
      D=X(7)*X(1)+X(8)*X(2)
      R3=R**3
      R5=R**5
      XP(1)=X(3)*X(9)
      XP(2)=X(4)*X(9)
      XP(3)=(-MU*X(1)/R3-B*X(7)/DSC)*X(9)
      XP(4)=(-MU*X(2)/R3-B*X(8)/DSC)*X(9)
      XP(5)=MU*(X(7)/R3-3.0d+00*D*X(1)/R5)*X(9)
      XP(6)=MU*(X(8)/R3-3.0d+00*D*X(2)/R5)*X(9)
      XP(7)=-X(5)*X(9)
      XP(8)=-X(6)*X(9)
      XP(9)=0.0d+00
      RETURN
      END
*
************************************************************
*
      SUBROUTINE FCNJ(N,T,X,PD)
      DOUBLE PRECISION T,X(N),PD(N,N),MU,R,R3,R5,R7,B,D,TH,
     *   MO,MD,E,F,G,DSC
      INTEGER N
      COMMON /ACOM/ MU /BCOM/ TH,MO,MD
      R=DSQRT(X(1)**2+X(2)**2)
      B=TH/(MO-MD*T*X(9))
      DSC=DSQRT(X(7)**2+X(8)**2)
      R3=R**3
      R5=R**5
      R7=R**7
      D=X(7)*X(1)+X(8)*X(2)
      E=X(7)*X(2)+X(8)*X(1)
      F=3.0d+00*X(7)*X(1)+X(8)*X(2)
      G=3.0d+00*X(8)*X(2)+X(7)*X(1)

      PD(1,1)=0.0
      PD(1,2)=0.0
      PD(1,3)=X(9)
      PD(1,4)=0.0
      PD(1,5)=0.0
      PD(1,6)=0.0
      PD(1,7)=0.0
```

116

```
PD(1,8)=0.0
PD(1,9)=X(3)

PD(2,1)=0.0
PD(2,2)=0.0
PD(2,3)=0.0
PD(2,4)=X(9)
PD(2,5)=0.0
PD(2,6)=0.0
PD(2,7)=0.0
PD(2,8)=0.0
PD(2,9)=X(4)

PD(3,1)=MU*(-1.0d+00/R3+3.0d+00*X(1)**2/R5)*X(9)
PD(3,2)=3.00d+00*MU*X(1)*X(2)/R5*X(9)
PD(3,3)=0.0
PD(3,4)=0.0
PD(3,5)=0.0
PD(3,6)=0.0
PD(3,7)=-B*X(8)**2/DSC**3*X(9)
PD(3,8)=B*X(8)*X(7)/DSC**3*X(9)
PD(3,9)=-MU*X(1)/R3-B*X(7)/DSC

PD(4,1)=PD(3,2)
PD(4,2)=MU*(-1.0d+00/R3+3.0d+00*X(2)**2/R5)*X(9)
PD(4,3)=0.0
PD(4,4)=0.0
PD(4,5)=0.0
PD(4,6)=0.0
PD(4,7)=PD(3,8)
PD(4,8)=-B*X(7)**2/DSC**3*X(9)
PD(4,9)=-MU*X(2)/R3-B*X(8)/DSC

PD(5,1)=MU*(-3.0d+00*F/R5+15.0d+00*X(1)**2*D/R7)*X(9)
PD(5,2)=MU*(-3.0d+00*E/R5+15.0d+00*X(1)*X(2)*D/R7)*X(9)
PD(5,3)=0.0
PD(5,4)=0.0
PD(5,5)=0.0
PD(5,6)=0.0
PD(5,7)=-PD(3,1)
PD(5,8)=-PD(3,2)
PD(5,9)=MU*(X(7)/R3-3.0d+00*X(1)*D/R5)

PD(6,1)=PD(5,2)
PD(6,2)=MU*(-3.0d+00*G/R5+15.0d+00*X(2)**2*D/R7)*X(9)
PD(6,3)=0.0
PD(6,4)=0.0
PD(6,5)=0.0
PD(6,6)=0.0
PD(6,7)=PD(5,8)
PD(6,8)=-PD(4,2)
PD(6,9)=MU*(X(8)/R3-3.0d+00*X(2)*D/R5)
```

```
          PD(7,1)=0.0
          PD(7,2)=0.0
          PD(7,3)=0.0
          PD(7,4)=0.0
          PD(7,5)=-X(9)
          PD(7,6)=0.0
          PD(7,7)=0.0
          PD(7,8)=0.0
          PD(7,9)=-X(5)

          PD(8,1)=0.0
          PD(8,2)=0.0
          PD(8,3)=0.0
          PD(8,4)=0.0
          PD(8,5)=0.0
          PD(8,6)=-X(9)
          PD(8,7)=0.0
          PD(8,8)=0.0
          PD(8,9)=-X(6)

          PD(9,1)=0.0
          PD(9,2)=0.0
          PD(9,3)=0.0
          PD(9,4)=0.0
          PD(9,5)=0.0
          PD(9,6)=0.0
          PD(9,7)=0.0
          PD(9,8)=0.0
          PD(9,9)=0.0

          RETURN
          END
*
************************************************************
*
          SUBROUTINE FCNB(N,XA,XB,F)
          DOUBLE PRECISION XA(N),XB(N),F(N),KM,KS,RB3,XBP3,XBP4,
     *     TH,MO,MD,MU,BF,XBNOM(4),DCB,W,TP,AL
          INTEGER N
          COMMON /ACOM/ MU /BCOM/ TH,MO,MD /CONV/ KM,KS /DCOM/ TP
          COMMON /CONST/ AL
          W=KS/KM
          RB3=KM**3
          BF=TH/(MO-MD*XB(9))
          DCB=DSQRT(XB(7)**2+XB(8)**2)
          XBP3=XB(7)*(-MU*XB(1)/RB3-BF*XB(7)/DCB)
          XBP4=XB(8)*(-MU*XB(2)/RB3-BF*XB(8)/DCB)
          XBNOM(1)=KM*DCOS(W*XB(9)+TP)
          XBNOM(2)=KM*DSIN(W*XB(9)+TP)
          XBNOM(3)=-KS*DSIN(W*XB(9)+TP)
          XBNOM(4)=KS*DCOS(W*XB(9)+TP)
```

118

```
      F(1)=XA(1)-.332645d+01
      F(2)=XA(2)-.573847d+01
      F(3)=XA(3)+.335233d+00
      F(4)=XA(4)-.194326d+00
      F(5)=(1+XB(5)*XB(3)+XB(6)*XB(4)+XBP3+XBP4)*XB(9)
     *    +(XB(5)*XBNOM(2)-XB(6)*XBNOM(1)+XB(7)*XBNOM(4)
     *    -XB(8)*XBNOM(3))*W
      F(6)=XB(1)+4.54425d+00*AL+(AL-1.0d+00)*XBNOM(1)
      F(7)=XB(2)-4.81623d+00*AL+(AL-1.0d+00)*XBNOM(2)
      F(8)=XB(3)+.282583d+00*AL+(AL-1.0d+00)*XBNOM(3)
      F(9)=XB(4)+.266625d+00*AL+(AL-1.0d+00)*XBNOM(4)
      RETURN
      END
```

Bibliography

1. Baker, M. L. Jr. *Astrodynamics*. New York: Academic Press, 1967.

2. Barclay, Capt Richard C. *A Computer Model for Evaluation of Launch Vehicle and Target Tracking Error Assignments for Direct Ascent, Deep Space ASAT Systems*. MS Thesis, AFIT/GSO/OS/83D-1. School of Engineering, Air Force Institute of Technology (AU), Wright-Patterson AFB OH, December 1983.

3. Bate, Roger R. et al. *Fundamentals of Astrodynamics*. New York: Dover Publications, Inc., 1971.

4. Bryson, Arthur E., Jr. and Yu-Chi Ho. *Applied Optimal Control*. New York: Hemisphere Publishing Corporation, 1975.

5. Burk, Capt Robert C. *Minimum Impulse Orbital Evasive Maneuvers*. MS Thesis, AFIT/GSO/AA/85D-3. School of Engineering, Air Force Institute of Technology (AU), Wright-Patterson AFB OH, December 1985.

6. Carnahan, Brice et al. "The Approximation of the Solution of Ordinary Differential Equations," *Applied Numerical Methods*. New York: John Wiley and Sons, Inc., 1969.

7. Isaacs, R., *Differential Games*. New York: John Wiley and Sons, Inc., 1965.

8. Kelley, H. J. et al. *Orbital-Maneuver-Sequence Optimization*. AFRPL TR-85-090. Washington: Government Printing Office, 1985.

9. Lawden, D. F., *Optimal Trajectories for Space Navigation*. London, England: Butterworth and Co, Ltd., 1963.

10. Marec, J. P., *Optimal Space Trajectories*. Amsterdam, the Netherlands: Elsevier Scientific Publishing Co., 1979.

11. National Aeronautics and Space Administration Lewis Research Center, *Ion Propulsion for Spacecraft*. Washington: Government Printing Office, 1977.

12. Pereyra, V. "PASVA3: An Adaptive Finite Difference
     Fortran Program for First Order Nonlinear, Ordinary
     Boundary Problems," _Lecture Notes in Computer Science,
     Volume 76, Codes for Boundary-Value Problems in
     Ordinary Differential Equations_. Berlin:
     Springer-Verlag, 1979.

13. Preissinger, Capt Robert D. _Optimal Continuous Thrust
     Orbital Evasive Maneuvers from Geosynchronous Orbit_.
     MS Thesis, AFIT/GA/AA/86D-12. School of Engineering,
     Air Force Institute of Technology (AU),
     Wright-Patterson AFB OH, December 1986.

14. Widhalm, J. W. and S. A. Eide. "Optimal Continuous
     Thrust In-Plane Orbital Evasive Maneuvers," _Proceedings
     of the AIAA 26th Aerospace Sciences Meeting_.
     Unpublished Paper, 1987.

121

Vita

Second Lieutenant Sharon A. Eide was born on ███████ ██ ████████ ████████ She graduated from Newport High School in ████████ ████████ in 1982. Lieutenant Eide then attended the University of Washington in Seattle, from which she graduated Magna Cum Laude in 1986 with the degree of Bachelor of Science in Aeronautics and Astronautics. Upon graduation, Lieutenant Eide received her commission through the Air Force Reserve Officer Training Corps and entered the School of Engineering, Air Force Institute of Technology in June 1986.

Permanent Address: ███ ████████████████████ ████████ ██████████████

A181544

REPORT DOCUMENTATION PAGE	Form Approved OMB No. 0704-0188

1a. REPORT SECURITY CLASSIFICATION UNCLASSIFIED	1b. RESTRICTIVE MARKINGS

2a. SECURITY CLASSIFICATION AUTHORITY	3. DISTRIBUTION/AVAILABILITY OF REPORT
2b. DECLASSIFICATION/DOWNGRADING SCHEDULE	Approved for public release; distribution unlimited

4. PERFORMING ORGANIZATION REPORT NUMBER(S) AFIT/GA/AA/87D-2	5. MONITORING ORGANIZATION REPORT NUMBER(S)

6a. NAME OF PERFORMING ORGANIZATION School of Engineering	6b. OFFICE SYMBOL (If applicable) AFIT/ENY	7a. NAME OF MONITORING ORGANIZATION

6c. ADDRESS (City, State, and ZIP Code) Air Force Institute of Technology (AU) Wright-Patterson AFB, Ohio 45433-6583	7b. ADDRESS (City, State, and ZIP Code)

8a. NAME OF FUNDING/SPONSORING ORGANIZATION	8b. OFFICE SYMBOL (If applicable)	9. PROCUREMENT INSTRUMENT IDENTIFICATION NUMBER

8c. ADDRESS (City, State, and ZIP Code)	10. SOURCE OF FUNDING NUMBERS			
	PROGRAM ELEMENT NO.	PROJECT NO.	TASK NO	WORK UNIT ACCESSION NO

11. TITLE (Include Security Classification)
OPTIMAL THRUST VECTOR CONTROL OF COPLANAR ORBITAL EVASIVE MANEUVERS

12. PERSONAL AUTHOR(S)
Sharon A. Eide, B.S., 2Lt, USAF

13a. TYPE OF REPORT MS Thesis	13b. TIME COVERED FROM _____ TO _____	14. DATE OF REPORT (Year, Month, Day) 1987 December	15. PAGE COUNT 138

16. SUPPLEMENTARY NOTATION

17. COSATI CODES			18. SUBJECT TERMS (Continue on reverse if necessary and identify by block number)
FIELD	GROUP	SUB-GROUP	Evasive Maneuvers
22	03		Geosynchronous Satellite Orbits
22	01		Optimization, Continuous Thrust Programming

19. ABSTRACT (Continue on reverse if necessary and identify by block number)

Thesis Advisor: Joseph W. Widhalm, Lt Col, USAF
Assistant Professor of Aerospace Engineering

Approved for public release: IAW AFR 190-1.

Dean for Research and Professional Development
Air Force Institute of Technology (AU)
Wright-Patterson AFB OH 45433

20. DISTRIBUTION/AVAILABILITY OF ABSTRACT ☒ UNCLASSIFIED/UNLIMITED ☐ SAME AS RPT. ☐ DTIC USERS	21. ABSTRACT SECURITY CLASSIFICATION UNCLASSIFIED
22a. NAME OF RESPONSIBLE INDIVIDUAL Joseph W. Widhalm, Lt Col, USAF	22b. TELEPHONE (Include Area Code) 513-255-4372	22c. OFFICE SYMBOL AFIT/ENY

DD Form 1473, JUN 86   Previous editions are obsolete.

Optimal in-plane orbital maneuvers enabling a target spacecraft in geosynchronous orbit to avoid interception by a threat in direct coasting ascent are examined. Given constant magnitude, low thrust electric propulsion, the thrust vector control history is determined to propel the spacecraft to either a maximum or minimum orbit radius in a specified time of flight. The evasive maneuver is studied from two aspects. First, an orthogonality constraint is applied at the final time of the maneuver, such that the target spacecraft's position vector is orthogonal to its velocity vector. This requirement is then removed to allow the spacecraft to travel without influence of a terminal constraint. Results demonstrate the adverse shaping effect the orthogonality constraint applies over the entire evasive maneuver.

Upon completion of the evasive maneuver, the spacecraft returns in minimum time to its nominal orbit, in a position as if no evasive thrusting had occurred. Results show the time required to rendezvous with the nominal orbit may be significantly greater than the time of flight of the evasive maneuver.

Optimal control is applied to formulate the evasive and rendezvous maneuvers using Euler-Lagrange theory and the calculus of variations. The behavior of the Lagrange costates is examined in terms of their effect upon solution convergence. The resulting two point boundary value problem is solved by numerical methods to yield the optimal spaceflight trajectory. (Theses)